YUNIBESITI YA BOKONE-BOPHIRIMA
NORTH-WEST UNIVERSITY
NOORDWES-UNIVERSITEIT

ASSESSMENT OF THE CHARACTERISTICS OF CHITOSAN PROCESSED BY SPHERICAL AGGLOMERATION

Abel Hermanus van der Watt (B.Pharm.)

Dissertation submitted in partial fulfilment of the requirements for the degree Magister Scientiae in the Department of Pharmaceutics at the North–West University

Supervisor: *Dr. A.F. Marais*

June 2005

Potchefstroom

Dedicated to Jakkie van der Watt

ACKNOWLEDGEMENTS

This study would not have been possible without the assistance and encouragement of several people. I would like to extend my gratitude towards the following people:

- Dr. A.F. Marais for his tremendous hard work, administration and contribution in making this study possible and most importantly enjoyable for me.
- Dr. Louwrens Tiedt for the SEM micrographs.
- Dr. EC van Tonder.
- Prof. Faans Steyn for his help with the statistical analysis of the data.
- Prof. FC van Graan for his statistical advice.
- Me. Anriëtte Pretorius for ensuring that the references are correctly noted.
- My friends and colleagues at the Research Institute for Industrial Pharmacy and at the Department of Pharmaceutics.
- Elsa-Marie van der Watt for her love and financial support.
- Dalene Delport for her patience, love and emotional support.

Finally, our Father in Heaven.

AIM AND OBJECTIVES OF THE INVESTIGATION

1.1 AIM

The aim of the study was to investigate the parameters contributing to the spherical agglomeration of chitosan powder in an effort to improve the micrometric properties of chitosan powder. Furthermore, to determine the applicability of spherical chitosan agglomerates and formulations in sustained release directly compressed tablets by analysis of the dissolution profiles of a water soluble tracer drug.

1.2 BACKGROUND

Chitosan is a fiber type polymer derived from chitin, a polysaccharide found in the exoskeletons of crabs, shrimp and other shellfish. Chitosan is applied in numerous products as it is widely available and inexpensive. In contrast, chitosan lacks the properties a pharmaceutical excipient has to comprise. Chitosan is characterized by its relatively weak flowability and poor compactibility. Good flowability and compactibility are just two of the properties an excipient intended for direct compression has to possess. The poor flowability and compressibility can be the result of chitosan having an asymmetrical, fibre type of structure in addition to its physical properties.

Spherical agglomeration is a size enlargement technique that facilitates operations of solid processing and conserves the solubilization properties of fine particles. The spherical agglomeration technique is rarely used industrially because its kinetics and mechanisms are poorly understood. Although the process of spherical agglomeration is inadequately understood, it bears some advantages over traditional techniques employed for the size enlargement of particles. In addition to being a time sparing technique, the spherical agglomeration procedure can be utilized to optimize the compactibility and flowability due to the dense spherical product an agglomerated material produces. An agglomerated powder is desirable in many solid processing and handling applications. It contains little or no dust, flows freely for easy metering, and has good storage and handling characteristics.

Chitosan can be compressed with the use of expensive hydraulic presses, designed for material compactibility studies, apart from the commercially available tablet presses. If

chitin, the most abundant natural polymer available next to cellulose, and the fiber structure of chitosan derived from chitin can be transformed into a spherical shape, flow properties and compactibility are prone to improve, thus creating an acceptable powder to be used for pharmaceutical purposes, which will ultimately be inexpensive and easily produced.

Many methods are employed to delay the dissolution rate of drugs. Film coating and microencapsulating are costly, time consuming and complex techniques. The spherical agglomeration of drug particles has revealed to deliver matrix type drug release. The simple, but yet to date a poorly understood technique, necessitates the spherical agglomeration method for the development of a dosage form including chitosan to delay the dissolution of a highly water soluble tracer drug.

1.3 OBJECTIVES

The aim of the study necessitates the following investigations:

- *Determination of the possibility of chitosan to be spherically agglomerated.*
- *Determination of the parameters contributing to the spherical agglomeration of chitosan.*
- *Investigation of the effect of each operating parameter on agglomerate formation and recovery.*
- *Comparison of the micrometric properties of chitosan prior to and after spherical agglomeration.*
- *Establishment of the applicability of the spherical agglomeration process and the formulations in terms of efficiency and reliability compared to a commercially available product.*
- *Comparison of the dissolution profiles of propranolol hydrochloride from different spherically agglomerated chitosan tablet formulations with the dissolution profiles of a commercially available capsule formulation.*

- *Establishment of the type of drug release from spherically agglomerated chitosan tablets.*

- *Comment on the spherical agglomeration of chitosan.*

ABSTRACT

ASSESSMENT OF THE CHARACTERISTICS OF CHITOSAN PROCESSED BY SPHERICAL AGGLOMERATION

Chitosan, derived from the most abundant natural polymer available next to cellulose, lacks the micrometric properties a pharmaceutical excipient intended for direct compression has to comprise. Excellent flowability, compactibility and dust freeness are primary micrometric properties required from direct compression excipients to ensure the success of the method. The successful exploitation of direct compression as a tablet manufacturing process could result in phenomenal time saving and economical benefits.

Size enlargement is a technique utilized to alter the micrometric properties of powders on a physical level. Several methods are available to enlarge particle size, but no techniques experimented offered the same advantages in terms of efficiency, simplicity, time and cost effectiveness than the spherical agglomeration technique.

An intensive preliminary experimental study revealed the predominant factors contributing to the successful spherical agglomeration of chitosan. A factorial design identified the optimum factors and factor levels. An agitation speed of 400 rpm provided agglomerates of desirable size and shape. Higher speeds disrupted the process. A suspension agglomeration time of 15 minutes produced perfectly spherical agglomerates, but had no influence on tablet properties. A bridging liquid volume of 3 ml per 3 g powder was sufficient to wet the suspended particles. Higher volumes per powder weight produced large undesirable agglomerates which failed during compression. A bridging liquid concentration of 5% v/v facilitated adequate wetting. The optimum binder was identified as Kollidon® K25 and a binder concentration of 30% w/w seemed adequate to coat the entire powder mass, as SEM micrographs indicated.

The optimal parameters and levels of the spherical agglomeration of chitosan were recognized and further investigated. A study on the effect of each variable level was conducted in an attempt to explore the influence of a factor level on spherical chitosan agglomerate recovery and formation. Results indicated that no trends were present and that it could be suggested that agglomerate recovery was the result of the interaction of certain factors and specific factor levels.

Spherically agglomerated chitosan possessed phenomenally enhanced flow, compressibility and dust free properties. An angle of repose test indicated an improvement in fluidity from 23.2° to 2.5°. No lamination during compression was encountered. Spherically agglomerated chitosan was compressed successfully and used in tablet formulations without any tableting excipients other than Kollidon® K25, an excipient that proved essential in the agglomeration step. No glidants were necessary, as the powder flowed freely into the tablet die. In addition, the formulations required no lubrication in view of the fact that the tablets underwent no friction during compression. The tablets were hard (>100 Newton), and had minimum friability and complied with the weight variation standards of the British Pharmacopoeia.

Propranolol hydrochloride is an extremely poor flowing powder and could only be compressed with chitosan after being spherically agglomerated with chitosan. The drug remained stable during and after spherical agglomeration. The process proved safe, given the results obtained from the X-ray powder diffraction and infrared absorption spectroscopy.

Dissolution parameters in 0.1 M HCl and Sörensen buffer pH 4.5 were tested. The Inderal® LA 80 mg was the norm (1.000). Formulation 1 presented an average $(DR_i)_n$ of 1.42 and a $(AUC)_n + (DR_i)_n$ (combined) of 3.52. Formulation 2 displayed an average $(AUC)_n$ of 2.05. Formulation 3 had the overall best dissolution performance compared to Inderal® LA 80 mg, with an f2--value in both mediums of 34.46. Formulation $1_{10\ minutes}$ had an f2-value in 0.1 M HCl of 51.45, an $(AUC)_n$ of 1.30 and a $(DR_i)_n$ of 1.46.

The initial dissolution rate decreased with an increase in crushing strength and concentration propranolol and chitosan per tablet formulation. The incorporation of spherically agglomerates of chitosan into tablets resulted in sustained release of the drug.

It can be concluded that the release of propranolol from spherically agglomerated chitosan tablets is in accordance with the matrix model where diffusion is the rate limiting factor, with an almost desirable linear dependency for zero order drug release. A linear correlation is present between the percentage of drug released and the square root of

time (R^2 = 0.9434). Additionally, a linear relationship was found between the logarithm of the amount of drug released and the logarithm of time (R^2 = 0.9172). With a slope of 0.6594, it can be concluded that drug release took place passing through a porous system and as a result of a combination of diffusion through a polymer and diffusion through pores in the system.

The suitability of chitosan as a multipurpose excipient was illustrated. An effective method was developed, chitosan obtained enhanced micrometric properties as a result of the method, and spherically agglomerated chitosan sustained release tablets were obtained.

UITTREKSEL

EVALUERING VAN DIE EIENSKAPPE VAN SFERIES GEAGGLOMEREERDE KITOSAAN

Kitosaan is 'n polimeer en 'n derivaat van kitien. Kitien is naas sellulose die polimeer wat die mees algemeenste voorkom in die natuur. Kitosaan besit egter nie die gunstige mikrometriese eienskappe wat die meeste ander kommersieel beskikbare vulstowwe omvat nie. Uitstekende vloei-,hanterings- en tabletteringseienskappe is belangrik om die sukses van die direkte samepersingsproses te verseker. Die metode lei tot beduidende tydsbesparing vanweë die eenvoud van die proses. Die bestanddele word eenvoudig vermeng, waarna tablettering geskied.

Die vergroting van die afsonderlike deeltjies van 'n farmaseutiese poeier lei gewoonlik tot 'n verandering van die mikrometriese eienskappe van die poeier. Menigte tegnieke en apparaat is beskikbaar om die vergroting van deeltjies op 'n fisiese manier te bewerkstellig. Die sferiese agglomerasie tegniek bied die voordeel dat dit 'n tydsbesparende, koste-effektiewe en eenvoudige tegniek is.

'n Aanvanklike studie het getoon dat sekere faktore op sekere vlakke bygedra het tot die sferiese agglomerasie van kitosaan. Die optimum faktore en vlakke is met behulp van 'n faktoriaal ontwerp geïdentifiseer. 'n Roerspoed van 400 revolusies per minuut (met die behulp van 'n roerder in 'n beker) het agglomerate van aanvaarbare vorm en grootte gelewer. Hoër roersnelhede in die sisteem het in die algemeen gelei tot swak agglomeraat opbrengste. 'n Suspensie agglomerasie tydperk van 15 minute het geen invloed getoon op poeier en tableteienskappe nie, alhoewel die agglomerate wat bloot gestel was aan 'n langer agglomerasie tydperk wel oor 'n ronder voorkoms beskik het as die agglomerate wat aan korter agglomerasie tye blootgestel was. 'n Hoeveelheid van 1 ml/g brugvloeistof (ysasynsuur) was voldoende om al die gesuspendeerde deeltjies te benat. 'n Ysasynsuuroplossing van 5% was benodig vir die volkome benatting van die gesuspendeerde deeltjies. Kleiner hoeveelhede het geen agglomerasie tot gevolg gehad, terwyl groter hoeveelhede gelei het tot die gedeeltelike oplos van kitosaan met geen tablettering as gevolg. Kollidon® K25 het hoër agglomeraat opbrengste gelewer as Kollidon® K30, en het optimum agglomerate gevorm in verhoudings van 7 dele

bindmiddel en 3 dele kitosaan. SEM foto's het addisionele bewyse getoon van die struktuur en wyse van agglomerate vorming.

Die optimale parameters en vlakke van die sferiese agglomerasie van kitosaan is geïdentifiseer. 'n Ondersoek is ingestel om die effek van elke veranderlike se vlakke op agglomeraat opbrengste te ontleed. Resultate het getoon dat geen verwantskappe gevind kon word nie en dat agglomeraat opbrengste afhanklik was van die interaksies van spesifieke faktore op spesifieke vlakke.

Sferiese geagglomereerde kitosaan het fenominale verbeteringe in vloei, tabletteerbaarheid en hanteringseienskappe getoon. Die rushoek van kitosaan poeier was voor agglomerasie 23.2° en na agglomerasie 2.5°. Laminering en friksie was afwesig tydens tablettering. Geen bykomende hulpstowwe, glymiddels en smeermiddels was benodig nie. Slegs Kollidon® K25 was bygevoeg voor agglomerasie en was noodsaaklik tydens die agglomerasieproses. Die tablette was hard (>100 Newton) en het minimum verbrokkeling vertoon. Die tablette se massavariasie was binne die perke van die BP se vereistes.

Propranolol hidrochloried beskik oor swak vloeieienskappe en kon slegs saam met kitosaan getabletteer word nadat beide poeiers saam sferies geagglomereer was. Propranolol hidrochloried was stabiel gedurende en na die sferiese agglomerasie proses. X – straalpoeierdiffraksie- en infrarooi absorpsietoetse het bevestig dat propranolol hidrochloried nie as gevolg van die sferiese agglomerasie proses afbraakprodukte gevorm het nie.

Dissolusietoetse is uitgevoer in 0.1 M HCl (pH 1.2) en in Sörensen buffer pH 4.5. Inderal® LA 80 mg is as die norm gebruik (1.000). Formule 1 het 'n gemiddelde $(DR_i)_n$ van 1.42 en 'n gekombineerde $(AUC)_n + (DR_i)_n$ – totaal gehad van 3.52. Formule 2 het 'n gemiddelde $(AUC)_n$ getoon van 2.05. Formule 3 het die beste in beide mediums vergelyk teenoor Inderal® LA 80 mg kapsules, met 'n gemiddelde f2–waarde van 34.46. Formule $1_{10\ minute}$ het 'n f2–waarde van 51.45 in 0.1 M HCl gehad, 'n $(AUC)_n$ van 1.30 en 'n $(DR_i)_n$ van 1.46.

Die aanvanklike dissolusie tempo van tablette het verminder met 'n toename in breeksterkte en 'n toename in die hoeveelheid kitosaan en propranolol per tablet. Die vorming van 'n gellaag rondom die sferies geagglomereerde kitosaan en die propranolol hidrochloried deeltjies het waarskynlik gelei tot die verlengde vrystelling en 'n afname van die tempo van dissolusie van die getabletteerde propranolol.

Dit kan veronderstel word dat die vrystelling van propranolol hidrochloried volgens die matriksmodel verloop met diffusie as die snelheids bepalende faktor. Die vrystelling van propranolol hidrochloried het byna 'n liniêre verwantskap getoon teenoor die hoogs aangeskrewe zero orde vrystellingsmodel. 'n Liniêre verwantskap was gevind tussen die vierkantswortel van tyd en persentasie van geneesmiddel reeds vrygestel (R^2 = 0.9434). 'n Bykomende liniêre verwantskap was gevind tussen die logaritme van die persentasie geneesmiddel vrygestel en die logaritme van tyd (R^2 = 0.9172). Die helling van die lyn (0.6594) het getoon dat die vrystelling van propranolol hidrochloried deur 'n porieuse sisteem plaasgevind het. Die vrystelling van propranolol was 'n funksie van die kombinasie van geneesmiddel diffusie deur 'n polimeer en diffusie deur 'n porieuse sisteem.

Die geskiktheid van kitosaan as 'n meerdoelige vulstof is gedemonstreer. 'n Effektiewe metode is ontwikkel, kitosaan het verbeterde mikrometriese eienskappe verkry as gevolg van sferiese agglomerasie, en die verlengde vrystelling van propranolol vanuit kitosaan tablette is verkry.

TABLE OF CONTENTS

1. CHAPTER 1

CHITOSAN, CONTROLLED RELEASE METHODOLOGY AND SPHERICAL AGGLOMERATION

1.1 INTRODUCTION

Chitin is the most abundant natural amino polysaccharide (Shepard *et al.*, 1997:535) and its annual production equals that of cellulose, a well known powder utilized in the tablet manufacturing industry. Chitosan is a powder formed by the deacetylation of chitin. The widespread availability of chitosan however, does not compensate for its poor flow and compressibility which are properties that an excipient intended for direct compression should comply to.

Tableting is easily process-validated and automated toward unmanned operation overnight. To do this, highly compactable properties of drug particles are required; otherwise a lot of powder binder such as microcrystalline cellulose, dicalcium phosphate dihydrate and other excipients are necessary to be mixed in the formulation, ensuing in larger sized tablets and additional formulation costs (Kawashima *et al.*, 2002:283).

The improvement of the micromeritic properties of chitosan with the least amount of effort, and to achieve matrix type drug release additionally from a chitosan formulation through an alternative granulation technique could be of great advantage.

1.2 BIOPOLYMERS

Biopolymers are compounds that are produced in nature by living organisms and plants, participate in the natural biocycle and are eventually degraded and reabsorbed in nature. The most widespread biopolymers are polysaccharides, cellulose, starch and lignin, whose swellability in water and viscous solution/gel-forming properties are already utilized to manufacture a number of industrial and consumer products.

The plentiful amount of natural polymers available does not compensate for its relatively low utilization compared to synthetic polymers within the pharmaceutical industries.

In view of growing public health and ecological awareness, accompanied by an increasing amount of ever stricter environmental policies on discharged wastes, attention has been

focused on the use of biopolymers from renewable resources as alternatives to synthetic polymers (Krajewska, 2005:306).

Chitin and chitosan are also biopolymers from renewable resources, obtainable from shells of shellfish, the wastes of the seafood industry.

1.2.1 Chitin

Every year, approximately 100 billion tons of chitin is produced on the earth by crustaceans, molluscs, insects, fungi, and related organisms. This amount is comparable to that of cellulose produced by higher plants, but chitin is not widely used by the pharmaceutical industry at present (Rege *et al.*, 2003:41).

Chitin is the most abundant natural amino polysaccharide. It has become of great interest not only as an underutilized resource, but also as a new functional material of high potential in various fields, and recent progress in chitin chemistry is quite noteworthy. Chitin, a naturally abundant mucopolysaccharide, and the supporting material of crustaceans, insects, etc., is well known to consist of 2-acetamido-2-deoxy-β - *D* -glucose through a β (1→4) linkage (Shepard *et al.*, 1997:535).

1.2.2 Chitinosans

The term 'chitinosans' embraces the spectrum of acetylated poly (*N*-glucosamines), ranging from chitin (0% deacetylated) to chitosan (100% deacetylated) (Rege *et al.*, 1999:49). Chitosan is a linear polycationic macromolecule which exhibits a variety of physicochemical and biological properties resulting in numerous applications in fields such as waste and water treatment, agriculture, fabric and textiles, cosmetics, nutritional enhancement, and food processing.

The main driving force in the development of new applications for chitinosans lies in the fact that this cationic polymer is not only readily and economically processed from naturally abundant chitin, but also is non-toxic, biodegradable, and multifunctional (Rege *et al.*, 1999:50).

In addition to its lack of toxicity and allergenicity, its biocompatibility, biodegradability, mucoadhesion and bioactivity make it a very attractive substance for diverse applications as a biomaterial in pharmaceutical and medical fields, where it has been used for systemic and local delivery of drugs and vaccines (Şenel & McClure, 2004:1467).

The structures of cellulose, chitin and chitosan are presented in figure 1.1 (Ravi Kumar, 2000:2).

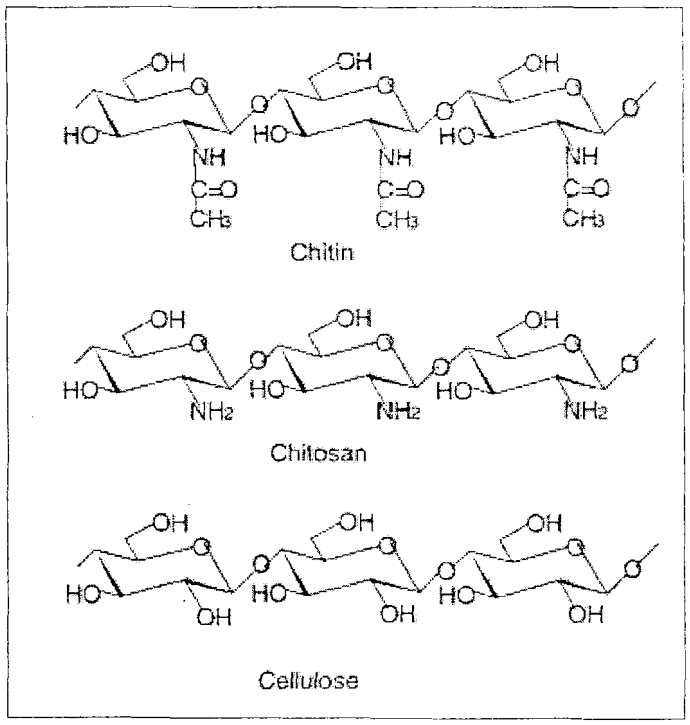

Figure 1.1: The structures of cellulose, chitin and chitosan. Note the close structural relationship (Ravi Kumar, 2000:2).

1.2.3 Processing of chitin and chitosan

Commercially, chitosan is available in the form of dry flakes, solution and fine powder. Chitin is easily obtained from crab or shrimp shells and fungal *mycelia*. Chitin production is associated with food industries such as shrimp canning. The production of chitosan-glucan complexes is associated with fermentation processes, similar to those for the production of citric acid from *Aspergillus niger*, *Mucor rouxii*, and *Streptomyces*, which involves alkali treatment yielding chitosan-glucan complexes. The alkali removes the protein and deacetylates chitin simultaneously (Ravi Kumar, 2000:3). The deacetylation process of chitin to produce chitosan is described in figure 1.2.

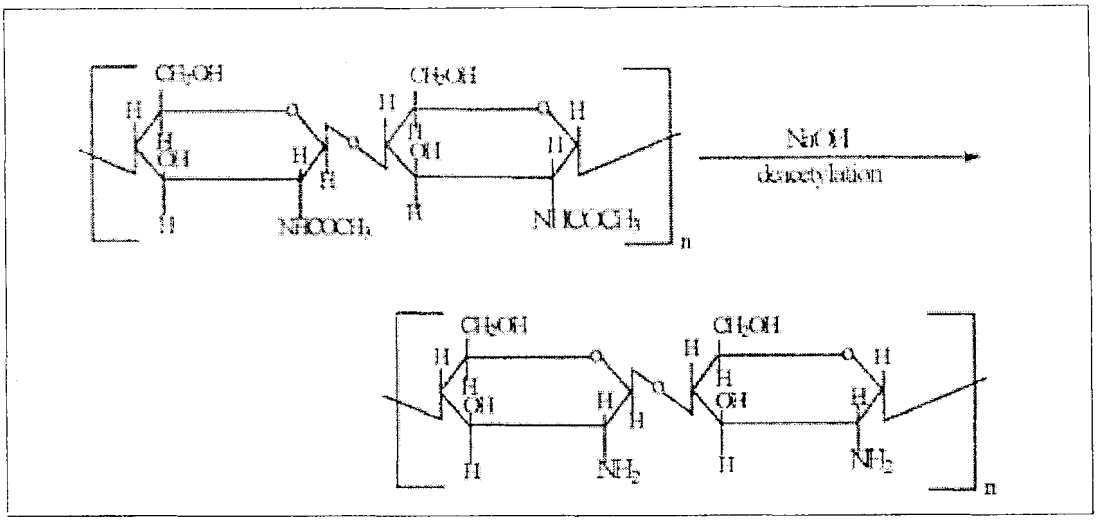

Figure 1.2: The deacetylation process of chitin to produce chitosan (Ravi Kumar, 2000:2).

The processing of crustacean shells mainly involves the removal of proteins and the dissolution of calcium carbonate which is present in crab shells in high concentrations. The resulting chitin is deacetylated in 40% sodium hydroxide at 120° C for 1-3 hours. This treatment produces 70% deacetylated chitosan (figure 1.2).

1.3 SIZE ENLARGEMENT

1.3.1 Introduction

Tablets can be compacted by direct compression or after a granulation step. Direct compression is always preferred, but is only possible for a limited number of substances due to problems such as poor powder flow properties, low tablet strength, capping and segregation. Size enlargement is an approach to overcome these problems and usually results in better flowability and compactibility of the powder.

Tablets are the most popular drug dosage form on the market nowadays. As a result of the oral administration market being so vastly popular, a great deal of effort is put into developing powders ultimately serving as directly compressible pharmaceutical excipients. Powders unable to be directly compressed are typically used in conjunction with capsules to ease administration. The most economical approach would thus be to compress the powder mixtures directly into tablets.

There are several reasons for this type of oral solid dosage form being fashionable:

- Oral administration is usually the most acceptable route for drug administration.
- The active drug dose is contained in a relatively small volume, leading to ease of packaging, transport, storage and eventual administration.
- A high dose accuracy is acquired
- Large quantities of tablets can be manufactured over a reasonably short period of time
- Alternative formulation can promote altered drug release

Various tablets differ from functional as well as a production approaches. Dissimilar types of tablets require different production techniques, though these techniques vary extensively in the amount of time put into development and the manufacturing difficulty.

1.3.2 Granulation

Granulation is a particle designing technique. A granulation step improves the micrometric properties of a powder. Some additional properties of granulated products include (Iveson *et al.*, 2001:4) :

- reduced dustiness which minimizes losses, inhalation and explosion risks
- improved handling which facilitates controlled metering
- increased bulk density
- controlled dissolution rates
- and the co-mixing of particles which would otherwise segregate during handling

However, in spite of its widespread use, economic importance and almost 50 years of research, granulation has in practice remained more of an art than a science. Existing continuous industrial plants frequently operate with recycle ratios as high as 5:1 and suffer from cyclic behaviour, surging, erratic product quality and unplanned shutdowns. In addition, improper granulation causes problems in down-stream processes such as caking, segregation and poor tableting performance (Iveson *et al.*, 2001:4).

Understanding of the mechanisms by which granules are formed, interact with each other, and change in size has increased greatly. Frustratingly still, granulation processes remain difficult to control. Another challenge however is to develop better models for granule coalescence. Although there have been significant advances on understanding of the processes of granule adhesion and coalescence, more needs to be done. An additional challenge is to learn how to design mixers that inherently give a better control of granule size. This requires an

understanding of the motion of material within granulators and how the granulator interacts with the material being granulated (Knight, 2004:156).

1.3.3 Wet granulation

The wet granulation method is a size enlargement process capable of producing uniformly distributed components. An adhesive are employed to stick particles together to manufacture a granular product with enhanced flow properties and an increased ability to cohere under pressure. Compressibility of certain substances can improve due to the uniform distribution of components.

A distinction is made between wet and dry granulation. Both dry and wet granulation methods have some advantages and disadvantages, but for drugs requiring relatively high loading, then the wet process is usually the method of choice (assuming adequate drug stability) as it can provide particles with superior processing characteristics (Williams *et al.*, 2004:29)

1.4 SIZE ENLARGEMENT BY AGGLOMERATION AS AN INTERDISCIPLINARY SCIENCE

Until very recently, agglomeration technologies, as all the other unit operations and associated techniques of mechanical process technology had been developed independently in the particular industries in which they were applied (Ennis, 1996:206).

Agglomeration is the size enlargement of particles by various mechanisms, such as particle interlocking, molecular (van der Waals), electrostatic or magnetic forces, chemical reaction, or the use of a hardening binder. In the mineral and mining industry any agglomerated material is desirable in many solids processing and handling applications. It contains little or no dust, flows freely for easy metering, and has good storage and handling characteristics (Ennis, 1996:203). An agglomerate also has a defined shape, high bulk density, and low bulk volume. Its porosity and density can be controlled, within limits, to influence the material's solubility, reactivity, heat conductivity, and other properties. An agglomerate often has better product appeal and sales value than a fine particle product.

Because the process requirements are fundamentally different in such unlike industries that handle, for example, coal and ores on one hand or food and pharmaceuticals on the other, no interdisciplinary contact and exchange of information took place. In fact, although agglomeration techniques developed along similar lines, application-related "theories" were defined which

were derived from investigations of specific requirements and their solutions together with a terminology that was often incomprehensible and, therefore, not useable by the "agglomeration expert" of another industry (Pietsch, 2003:11).

Agglomeration, as a science, began when an effort was made to interdisciplinary combine the extensive knowledge that had been accumulated during sometimes hundreds of years in specific fields of human activities. Agglomeration however, is still regarded as an art by some engineers in various industries

1.4.1 Spherical agglomeration

Spherical agglomeration is a granulation method of particle design, and seems related to wet granulation in terms of agglomerate behaviour and growth. The process is illustrated in figure 1.3 (Rossetti & Simons, 2003:49).

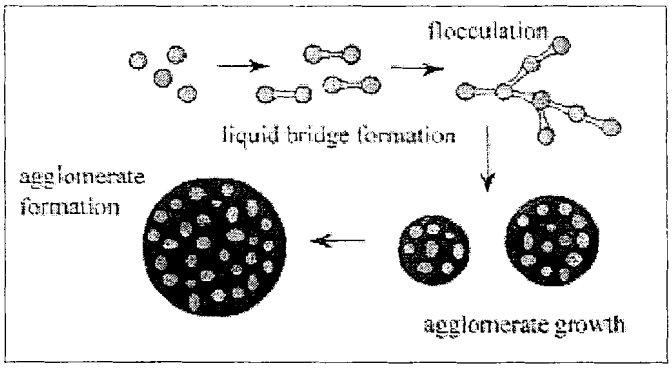

Figure 1.3: Spherical agglomeration (Rossetti & Simons, 2003:49).

Various studies have been done to separate dispersed fine particles efficiently from liquid suspensions in the powder technology, pharmaceutical and chemical engineering fields. With the addition of flocculants to the system, particles can be aggregated. However, the flocs obtained by this procedure are frequently bulky, which prevents subsequent processing (Kawashima *et al.,* 1981: 211).

Spherical agglomeration has many fine qualities as an industrial process for the recovery and separation of particles, including minerals. The process has been used in the mineral industry for many industrial applications, due to both the simplicity of the equipment required and to the possibility of agglomerating particles of around 10 μm in diameter with a high grade of recovery (Rossetti & Simons, 2003:49).

Like wet granulation, spherical agglomeration is also a size enlargement process, which uses as an agglomerating agent a liquid which is immiscible with the dispersion medium and which preferentially wets the dispersed particles. The technique was first developed by Kawashima and Capes to produce coal agglomerates (Kawashima & Capes, 1974:85).

Relatively strong and dense agglomerates from fine particles are formed if a suspension is agitated in conjunction with the addition of a bridging liquid. The bridging liquid wets the dispersed particles and must be immiscible with the external phase (Kawashima & Capes, 1980:312). The spherical agglomeration technique proved to be an inexpensive, time efficient and uncomplicated process to produce spherical coal agglomerates (Kawashima *et al.*, 1981b:913). The spherical agglomeration technique was developed by the National Research Council of Canada and was applied in the coal mining industry (Kawashima *et al.*, 1981c:1403).

Although several studies have been conducted on spherical agglomeration, the mechanics of this method have not been entirely elucidated. The reasons for the use of the specific bridging liquids and/or reagents in the literature concerned were often not stated. Therefore it would appear that further applications of the technique to other compounds could only be based on trial and error (Chow & Leung, 1996:358).

1.4.1.1 *Principles of the spherical agglomeration method*

Compound classification

Four different groups can be classified according to their solubilities in the relevant bridging liquids (Chow & Leung, 1996:358).

- Group I includes the compounds most soluble in water (>1 in 20).
- Group II encompasses those which are soluble in organic solvents (>1 in 20), such as chloroform but not water.
- Group III contains those compounds which are most soluble in ethanol, methanol, or acetone (>1 in 20).
- Group IV are compounds which are not sufficiently soluble in water.

Solvents used in Group III differ from the solvents used in Group II in that the solvents used in Group III are highly miscible with water.

1.4.1.2 *The process of agglomerate formation*

Kawashima and co-workers studied the parameters affecting agglomeration behaviour and showed that agglomeration obeyed first order kinetics (Kawashima *et al.*, 1981:211, Kawashima *et al.*, 1983:255).

Several factors contribute to the formation of sphere-shaped agglomerates. A primary aspect is the amount and distribution of bridging liquid poured into the system. With relatively great amounts of bridging liquid, two immiscible phases are formed in which particles are transferred from the suspending to the collecting liquid. In contrast, with smaller amounts of bridging liquid, compact spherical agglomerates may be formed. With even smaller amounts of bridging liquid, micro-agglomerates or flocs are formed (Kawashima & Capes, 1974:85).

Factors influencing the spherical agglomeration process include:

- Agitation speed
- Particle wettability
- Liquid bridge formation
- Particle size distribution
- External phase viscosity
- Bridging liquid applying mechanism
- Agglomeration time

Spherical agglomeration as a size enlargement and particle design process deliver products with the following benefits:

- Spherically shaped particles
- Better flow
- Segregation of powder mixtures is limited
- Fewer steps involved
- Less time
- Economical
- The suspension liquid can be recycled by distillation

Homogeneity in a powder formulation offers some advantages. A homogenous distribution of paracetamol decreased lamination (Nortjè, 1992:19). By melting paracetamol with various

excipients, a more homogenous distribution of paracetamol was obtained. The authors claimed that a reduction in tablet lamination was observed after milling the homogenous paracetamol and excipient powder.

A disadvantage however is the utilisation of organic solvents if water soluble substances need to be agglomerated (Nortjè, 1992:35).

Size enlargement by means of spherical agglomeration delivers a homogenous product without heating in contrast with a melting process.

1.4.1.3 *Agglomerate growth*

Forces contributing to the formation of agglomerates are of two kinds: natural (or physical) and applied (or mechanical) (Sastry & Fuerstenau, 1973:97).

The natural forces responsible for the formation of agglomerates can result from a number of sources:

- The attraction between solid particles due to van der Waals' forces, magnetic forces, or electrostatic charges.
- The interlocking effects between particles, depending on the shape of particles
- The adhesional and cohesional forces in bridging bonds, which are not freely moveable.
- The interfacial and capillary forces are due to the presence of a liquid phase.

Agglomerate growth mechanisms

Agglomerate growth can be related to three possible mechanisms. The mentioned mechanisms can occur simultaneously, whilst the experimental procedure and the physico-chemical properties of the substance determine the prevailing mechanism.

Coalescence

In the event of coalescence, two or more agglomerates combine to form a larger agglomerate. Additional agitation causes the agglomerate to obtain a spherical structure (Buys, 1988:24).

Layer formation

Layer formation is another mechanism when loose particles adhere to the outer layer of an existing agglomerate.

Fracturing

Thirdly, during agitation, agglomerates are exposed to forces, causing agglomerates to fracture, be dispersed once more and combining again with larger agglomerates. A definite size is finally achieved when a balance between coalescence and fracturing occur (Chow & Leung, 1996:370).

The modern approach and the traditional description of agglomerate growth are described in figure 1.4.

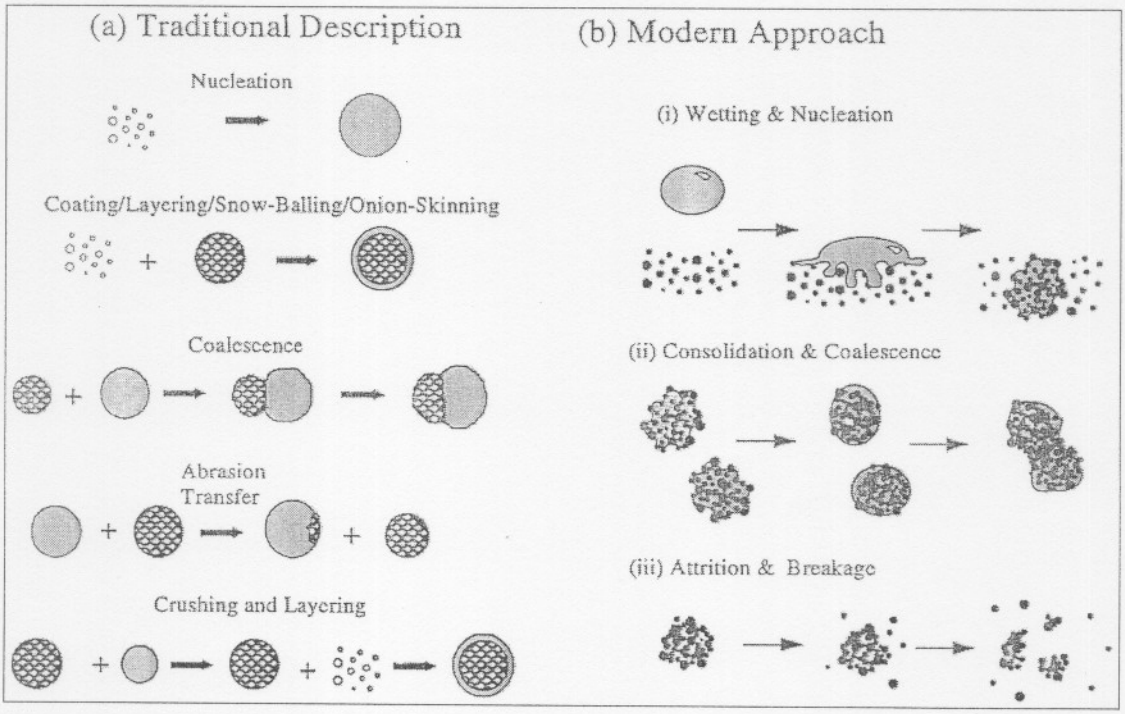

Figure 1.4: The modern approach versus the traditional approach of agglomerate growth (Iveson et al., 2001:5).

1.4.1.4 *Agglomerate structure*

The agglomerate structure depends on the mechanism by which the bridging liquid fills the spaces between the particles. Pendular (liquid trapped), funicular (air trapped) and capillary (air expelled-liquid saturated) are the mechanisms by which the secondary liquid fills the voids between particles (Sastry & Fuerstenau, 1973:98) and is described in figure 1.5.

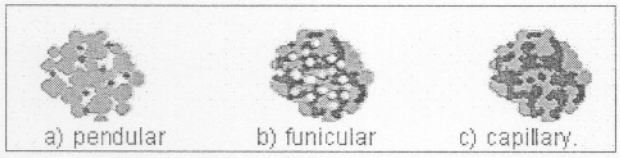

Figure 1.5: a) pendular b) funicular and c) capillary. Distribution of bridging liquid in agglomerates (Sastry & Fuerstenau, 1973:98).

Mechanical forces are required to bring the individual wetted particles, clusters or agglomerate species into contact with one another so that the natural forces can bring about their growth (Sastry & Fuerstenau, 1973:98). This mechanical action of moving the material is imparted by means of rolling, tumbling, agitating, kneading, extruding or compressing in a suitable apparatus.

Agglomeration of damp powders makes use of tumbling or agitating the material in balling drums, discs or cones. The tumbling properties of the agglomerate charge are dependent on the physical properties of the powder, size distribution of the growing species and size, geometry and speed of rotation of the balling device (Sastry & Fuerstenau, 1973:98).

1.4.2 Chitosan

All chitosan formulations developed to date necessitate the addition of other ingredients to facilitate compression. This reflects the fact that this commercially available polymer, as supplied, lacks good flow properties, packability and compressibility (Rege, 1999:50).

However several techniques, i.e. spray drying and coating are inappropriate due to high costs and exertion involved to enlarge and alter the particles. There is an increasing need for alternative processes that are more economic, reliable and reproducible, taking into consideration the possibility of automation and process continuity (Keleb *et al.*, 2004:183). The spherical agglomeration technique has proved to advance the micromeritic properties of powder substances, however little is written in literature involving chitosan and the spherical agglomeration technique.

1.5 CHITOSAN AND PROLONGED-RELEASE TECHNOLOGY

1.5.1 Introduction

Results of *in vitro* studies have shown that chitosan adheres to mucosal tissues, e.g. gastric or intestinal mucosa (Lehr *et al.*, 1992:43, Gåserød *et al.*, 1998:237). These adhesive properties

have led to increasing interest in the development of slow release chitosan dosage forms with prolonged gastric residence times.

1.5.2 Drug-delivery systems

1.5.2.1 *Conventional dosage forms*

Conventional dosage forms frequently lead to irregular changes in serum drug concentrations, as can be seen from figure 1.6. The majority of the drug content is released soon after administration, causing agent levels in the body to rise rapidly, peak and then decline sharply. For drugs whose actions show a relationship with their serum drug concentration, the sharp fluctuations often cause inappropriate side-effects at the peaks, followed by insufficient therapy at the troughs (Ravi Kumar, 2000:14).

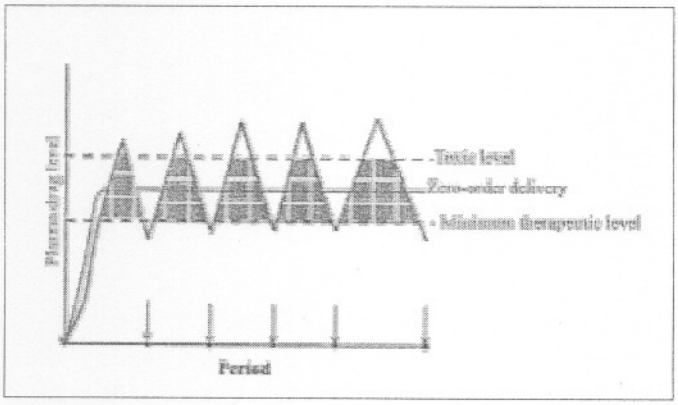

Figure 1.6: Controlled drug delivery versus immediate release (Ravi Kumar, 2000:14).

1.5.2.2 *Controlled-release*

Controlled-release technology emerged during the 1980's as a commercially sound method to administer drugs. The ability to predict and reproduce the release of an agent into a specific environment over an extended period of time has much remarkable merit. According to Ravi Kumar (2000:13) advantages of controlled-release dosage forms include:

- Controlled-release dosage forms create a preferred environment with optimal response, minimum side-effects and extended efficiency.
- Safety, effectiveness and reliability of drug therapy are desirable aspects produced by controlled-release drug administration.
- Such dosage forms regulate the drug release rate and lessen the frequency of drug administration to encourage patients to comply with dosing instructions.

According to Buys (1988:5) the disadvantages of controlled-release dosage forms are:

- Over dosage can occur if the release of the agent from the preparation takes place to fast, whilst an unnecessary slow release of agent can result in inadequate therapy
- Controlled-release dosage forms enhance the difficulty to effectively treat emergency cases of poisoning resulting from a drug over dose The process of formulation and producing a controlled-release dosage form is time consuming and expensive

Llittle information on the behaviour in man of stomach-specific dosage forms containing chitosan is available. Possible benefits of such dosage forms are under investigation (Säkkinen, 2003:227).

Dosage forms that release drugs slowly in the upper regions of the gastrointestinal tract could be of value if bioavailability of the drugs concerned were low or if toxic metabolites were formed distally in the intestine. If the bioavailability of a drug is low because it is specifically absorbed from sites in the upper regions of the gastrointestinal tract, use of chitosan as an excipient could result in amounts of drug absorbed being increased as a result of prolongation of gastric residence time (Säkkinen, 2003:228).

1.5.3 Bioadhesiveness

The incentives to utilize chitosan as a matrix forming agent can be attributed to the fact that chitosan is non-toxic and easily bioabsorbable (Şenel & Mcclure, 2004:1467), with gel-forming ability at low pH (Krajewska, 2005:305).

The bioadhesive systems are new delivery systems used to reduce bioavailability problems resulting from a too short stay of the pharmaceutical form at the activity or resorption site (Prudat-Christiaens *et al.*, 1996:109).

Additionally, chitosan has antacid and antiulcer activities which prevent or weaken drug irritation in the stomach (Ravi Kumar, 2000:14). Also, chitosan matrix formulations appear to float and gradually swell in an acid medium. Gel formation by chitosan at pH values of 1-2, as in the stomach, makes chitosan interesting for study as an excipient for development of slow release oral dosage forms.

These properties of chitosan make this natural polymer an ideal candidate for controlled drug release formulations.

1.6 DRUG RELEASE MECHANISMS

The ideal controlled release preparation would release its contents according to a zero order model. A graph of the percentage released versus time would represent a straight line. It is though highly unlikely to obtain a zero order rate of drug release from preparations utilising diffusion and erosion to release a drug (Buys, 1988:6).

Controlled release preparations can be categorized according to the mechanism by which drug release take place. According to Bruck (1983:6), the preparations are categorized in:

- Mechanical pumps
- Osmotic pumps
- Dissolution systems
- Diffusion systems

1.6.1 Mechanical pumps

Originally developed to release insulin and heparin directly into the blood circulation (Bruck, 1983:8). A constant drug level is maintained as long as the pump is functional. Disadvantages include the requirement of a surgical procedure and the additional high costs involved.

1.6.2 Osmotic pumps

A system utilizing osmotic pressure to accomplish zero order drug release was described by Theeuwes (1975:1987). The system comprises a water soluble drug and an osmotic active substance surrounded with a semi permeable membrane with a delivery orifice. When exposed to water, the core imbibes water osmotically at a controlled rate, determined by the membrane permeability to water and by the osmotic pressure of the core formulation.

Water moves into the system across the membrane by means of diffusion and dissolves the enclosed drug. The dissolved drug exits the system as a result of osmotic differences. A constant drug release is maintained as long as the osmotic active substance is present (Buys, 1988:6).

However, the rate of drug release is reduced remarkably if the osmotic active substance concentration decreases below the satisfied level (Lee & Robinson, 1978:172). The osmotic pump delivers between 60–80% of the drug at a constant tempo (Theeuwes, 1984:293).

1.6.3 Systems regulated by dissolution

Two types (encapsulated preparations and dissolution matrices) of systems demonstrate a dissolution regulated drug release.

1.6.3.1 *Encapsulated preparations*

Encapsulated preparations have enclosed granules coated with a slow dissolving film layer. The release rate is determined by the film solubility and layer thickness.

1.6.3.2 *Dissolution matrices*

Matrix systems can be obtained via various microencapsulation processes. The drug is compressed together with a weak water soluble excipient. The release of drug is a function of the filler solubility, tablet porosity and the presence of hydrophobic substances and tablet wettability. Compression force, dissolution medium, drug and excipient properties additionally influence dissolution (Parrot, 1981:162). The rate of dissolution from a solid is described in equation 1.1:

$$dc/dt = k_D A(C_s - C) \qquad \text{Equation 1.1}$$

Where:

dc/dt	=	dissolution tempo.
k_D	=	constant (dissolution tempo).
A	=	area.
C_s	=	saturated solubility of drug.
C	=	drug concentration in dissolution medium.

The dissolution rate will remain constant as long as there is a sufficient amount of drug available to stabilize C_s , and on condition that the area, A remains steady. The dissolution process however alters the surface area of the drug if exposed to the dissolution medium.

For spherical particles, the varying area can be substituted by the mass of the particles. The release of drug according to the mass of spherical particles can be given by the law of the cube roots (Ritchel & Udeshi, 1987:739):

$$W_0^{1/3} - W^{1/3} = k_D \qquad \text{Equation 1.2}$$

Where:

$W_0^{1/3}$	=	initial drug amount in the core.
$W^{1/3}$	=	amount of drug remaining in the core.
k_D	=	cube root dissolution rate constant.

1.6.4 Systems regulated by diffusion

Both diffusion and dissolution is present in a specific dosage form. However, one mechanism usually dominates the other mechanism (Lee & Robinson, 1978:140).

1.6.4.1 *Systems coated with a water immiscible membrane*

A water immiscible polymer or a combination of a water immiscible and a water soluble polymer coated upon drug nucleus is one technique to produce a diffusion based system. Equation 1.3 explains this particular drug release:

$$dM/dt = ADK\Delta C/\ell \qquad \text{Equation 1.3}$$

Where:

A	=	area.
dM/dt	=	release rate.
D	=	diffusion coefficient.
K	=	coefficient of drug between membrane and nucleus.
ℓ	=	membrane thickness.
ΔC	=	concentration difference across membrane.

1.6.4.2 *Systems coated with a semi-soluble membrane*

The drug nucleus is coated with a semi soluble membrane, containing a complex of a water soluble and water insoluble polymer. The water soluble polymer dissolves and the drug diffuse

through the membrane pores (Lee & Robinson, 1978:141). Equation 1.4 explains this particular drug release:

$$dM/dt = AD(C_1 - C_2)/\ell \qquad \text{Equation 1.4}$$

Where:

C_1	=	drug concentration inside nucleus.
C_2	=	drug concentration in dissolution medium.
A	=	area.
D	=	diffusion coefficient.
ℓ	=	membrane thickness.

1.6.5 Matrix release subject to drug diffusion

The Higuchi equation (1963:1145) explains the drug release dependent on diffusion out of an inert matrix. According to Schwartz *et al.* (1968:275), the Higuchi equation can be transformed to equation 1.5:

$$Q' = KSt^{1/2} \qquad \text{Equation 1.5}$$

Where:

Q'	=	amount of drug released.
S	=	area.
K	=	$(D.\varepsilon/\tau(2A - \varepsilon.C_s)C_s)^{1/2}$
A	=	amount of drug present in matrix.
C_s	=	drug solubility in matrix.
ε	=	porosity factor.
τ	=	crinkle factor.

A linear correlation would be possible between amount of drug released and the square root of time. Schwartz *et al.* (1968:275) differentiated the above equation to:

$$dQ'/dt = K^2.S^2/2Q \qquad \text{Equation 1.6}$$

Where:

dQ'/dt	=	release rate

The equation can logarithmically be altered to equation 1.7:

$$\log Q' = \log K + \frac{1}{2}\log t \qquad \text{Equation 1.7}$$

A graph of log Q' and log t would supply a straight line with an inclination of 0.5 if the drug is released by means of fickian diffusion.

1.6.5.1 *Diffusion out of an inert matrix*

Two types of inert matrices are defined:

- Drug particles coated individually
- Drug particles not coated individually and with canals and pores present, otherwise known as a granular matrix (Buys, 1988:13).

1.6.6 Conclusion

Several techniques are utilized to impart a delay in drug release. The coating process plays a major role in the field of matrix and controlled release methodology.

1.7 PREPARATION OF CONTROLLED RELEASE DOSAGE FORMS

A vast variety of controlled release preparations exist which can be classified according to its manufacturing procedure, i.e. coating or microencapsulation. The release of drug from these preparations is a result of erosion (dissolution) or diffusion. Some preparations utilize ion exchange, osmoses and mechanical mechanisms to release drug in its intended environment (Buys, 1988:19).

1.7.1 Coating

Many solid pharmaceutical dosage mediums are produced with coatings, either on the external surface of tablets, or on materials dispensed within gelatine capsules. According to Eurotherm (2003:1) coating serves a number of purposes:

- Protects the tablet (or the capsule contents) from stomach acids
- Protects the stomach lining from aggressive drugs such as enteric coated aspirin
- Provides a delayed release of the medication
- Helps maintain the shape of the tablet

The coating can be specially formulated to regulate how fast the tablet dissolves and where the active drugs are to be absorbed into the body after ingestion. Many factors can affect the end-use properties of pharmaceutical tablets:

- Chemical composition

- Coating process
- Drying time
- Storage and environmental monitoring.

1.7.1.1 *Coating process design and control*

The coating process is usually a batch driven task consisting of the following phases:

- Batch identification and recipe selection (film or sugar coating)
- Loading/Dispensing (accurate dosing of all required raw materials)
- Warming
- Spraying (application and rolling are carried out simultaneously)
- Drying
- Cooling
- Unloading

The coating process is described in figure 1.7. Tablet coating takes place in a controlled atmosphere inside a perforated rotating drum. Angled baffles fitted into the drum and air flow inside the drum provides means of mixing the tablet bed. As a result, the tablets are lifted and turned from the sides into the centre of the drum, exposing each tablet surface to an even amount of deposited/sprayed coating.

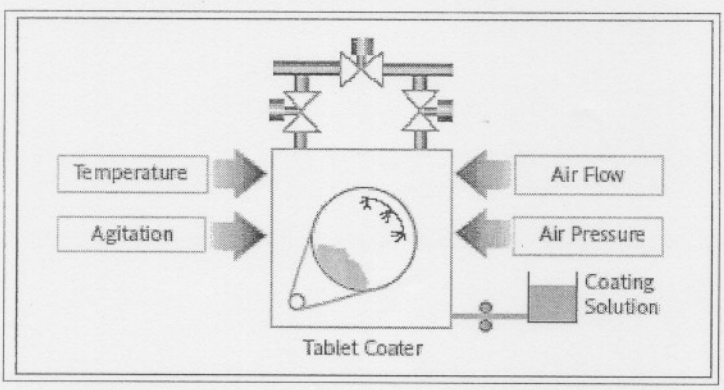

Figure 1.7: The coating process (Eurotherm, 2003:1).

The liquid spray coating is then dried onto the tablets by heated air drawn through the tablet bed from an inlet fan. The air flow is regulated for temperature and volume to provide controlled drying and extracting rates, and at the same time, maintaining the drum pressure slightly negative relative to the room in order to provide a completely isolated process atmosphere for the operator.

Tablet coating equipment may include spray guns, coating pan, polishing pans, solution tanks, blenders and mixers, homogenisers, mills, peristaltic pumps, fans, steam jackets, exhaust and heating pipes, scales and filters. Tablet coating processes may include sugar coating (any mixtures of purified water, cellulose derivatives, polyvinyl, gums and sugar) or film coating (purified water, cellulose derivatives)

1.7.2 Coated tablets

Coated tablets are tablets covered with one or more layers of mixtures of various substances such as natural or synthetic resins, gums, gelatin, inactive and insoluble fillers, sugars, plasticizers, polyols, waxes, coloring matter authorized by the competent authority and sometimes flavoring substances and active substances.

As described above the coating process can be a costly and time consuming process, and considering the expensive equipment involved a less time consuming process is highly sought-after.

The substances used as coatings are usually applied as a solution or suspension in conditions in which evaporation of the vehicle occurs. When the coating is a very thin polymeric coating, the tablets are known as film-coated tablets. Koizumi *et al.* (2000:277) film coated propranolol hydrochloride (p-HCl) loaded tablets with chitosan to establish a model of drug release to improve goodness-of-fit models compared to conventional models.

The delivery of drugs directly to the colon via the oral route has several useful therapeutic advantages. Macleod *et al.* (1999:251) showed the potential of mixed pectin:chitosan:hydroxypropyl methylcellulose films for colonic drug delivery. These coatings were capable of retarding the release of tablet core materials until they reached the colon, an environment rich in bacterial enzymes, which degraded the coating allowing drug release to occur.

Buys (1988:100) coated frusemide with polyvinylpyrrolidone in an alternative size enlargement technique, termed spherical agglomeration, and delayed the release of frusemide in a McIlIvaine buffer. The spherical agglomeration technique consisted of fewer steps than conventional coating techniques.

1.7.3 Spherical agglomeration

Relatively strong and dense agglomerates from fine particles are formed if a suspension is agitated in conjunction with the addition of a bridging liquid. The bridging liquid wets the dispersed particles and must be immiscible with the external phase (Kawashima & Capes, 1980:312). By utilizing the spherical agglomeration technique, Kawashima *et al.* (1981b:913) developed an inexpensive, time efficient and uncomplicated process to produce spherical coal agglomerates. The spherical agglomeration technique was developed by the National Research Council of Canada and was applied in the coal mining industry (Kawashima *et al.,* 1981c:1403).

Conventional microencapsulation processes occasionally use extreme temperatures and complicated steps during production stages. In contrast with conventional microencapsulation processes, the spherical agglomeration technique is uncomplicated and open for heat labile substances. Additionally, the spherical agglomeration technique coats individual particles (Buys, 1988:19).

Kawashima *et al.* (1981b:913) utilized the spherical agglomeration technique to develop an inexpensive and simple method to produce spherical agglomerates which delayed the release of sulfamethoxazole.

1.8 CONCLUSION

Chitosan has not been widely adopted as a pharmaceutical excipient or a formulation component and has not been used extensively despite of its abundant availability. One area of concern involves their utilization in directly compressible tablet formulations after being spherically agglomerated.

Granulation has been described by scientists as an art rather than a science, and the same applies for spherical agglomeration. In contrast, spherical agglomerates opposed to granules possess more advanced tableting properties obtained from a simple and straightforward manufacturing technique.

Spherical agglomeration was employed in previous studies to obtain matrix type drug release. In addition, the mucoadhesive properties of chitosan could provide some interesting prospects regarding drug targeting technology.

Currently, advances are made concerning spherical crystallization without the use of any binder as well as the spherical agglomeration of proteins.

Following in chapter 2 is the experimental methods and apparatus employed and the substances used throughout the study.

2. CHAPTER 2

EXPERIMENTAL METHODS, MATERIALS AND APPARATUS

The experimental procedures and substances used in the different experiments are explained in this chapter. Methods for the production of spherical chitosan agglomerates and a technique to deliver a directly compressible matrix type drug release tablet were developed. The effects of the different formulations and experimental procedures on the powder properties, agglomerate yield and dissolution profiles were investigated and the apparatus described.

2.1 MATERIALS

2.1.1 Chitosan

Chitosan (Batch number 021010, WarrenChem, WCI 7109, Durban, Republic of South Africa)

2.1.2 Binder

2.1.2.1 *Polyvinylpyrrolidone*

Kollidon® K25 and Kollidon® K30 (povidone: K-value: 25 and 30) (lot number 36-3790, BASF Aktiengesellschaft, Ludwigshafen, Germany) are well known binders and coating agents. Kollidon® K25 and Kollidon® K30 were used as binders for the reason that they have nearly the same solubility properties as chitosan and p-HCl (propranolol hydrochloride). The binders were critical for the spherical agglomeration of chitosan, playing a role in the binding phase of agglomerate formation.

2.1.3 Bridging liquid

2.1.3.1 *Acetic acid solution*

The bridging liquid has to wet the particles suspended in the external phase. Chitosan is well known to be soluble in a diluted acetic acid solution. P-HCl is a weak basic drug and highly soluble in water, thus an ideally suitable substance, possessing desirable qualities for spherical agglomeration in conjunction with chitosan and Kollidon® K25 and Kollidon® K30. These two binders are also very soluble in diluted acetic acid and could theoretically be wetted by a diluted acetic acid solution. Solutions of 0, 3, 5, 25, 50 and 100% v/v were used in the experiments as bridging liquid.

2.1.4 External phase

2.1.4.1 *Ethyl acetate*

Ethyl acetate were used as the suspension medium for the formulation mixtures hence its immiscibility with distilled water and acetic acid. Unlike most other water immiscible solvents, ethyl acetate has a low toxic potential (class 3, Materials Safety Data Sheet) and includes no health hazard at levels normally accepted in pharmaceuticals.

2.1.5 Tracer drug

2.1.5.1 *Propranolol hydrochloride (P-HCl)*

P-HCl, (Batch number PHC 030827, Kothari Phytochemicals International, Nagari, Thanichlhiyam, India). P-HCl is a powder with weak fluidity and fails to be directly compressed. Additionally the dry chitosan, polyvinylpyrrolidone and p-HCl powder mixtures also failed to be compressed and displayed poor powder flow as well.

Inderal® LA capsules are commercially available, long acting dosage form for p-HCl. The sustained release methodology was developed to increase patient compliance, offering a once daily dosage. In practice however, in contrast with capsule filling, the direct compression approach offers considerable savings in energy, equipment and materials handling.

An alternative method was to incorporate the p-HCl powder in the spherically agglomerated chitosan spheres. P-HCl is highly soluble in water, theoretically suitable to be integrated into the spherically agglomerated chitosan particles.

2.2 AGGLOMERATE PREPARATION

2.2.1 Mixture preparation

Powder mixtures consisted of a variety of formulations constructed according to a factorial design explained in the following chapter. Three gram mixtures of each of the different formulations were used in the range of spherical agglomeration experiments. The mixtures were transferred directly after weighing to the agglomeration apparatus without being mixed, as the formulations were thought to be thoroughly mixed by the motor blades prior to the start of agglomeration.

2.2.2 Suspension

Chitosan and polyvinylpyrrolidone were suspended in 100 cm^3 ethyl acetate and mixed with the Heidolph mechanical stirrer for sixty seconds prior to the onset of agglomeration.

2.2.3 Apparatus setup

The apparatus setup is displayed below in figure 2.1.

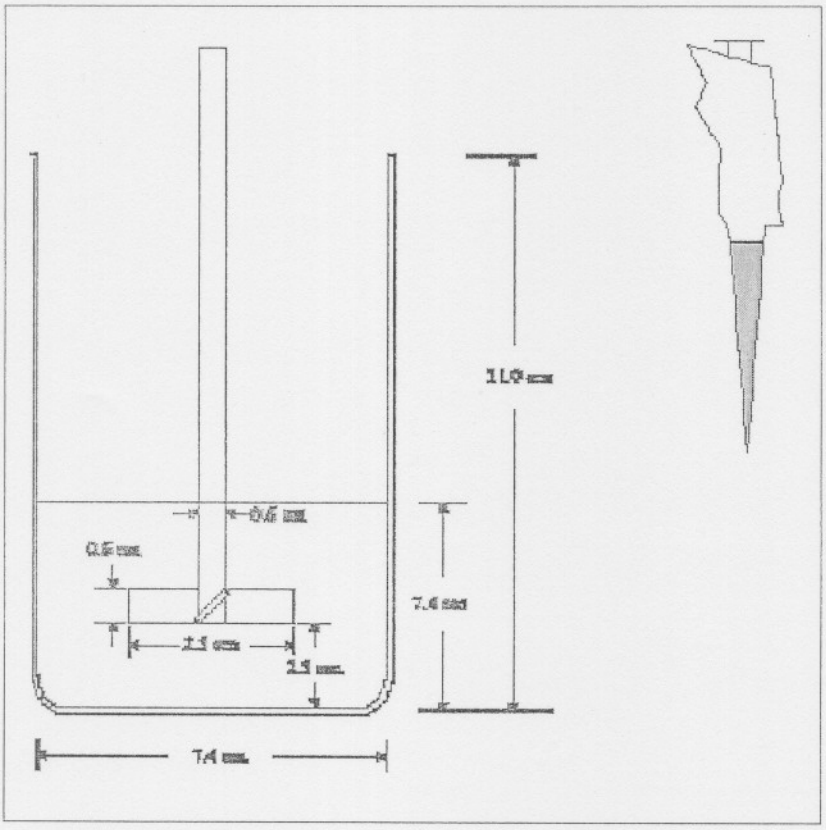

Figure 2.1: Apparatus setup as used in the agglomeration experiments.

The apparatus utilised in this study consisted of a 600 ml beaker containing a suspension of the powder, filled up to 100 ml with the external phase (ethyl acetate), with five baffles fixed to a Heidolph mechanical stirrer at the bottom to create turbulence. An Eppendorf pipette as well as a peristaltic pump were utilised for the addition of the bridging liquid (acetic acid). The agglomerates, if formed, were dried at room temperature for 48 hours and investigated.

2.2.4 Agglomerate recovery

The effectiveness of a particular experiment was described in terms of the amount of spherical particles it could produce. Agglomerate formation accounted for sphere shaped particles greater

than 1 mm. The agglomerate recovery is a value expressed in percentage and was calculated by determining the weight of the agglomerates and dividing it by the weight of the powder feed, multiplied with one hundred. The equation is given as:

$$AR = \frac{W_{agglomerates}}{Feed_{powder}} \times 100 \qquad \text{Equation 2.1}$$

Where:

AR	=	Agglomerate recovery
W	=	Sieved agglomerate weight
$Feed$	=	Powder amount used in agglomeration process.

2.3 *PHYSICAL CHARACTERIZATION OF SUBSTANCES*

2.3.1 Flow properties

Flow behaviour can often be described best by quantification of the process of flow. Numerous methods have been described either directly, using dynamic or kinetic methods, or indirectly, generally by measurements carried out on static powder beds (Staniforth 2000:601). These include the angle of repose, hopper flow rate and weigh variation.

2.3.1.1 *Angle of repose*

The angle of repose has been used as an indirect method of quantifying powder fluidity (Staniforth 2000:601) Particles will start to slide when the angle of inclination is large enough to overcome the friction forces between particles. An amount of powder was poured into a Perspex container with a 10 mm orifice fitted with a shutter. The shutter was opened and the powder discharged from a height of 15 cm onto a horizontal glass surface. The flow rate of a powder is proportional to the angle of repose. A large angle is indicative of poor flowability and a small angle of superior flow. The time of the powder discharged from the container was also noted to determine a flow rate through the 10 mm orifice (Staniforth 2000:601).

2.3.1.2 *Hausner ratio and Carr's index*

Carr's index and the Hausner ratio previewed the degree of densification which could occur during tabletting. The Carr's "percent compressibility" and the Hausner ratio were calculated using the equation $([\rho_{tap} - \rho_{bulk}]/\rho_{tap}) \times 100$ and ρ_{tap}/ρ_{bulk}, respectively.

2.3.1.3 *Bulk and tapped density*

A known quantity of each sample (25 g) was poured through a funnel into a 100 ml tarred graduated cylinder. The cylinder was then lightly tapped twice to collect all the powder sticking on the wall of the cylinder. The volume was then read directly from the cylinder and used to calculate the bulk density. For tap density, the cylinder was tapped from a height of 2.5 cm from the cylinder bottom 50 times on a wooden bench top to attain a constant volume reading from the cylinder.

2.3.2 Particle size and size distribution

Particle size analysis of chitosan powder was conducted by method of laser diffraction using a Malvern® Mastersizer X (Malvern Instruments Ltd., Worcestershire, UK) fitted to a MSX sample suspension unit and a 300 mm lens. Samples were prepared by suspension of 1.5 g chitosan in 15 cm^3 ethanol. The samples were cycled through the apparatus by addition of 300 cm^3 of dispersion liquid. The particle size and particle size distribution was calculated after four repeats.

2.3.3 Tablet compression

Agglomerates were tableted after being dried and sieved through a 1 mm sieve. Reference to compression settings was designated as the upper punch setting. An upper punch setting of 50 (applied load) was utilized. The filling volume of the die was maintained at a constant level by adjustment of the lower punch setting. Flat faced compression tooling was utilized to manufacture tablets that presented a flat surface. The tooling was chosen to produce tablets of approximately 9 mm in diameter. A Cadmach® eccentric press was employed during all tableting procedures. After manufacturing was completed, tablets were stored in sealed glass containers away from light at room temperature for 24 hours preceding the analysis.

2.3.4 Tablet crushing strength, diameter and thickness

Crushing strength, diameter and thickness were determined for 10 tablets of each formulation using a Pharma Test® (model PTB-311) tablet test unit (Pharma Test, Switzerland). Each tablet was mounted on a horizontal steel platform with a ram measuring diameter and thickness. The ram crushed the tablet in order to determine crushing strength. Tablet density was determined by dividing tablet weight by tablet volume.

2.3.5 Weight variation

Twenty tablets of each batch were dusted and weighed on a Precisa® analytical balance (model 240A, OERLIKON AG, Zurich).

Table 2.1: British Pharmacopoeia (2002) limits for tablet weight variation.

Average weight of tablet	Percentage deviation
80 mg or less	10
More than 80 mg and less than 250 mg	7.5
250 mg or more	5

2.3.6 Friability

Ten tablets of each formulation were tested on a Roche® friabilator for a duration of ten minutes at 50 rpm. Equation 2.2 was used to calculate the percentage friability.

$$\%F = 100\frac{w_b - w_a}{w_b} \qquad \text{Equation 2.2}$$

2.3.7 Shape and surface structure of particles

A supplementary method of characterization of the physicochemical properties of powders, agglomerates and tablets is by scanning electron microscopy (SEM) observations. The analysis of the physical powder, agglomerate and tablet properties is often the observation of an assortment of macroscopic occurrence. Electron micrographs deliver information on a micro level that might direct a better understanding of the macroscopic phenomenon e.g. under which circumstances process variables exert their actions. Electron micrographs are included in this study.

2.3.7.1 *Experimental conditions, sample preparation and apparatus for SEM*

Agglomerate and powder samples were positioned on a double-sided conductive carbon tape to a sampling tray and dusted with an inert gas. Samples were consequently sputter-coated with a gold/palladium (80:20) to form a layer of approximately 28 nm on the surface of the samples. An Eiko® ion coater (model IB-2, Eiko Engineering, Japan) was used in all coating procedures and operated under a vacuum superior than 0.06 Torr. Samples were studied using a Philips® XL 30 DX 4i SEM microscope (Eindhoven, The Netherlands).

2.3.8 Sieve analysis

Agglomerates were sieved with a Fritch Analysette, (Type 03.502) sieve apparatus, vibrated for ten minutes. Sieve fractions were determined by weighing the powder residue on each sieve. Sieve with mesh sizes of up to 1 mm were used.

2.3.9 X-ray powder diffraction (XRPD)

XRPD is an effective method to distinguish between different solid phases in different or the same powdered samples. The advantage of using X-ray powder diffraction is that this method does not require large single crystals, but instead can be readily applied to any powdered sample (Brits, 2003:67).

The X-ray powder diffractogram yields information about the diffraction characteristics of the sample. These diffraction characteristics include the intensities of the maxima diffraction peaks and the angles at which they occur. The pattern of scattered radiation that is unique to each crystal structure is called the diffraction pattern. The diffraction pattern could be used to determine the crystal structure.

X-ray powder diffraction patterns were obtained at room temperature using a Bruker D8 Advance diffractometer (Bruker, Germany). Approximately 200 mg p-HCl samples were weighed into aluminium sample holders, taking care not to induce a preferential orientation of crystals. The measurement conditions were: target Cu; voltage 40 kV, current, 30 mA; divergence slit, 2 mm; antiscatter slit, 0.6 mm; monochromator; scanning speed, 2°/min (step size, 0.025°; step time, 1.0 sec.).

The XRPD traces of the powders were compared with regard to peak position and relative intensity, peak shifting and the presence or lack of peaks in certain regions of °2θ values.

2.3.10 Infrared absorption spectroscopy (IR)

IR-spectra were recorded on a Nicolet Nexus 470-FT-IR spectrometer (Nicolet instrumentation corporation, Maddison, USA) over a range of 400 – 4000 cm^{-1} . The diffuse reflectance method was used. KBr was used as background material. The main absorptions in the IR – spectral results of the samples were compared to determine possible significant differences with regard to polymorphic form or polymorphic modifications.

Silverstein *et al.* (1991:91) stated that "A peak-by-peak correlation [of the IR spectra] is excellent evidence for identity. It is unlikely that two compounds, except enantiomers, give exactly the same IR spectrum." Therefore IR-analysis proves to be a suitable method to implement for the characterization of different crystal forms, thus an appropriate procedure to determine whether the spherical agglomeration process interfered with the p-HCl. The IR spectra of polymorphs may differ.

2.4 DISSOLUTION STUDIES

Dissolution testing is an essential requirement for the development, establishment of *in vitro* dissolution and *in vivo* performance, registration and quality control of solid oral dosage forms.

2.4.1 Apparatus and experimental conditions

Dissolution tests were performed in a six station dissolution apparatus. A thermostat regulated the temperature of the medium at 37±.05 °C. Dissolution studies were performed in 900 cm^3 of 0.1 M HCl (pH ~ 1.20) and 900 cm^3 Sörensen buffer (pH ~ 4.5). The standardised USP basket-method was used in all studies and baskets were rotated at a constant speed of 50 rpm.

2.4.2 Method of tablet dissolution

The dissolution vessels were filled with the dissolution medium and heated to a temperature of 37±.05 °C. The rods were pushed down into the vessels with the baskets reaching 25 mm–27 mm from the bottom of the vessel. The dissolution sampling was initiated when the baskets, rotating at a speed of 50 rpm reached the dissolution medium. The timing sequence was started at a starting point of t = 0. Samples of 5 cm^3 were withdrawn at t = 10, 20, 45, 60, 120, 240, 360 minutes. Samples were withdrawn at a constant height and the withdrawn volume was replaced immediately after sampling with new, preheated dissolution medium. A correction was calculated for the cumulative dilution caused by replacement of the sample with an equal volume of original medium. The sampling was performed through a filter unit fitted with 0.3 µm Millipore® prefilter and the samples were transferred to 10 cm^3 glass polytops. The samples were subsequently analysed.

2.4.3 Standard curve

Standard curves were constructed prior to each set of dissolution tests. Standard solutions from both mediums with concentrations ranging from 1 to 100 $\mu g.cm^{-3}$ were prepared from the mother solutions. The initial solution contained 10 mg of p-HCl dissolved in 100 cm^3 of the specified dissolution medium. The UV-absorbencies of the standard solutions were determined

spectrophotometrically at 289 nm against 0.1 M HCl as blank medium. The absorbencies were plotted against concentration and the best straight line through the data points was fitted using linear regression. All standard curves complied with the principles of Beer's law in the concentration range that was utilised and acceptable correlation coefficients were obtained ($r^2 \geq 0.999$). Additional parameters that were derived by regression, the slope (m) and y-intercept (c), were utilised to calculate the p-HCl concentration of the samples.

2.4.4 Computation of dissolution data

The concentration of p-HCl dissolved ($\mu g.cm^{-3}$) at each sampling time was calculated using equation 2.2 and the amount of drug lost during sampling was corrected by using equation 2.4:

$$x = \frac{y^* - c}{1000m} \qquad \text{Equation 2.3}$$

Where:

y^* is the corrected absorbency (from equation 2.5); x is the drug concentration ($\mu g.cm^{-3}$) and m and c are the slope and y-axis intercept respectively obtained from the standard curve.

$$y_n^* = y_n + \frac{V_s}{V_m}\sum^{n-1} y^* \qquad \text{Equation 2.4}$$

Where:

y^*_n is the corrected absorbency of n^{th} sample, y_n is the measured absorbency of n^{th} sample; V_s is the sampling volume; V_m is the dissolution medium volume and Σ^{n-1} y^* is the sum of all the corrected absorbencies prior to the n^{th} sample.

2.4.5 Content of p-HCl in agglomerates

The absorbance of the p-HCl was measured spectrophotometrically against the dissolution medium at 289 nm. The determined content was compared with the theoretical content of the tablets at the end of each dissolution experiment.

2.4.6 Dissolution parameters

2.4.6.1 *DR_i and AUC*

The initial slope of the dissolution curve between t_0 and t_5 was proposed to be a fair approximation of the initial dissolution rate (DR_i) ($\mu g.cm^{-3}.min^{-1}$) of p-HCl from the various tablet formulations. The significance of this parameter is discussed later. The area under the dissolution curve (AUC) was calculated from t_0 up to completion of the dissolution test at 360

minutes and would give an indication of the extent of dissolution of active ingredient during this period. The calculation of the *AUC* (μg.cm.min^{-3}) was made by application of the trapezoidal rule and the value was determined for the whole extent of the dissolution experiments. The trapezoidal rule is described by the equation 2.5:

$$AUC = 0.5 \times \sum_{t=n}^{t=0} (t_n - t_{n-1})(c_n - c_{n-1}) \qquad \text{Equation 2.5}$$

Where:

$(t_n - t_{n-1})$ = the time difference between two consecutive sampling intervals and c_n and c_{n-1} = corresponding concentrations of the tracer at t_n and t_{n-1}.

2.4.6.2 *Similarity equation*

Dissolution curves of the percentage drug dissolved *versus* time were plotted and compared. The similarities between the dissolution curves were calculated, using equation 2.6 described by Moore and Flanner (1996:66):

$$f2 = 50 \bullet \log\left\{\left[1 + \left(\frac{1}{n}\right)\sum_{n=1}^{n} wt(Rt - Tt)^2\right]^{-0.5} \bullet 100\right\} \qquad \text{Equation 2.6}$$

Where:

N	=	Number of dissolution time points.
Rt	=	Reference dissolution value at time t.
Tt	=	Test dissolution value, at time t.
wt	=	Optional weighing factor.

The value of f2 is 100 when the test and reference mean profiles are identical. Values of f2 between 50 and 100 indicate similarity of the two dissolution profiles.

2.5 CALCULATIONS

All calculations were made using Microsoft® Excel TM 2003 for Wndows™ (Microsoft® Corporation, Seattle, Washington, USA).

3. CHAPTER 3

THE PARAMETERS DETERMINING THE SPHERICAL AGGLOMERATION OF CHITOSAN

3.1 INTRODUCTION

Chapter 1 described the spherical agglomeration of a powder substance as a particle design method that comprises several imperative factors to ultimately deliver a product with suitable flow and compactibility properties. Particle flowability and compactibility are two critical process parameters tested when a material is designed for direct compression (Otto, 2002:1). Chitosan lacks both adequate fluidity and compressibility as shown by the experiments conducted in this chapter.

The aims of this chapter were to:

- evaluate chitosan powder and assess manipulated chitosan particle structures that were achieved by means of size enlargement and particle alteration techniques.
- determine the parameters that contribute to the spherical agglomeration of chitosan
- analyze the effects of the factors on agglomerate formation.
- design chitosan into a powder with desired tableting properties, for example, good flow, compressibility and handling properties. The interpretations of the results obtained by these experiments are discussed in this chapter.

3.2 ASSESSMENT OF CHITOSAN POWDER

3.2.1 Visual evaluation

A scanning electron microscope (SEM) photographic image revealed that some chitosan particles contained sharp edges and lacked particle uniformity. The rough surfaces and the fiber like structure of some particles seen in the image of chitosan particles may contribute to its weak fluidity, due to cohesiveness between particles (figure 3.1). The cohesiveness and poor fluidity of chitosan is a problem, and can cause difficulties in material blending and transfer operations.

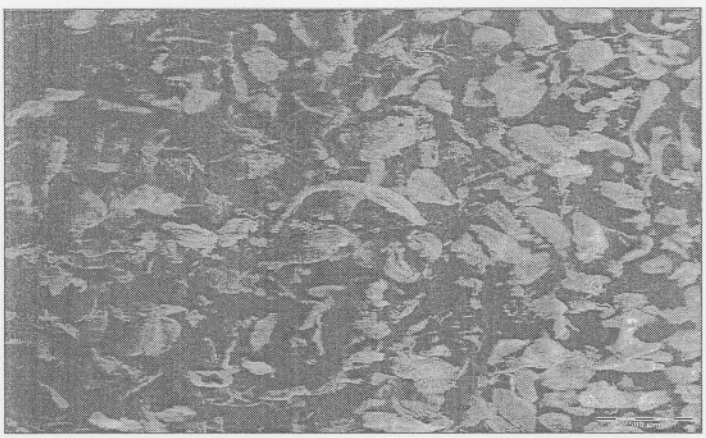

a)

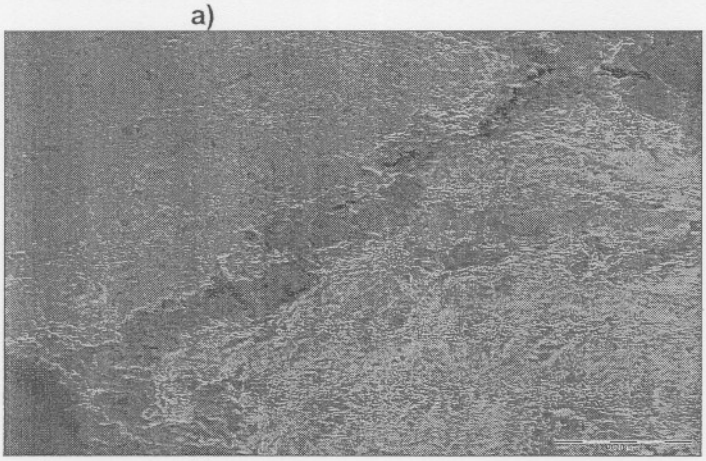

b)

Figure 3.1.

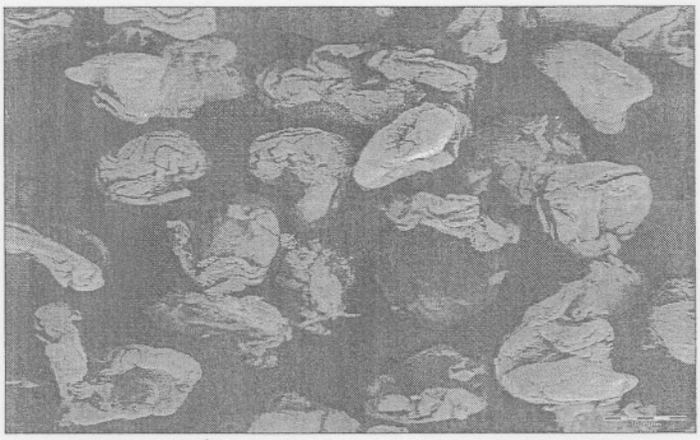

c)

Figure 3.1: SEM micrographs of a) chitosan particles b) ball milled chitosan c) grinded chitosan.

3.2.2 Physical characteristics of chitosan

The particle size, flow properties, particle size distribution, density, the Hausner ratio and Carr index of chitosan were assessed. Table 3.1 summarizes the data obtained from the various experiments conducted using the methods described in section 2.3.

Table 3.1: Physical characteristics of chitosan.

Property	Chitosan
Tapped density ($g.cm^{-3}$)	0.231
Untapped bulk density ($g.cm^{-3}$)	0.18
Hausner ratio	1.30
Carr's index	23.5
Mean particle size (µm)	208.9
Angle of repose (°)	23.2

Chitosan lacks the density most other commercial pharmaceutical excipients comprise. Emcompress®, a popular tablet filler for instance, has a bulk density of 0.402 $g.cm^{-3}$, and a tapped density of 0.985 $g.cm^{-3}$, which are more than double the values obtained for chitosan. The Carr's index and Hausner ratio preview the degree of densification which could occur during tabletting. Theoretically, if chitosan could be compressed, large amounts of chitosan have to fill a tablet die to ultimately produce a relatively small tablet. A denser powder shape of chitosan would be less bulky and would produce a relatively large tablet for the amount of chitosan filling a tablet die.

Evaluating sieve fractions is a simple process to determine powder particle size distribution. Chitosan powder (500 g) was sieved and photographed. Inspection of the SEM images showed that fine chitosan particles, together with larger, thinner particles were retrieved. The larger, thinner particles that were collected made it impossible to isolate smaller and rounded shaped particles to conduct a flow experiment to determine whether smaller particles could result in improved flow.

The particle size analysis was evaluated in accordance with section 2.3.2. The particle size of chitosan supplied varied dimensions to a large extent (annexure A1) and the bulk of chitosan particles presented a particle size of 208.9 µm. The extensive size distribution is disadvantageous regarding mixing and circumvention of segregation.

Another disturbing characteristic of chitosan, observed as a result of handling the powder, is that the powder distributes a lot of dust, thus resulting in large amounts of powder loss. Powder losses were observed in processes of weighing and tableting, both frustrating and redundant properties of chitosan powder. The lack of the dust freeness of chitosan is undesirable and would bear economical disadvantages.

3.3 EFFORTS TO ENHANCE THE MICROMETRIC PROPERTIES OF CHITOSAN

Although the chemical altering of a substance could produce a renewed substance with attractive micrometric properties, the initial compound structure of the substance is distorted. Ball milling and liquid nitrogen freezing were conducted during this study in an attempt to physically alter the size and shape of chitosan powder as an alternative to a chemical approach, to produce a free flowing, dust free and compressible excipient.

3.3.1 Ball milling

One liter of a 5% w/v chitosan suspension in water was poured into a ball mill. The suspension was milled for 24 hours after which the chitosan powder was collected, dried for 24 hours, and investigated. SEM images revealed that chitosan rolled up in wet laundry like fibers instead of being crushed into smaller pieces (figure 3.1b). The powder discolored and possessed weak flow properties. After an additional 24 hours the chitosan particles deformed into its original shape again. Thus, ball milling failed as a method to modify the microscopic shape of chitosan particles to enhance its micrometric properties.

3.3.2 Liquid nitrogen freezing

Liquid nitrogen was poured into a bowl over chitosan powder in an effort to freeze chitosan particles and crush the particles into smaller pieces. The powder was frozen after which crushing of the powder took place. This procedure failed to alter the shape of chitosan particles and was similar to what was experienced during the ball milling experiment, which was probably due to the elastic nature of chitosan. The deformed chitosan twisted into its original shape eventually.

3.3.3 Grinding

Grinded chitosan rolled up initially, but deformed into its original shape after a few days.

3.3.4 Wet granulation of chitosan

A 3 gram mixture of chitosan (70% w/w) and polyvinylpyrrolidone (30% w/w) was mixed in a Turbula® mixer for 10 minutes to ensure proper mixing. The effort was made to produce a directly compressible chitosan powder after a wet granulation step, and to compare the wet granulation process with the spherical agglomeration process utilizing the same conditions and substances where possible. Ethyl acetate was used as wetting agent. The wet granulation process was much more time consuming than spherical agglomeration process and failed with the specified conditions and quantities of resources. The wet granulation process was incomparable and inferior to the spherical agglomeration process.

It can be concluded that little can be done to physically alter and enhance the micrometric properties of chitosan in an economical method. A final approach to enlarge chitosan particles with a simple and inexpensive technique was through the process of spherical agglomeration.

3.4 FACTORIAL DESIGN OF THE PARAMETERS CONTRIBUTING TO THE SPHERICAL AGGLOMERATION OF CHITOSAN

At times, it is not feasible or desirable to include all possible combinations of factor levels for the different factors. A fractional factorial design was devised to study the effects of all the different factors in various combinations. Suppose a pharmaceutical company wished to study six different powder mixtures, five levels of binder content, and four compressing settings on a tablet press. A complete factorial study would then involve 6 x 5 x 4 = 120 experiments. Such a study might be extremely costly and time consuming.

Under these conditions, it may be possible to design a fractional factorial study containing only a fraction of the 120 factor level combinations, which will still provide information about the main effects of each of the three factors as well as about any important interactions of these factors.

The optimization tables contain the averages of values obtained for experiments involving the factor.

3.4.1 Fractional factorial design as employed in the study

Informed trial and error experimentation is used in product development, often utilizing experience obtained with similar materials and equipment. This may involve adjusting the particle size distribution of the solids, changing binder properties and selection of granulation conditions. Thus, the selection of suitable processing conditions can be time consuming. Frustratingly also, granulation processes remain difficult to control (Knight, 2004:156).

For this study, as a result of the exploratory nature of the experiment and the large amount of factors contributing to spherical agglomerate formation, factorial design was used to determine optimum conditions.

Spherical agglomeration took place according to the protocols described in section 2.2.

Table 3.2: Factors and level designation.

Factor	Designation	Level	
		0	1
Kollidon®	**A**	K25	K30
Kollidon (% w/w)	**B**	20% w/w	40% w/w
Agitation speed	**C**	400 rpm	1600 rpm
Agglomeration time	**D**	10 minutes	20 minutes
Bridging liquid volume	**E**	3 ml	7 ml

During a preliminary trial and error study it was determined that notable agglomerate recovery took place only within certain parameter limits. Five predominant factors on two extreme levels were investigated initially after which a carefully selected subsection/fraction was further investigated. A total of 32 formulations could be evaluated, however, the fractional design

necessitated the evaluation of only half of these combinations to determine the effect of each factor on agglomerate recovery.

Table 3.3: The factorial design employed to evaluate system variables and levels.

		A_0				A_1			
		B_0		B_1		B_0		B_1	
		C_0	C_1	C_0	C_1	C_0	C_1	C_0	C_1
D_0	E_0		X	X			X	X	
	E_1	X			X	X			X
D_1	E_0	X			X	X			X
	E_1		X	X			X	X	

3.4.2 Agglomerate recovery

The agglomerate recovery for each experiment was calculated according to the procedures described in section 2.2.4. The data obtained are summarized in the factorial design table 3.4.

3.4.3 Interpretation of the results obtained from the factorial design

The agglomerate recoveries for each of the experimental runs are displayed in table 3.4. Some experiments totally failed and delivered no agglomerates or unacceptable products.

Table 3.4: Factorial design.

		A_0				A_1			
		B_0		B_1		B_0		B_1	
		C_0	C_1	C_0	C_1	C_0	C_1	C_0	C_1
D_0	E_0		N/d	35.30%			N/d	29.50%	
	E_1	N/d			N/d	N/d			N/d
D_1	E_0	4.83%			1.35%	2.56%			0.06%
	E_1		N/d	N/d			N/d	N/d	

(N/d = No data obtained due to failed experiment)

The optimization table indicates the factors with the greatest effect on agglomerate formation and is displayed in table 3.5.

Table 3.5: Optimization table. (Highlighted values indicate the superior level of the agglomerate recovery).

$Factor_{level}$	Agglomerate recovery (%)
A_0	**5.19**
A_1	4.05
B_0	0.09
B_1	**8.28**
C_0	**9.02**
C_1	0.02
D_0	**8.11**
D_1	1.10
E_0	**9.24**
E_1	N/d

N/d = No data

It is worth mentioning that agglomerate formation is influenced by particle size. It was however extremely difficult to obtain various sieve fractions of chitosan due to its irregular size and shape distribution. Longer and thinner particles of approximately 350 µm, however only 20 µm in diameter were retrieved in the same sieve fraction as small 20 µm by 20 µm sized particles. No experiments to determine the effect of different particle sizes of chitosan on agglomerate formation were thus conducted.

The following factors in table 3.6 were identified as the optimum conditions, as they averaged the highest agglomerate percentages.

Table 3.6: Table of optimum conditions.

$Factor_{level}$	Factor	**Optimum condition**
A_0	Kollidon®	Kollidon® K25
B_1	Kollidon (% w/w)	40% w/w
C_0	Agitation speed	400 rpm
D_0	Agglomeration time	10 minutes
E_0	Bridging liquid volume	3 ml

3.4.4 Fractional factorial design

A fraction of the factorial design was further investigated if an experiment had a significant agglomerate recovery. The fraction was then redesigned into an additional factorial design, focusing in on the high agglomerate recovery factors and levels. For example, if a parameter and a specific level had a significant contribution towards agglomerate formation, the follow up fractional design contained the factor with two levels closer to the noteworthy level magnitude.

3.4.5 Results of the fractional factorial design

The factor and level notation of the fractional factorial design is displayed in table 3.7. Chitosan and Kollidon® were mixed in a 7:3 ratio as 6:4 and 8:2 ratios were considered not optimum. Scanning electron microscopy (SEM) images revealed entirely coated, individually shaped agglomerates which were easily removed and non sticky. The non stickiness could be attributed to the lesser amount of binder used in the mixture formulation, preventing adhesiveness between agglomerates and agglomerates and the beaker. Agglomerate formation was complete and no loose particles were present. The subsection selected from the previous factorial design table was based on the fact that chitosan and Kollidon® mixed in a 6:4 ratio had more binder than necessary to produce agglomerates of desirable size and shape, hence the tackiness of the product. All eight fractional experimental runs produced higher agglomerate recovery values, possibly as a result of the combination of optimal conditions.

Table 3.7: Factor and level notation of the fractional factorial design.

Factor	Designation	Level	
		0	1
Kollidon®	**A**		
Kollidon® (30% w/w)	**B**	K25	K30
Agitation speed	**C**	400 rpm	800 rpm
Agglomeration time	**D**	10 minutes	15 minutes
Bridging liquid volume	**E**	3 ml	5 ml

Table 3.8 displays the fractional factorial design.

Table 3.8: Fractional factorial design.

		B_0		B_1	
		C_0	C_1	C_0	C_1
D_0	E_0		X	X	
	E_1	X			X
D_1	E_0	X			X
	E_1		X	X	

The agglomerate recoveries for each of the experimental runs of the fractional factorial design are displayed in table 3.9.

Table 3.9: Agglomerate recoveries of the fractional factorial design.

		B_0		B_1	
		C_0	C_1	C_0	C_1
D_0	E_0		1.75%	29.20%	
	E_1	66.30%			2.10%
D_1	E_0	31.50%			1.80%
	E_1		1.88%	51.20%	

The optimization table indicates the factors from the fractional factorial design with the greatest effect on agglomerate formation and is displayed in table 3.10.

Table 3.10: Optimization table of the fractional factorial design.

Factor	Agglomerate recovery (%)
A_0	-
A_1	-
B_0	**25.61**
B_1	21.08
C_0	**44.55**
C_1	1.88
D_0	**24.84**
D_1	21.60
E_0	16.06
E_1	**30.37**

3.4.6 The effect of binder concentration on agglomerate formation

Results from the factorial design showed the importance of a binder and that the correct amount of binder is critical. Chitosan and Kollidon® were mixed in the ratios of 6:4 and 8:2. SEM micrographs showed that the 8:2 mixture ratios produced weak, brittle agglomerates and table 3.5 displayed low agglomerate recovery for 8:2 mixtures (B_1>B_0). The binder concentration was probably not sufficient enough to bind the particles together and SEM images revealed weak, irregular agglomerates with parts uncoated by the Kollidon®. Neither a change in stirring speed nor a different bridging liquid volume could contribute to notable agglomerate formation. A slight increase in the volume of bridging liquid added to the system contributed to an increase in agglomerate formation, producing an agglomerate recovery of 4.83% and 2.58% respectively for Kollidon® K25 and Kollidon® K30. A chitosan and Kollidon mixture in the ratio of 6:4 produced hard, entirely coated agglomerates. Agglomerate recovery was high, delivering values of 35.3% and 29.5% respectively for Kollidon® K25 and Kollidon® K30.

3.4.7 The effect of agitation speed

Initially, at an agitation speed of 1600 rpm (C_1), agglomerates seemed unable to form across the range of the factorial design, regardless of the change in binder concentration and bridging liquid volume (C_0>C_1). The agglomerates that did form were small, irregularly shaped (resembling the original powder) and sticky, thus unacceptable. Agglomerate recovery for the experiments conducted with 1600 rpm was minimal (1.35% and 0.06% respectively for the

Kollidon® K25 and Kollidon® K30) compared to the slower agitation speeds of 400 rpm and 800 rpm. The turbulence created in the beaker by the blades could be considered as one of the main factors influencing the formation of spherical particles. Higher agitation speeds delivered smaller, more irregular shaped particles than agglomerates formed under lower agitation speeds. The small, irregular size of these agglomerates could be the result of partial comminution caused by the collisions of the agglomerates with the cell walls, the blades and with each other (Sönmez and Cebecci, 2003:225).

3.4.8 The effect of agglomeration time

SEM images revealed that the experiments with agglomeration times of 20 minutes produced slightly more rounded and smooth shaped agglomerates than the experiments exposed to an agglomeration time of 10 minutes (D_0>D_1 for both the factorial design runs). However, the experiment with an agglomeration time of 10 minutes containing Kollidon® K25 had a higher agglomerate recovery of 66.3% compared to the 51.2% agglomerate recovery obtained from the experiment done for 20 minutes with Kollidon® K30. These two experiments differed only in agglomeration time and type of binder. Kollidon® K25 produced superlative results throughout the entire experimental runs. The more spherical particles may however be contributed to the agglomeration time.

3.4.9 The effect of the bridging liquid volume

Bridging liquid volume showed to be in excess in volumes of 7 ml (7 ml/3 g) and more for the system (E_0>E_1). It was observed that greater agglomerate recovery was achieved. However, undesirable gel-like, large and unsuitable particles for direct compression formed. During a study conducted previously, the powder migrated towards the bridging liquid and dissolved completely at very high volumes of bridging liquid, forming pasty slumps. At extremely low amounts of bridging liquid (<2.5 ml/3 g powder), agglomeration recovery was low, possibly due to the insufficient wetting of the particles in the system.

Volumes of 3 ml/3 g supplied more acceptable particles, though low agglomerate recovery. The particles were smaller and free flowing, although being slightly uncovered by PVP and still inadequately agglomerated. The statements mentioned above are in good agreement with the results given in literature (Sönmez & Cebecci, 2003:225). The bridging liquid probably failed to form additional bridges to enhance agglomerate strength.

3.4.10 Scanning electron micrographs

Agglomerates were investigated in accordance with procedures described in section 2.3.7.1. The images presented in figure 3.3 portrayed some agglomerates obtained from the various experimental runs and identified the contributive factors to specific obtained particle shapes.

3.4.11 Spherically agglomerated chitosan sieve analysis

A sieve analysis of the agglomerated chitosan showed a relatively narrow distribution of sizes amongst the particles. The particle size distribution may be primarily a function of the hydrodynamics of the system. The smaller agglomerates may have been formed near the area in the system most subjected to turbulence, in contrast with the larger agglomerates which may have been formed near the surface or the bottom possibly least effected by the turbulence of the blades.

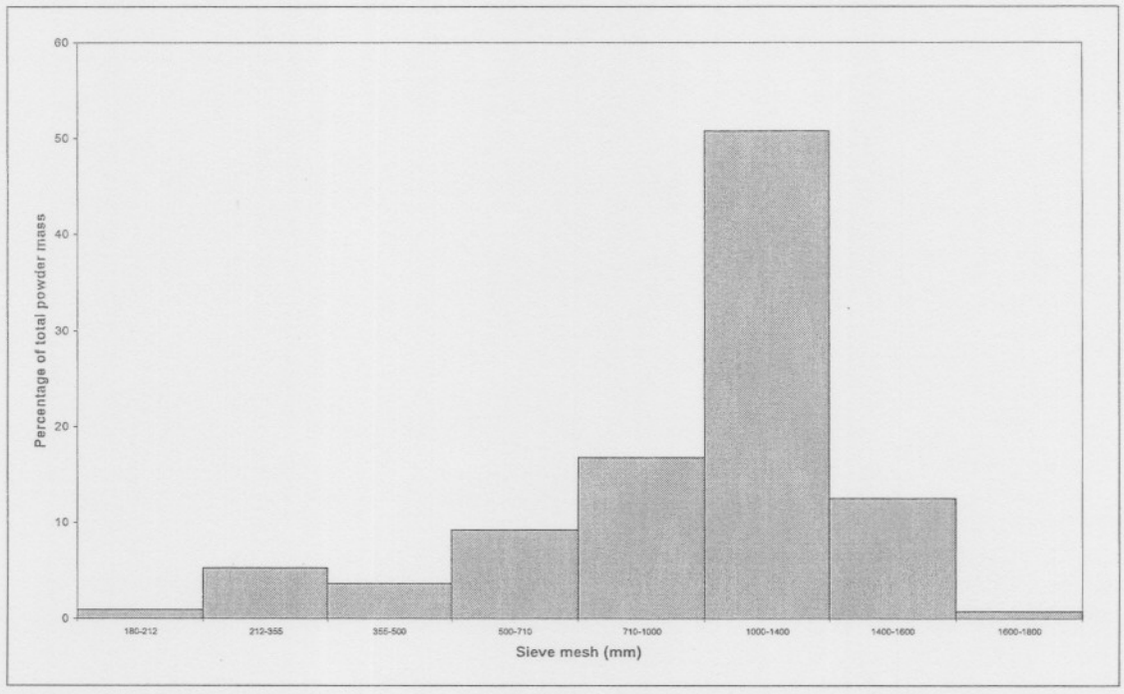

Figure 3.2: Sieve fractions from the sieve analysis of chitosan agglomerates.

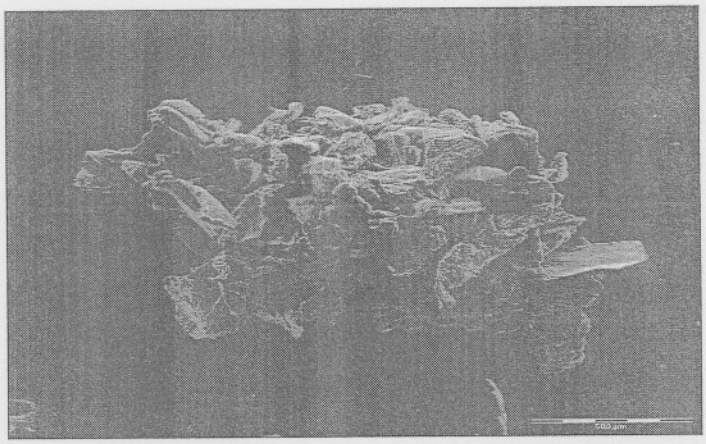

a)

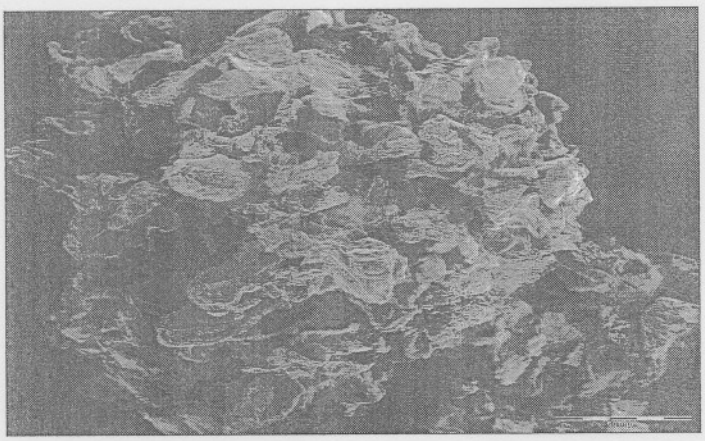

b)

c)

Figure 3.3.

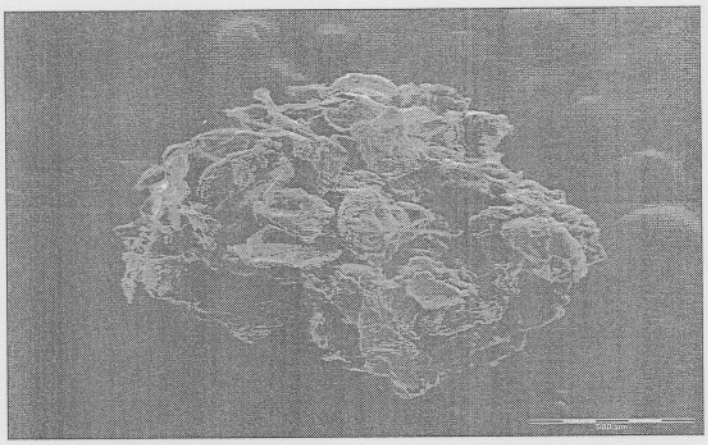

d)

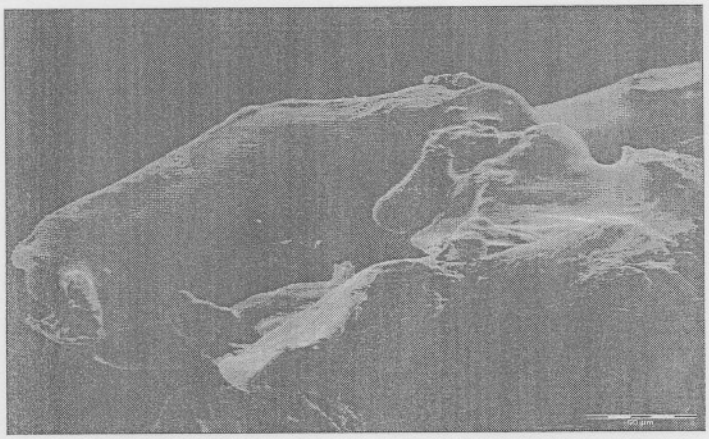

e)

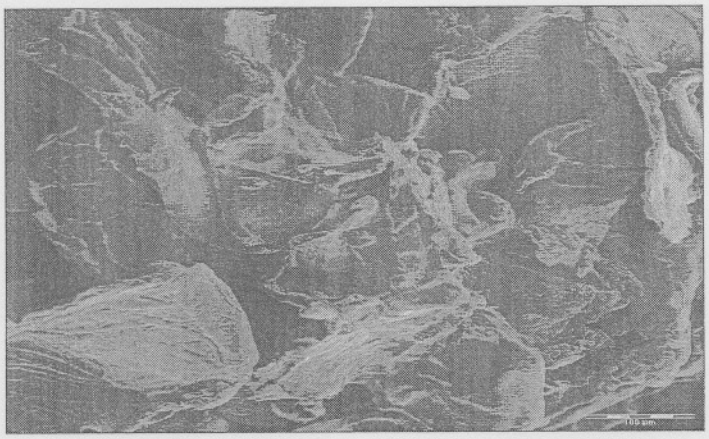

f)

Figure 3.3.

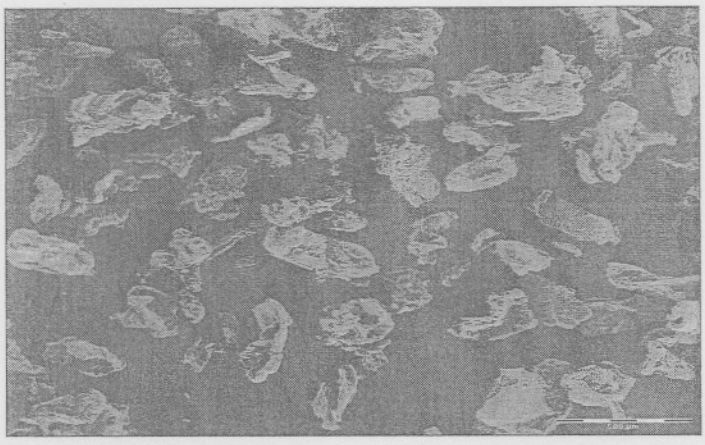

Figure 3.3: SEM micrographs of spherical agglomerated chitosan under various conditions: a) $A_1B_0C_0D_0E_0$ b) $A_0B_0C_0D_1E_0$ c) $B_0C_1D_0E_0$ d) $B_0C_0D_0E_1$ e) Kollidon® coated chitosan particle f) uncoated chitosan particle g) $B_0C_1D_0E_0$.

3.4.12 Summary

A factorial design was devised to study the effects of all the different factors in various combinations. Interactions between factors and factor levels determined the superior conditions for the spherical agglomeration of chitosan. The optimum parameters (table 3.11) were established and the effects of parameters and factorial interactions producing inferior agglomerates were stated.

Table 3.11: Optimum conditions contributing to the most desirable spherically agglomerated chitosan powder.

Condition	Factor level
Agitation speed	400 rpm
Agglomeration time	15 minutes
Bridging liquid volume	3 ml
Bridging liquid concentration	5% v/v
Binder	Kollidon® K25
Binder concentration	30% w/w

3.5 A STUDY ON THE SPHERICAL AGGLOMERATION OF CHITOSAN

In contrast with the parametrical analysis on a factorial design basis of section 3.4, this phase of chapter 3 deals with an advanced investigation of the optimum factors and levels observed

previously. For this purpose, effects of operating parameters were investigated utilizing one variable at a time of the optimum conditions.

In the experiments, effects of operating parameters such as; pH, stirring speed, amount of polyvinylpyrrolidone as a collector, and acetic as a bridging liquid, suspension and agglomeration time were investigated to define the effects of the optimum conditions.

3.5.1 Agitation speed

As seen in figure 3.4, agglomeration recovery reached a maximum at a stirring speed of 400 rpm and agglomerate recovery decreased remarkably at speeds of 800 rpm. Unfortunately the stirrer was unable to produce speeds slower than 400 rpm. Agglomerates almost ceased to form at speeds up to 2000 rpm. At the higher stirring speeds (800+ rpm), undersize amount increased and the agglomeration recovery decreased because of the partial comminution of the agglomerates caused by the collisions of the agglomerates with cell walls and with each other. There is also another factor to consider, and that is presence or lack thereof of microscopic gas bubbles which participate in the agglomeration mechanism. The decreasing recovery at high stirring speeds can be based on more gas entrained and the production of more micro bubbles, which results in less particle agglomeration in a given agglomeration time. Since particle–particle collision energy and collision speed increased with increasing the stirring speed, agglomerates having much more tight structures formed. Therefore, agglomerate size and agglomeration recovery increased.

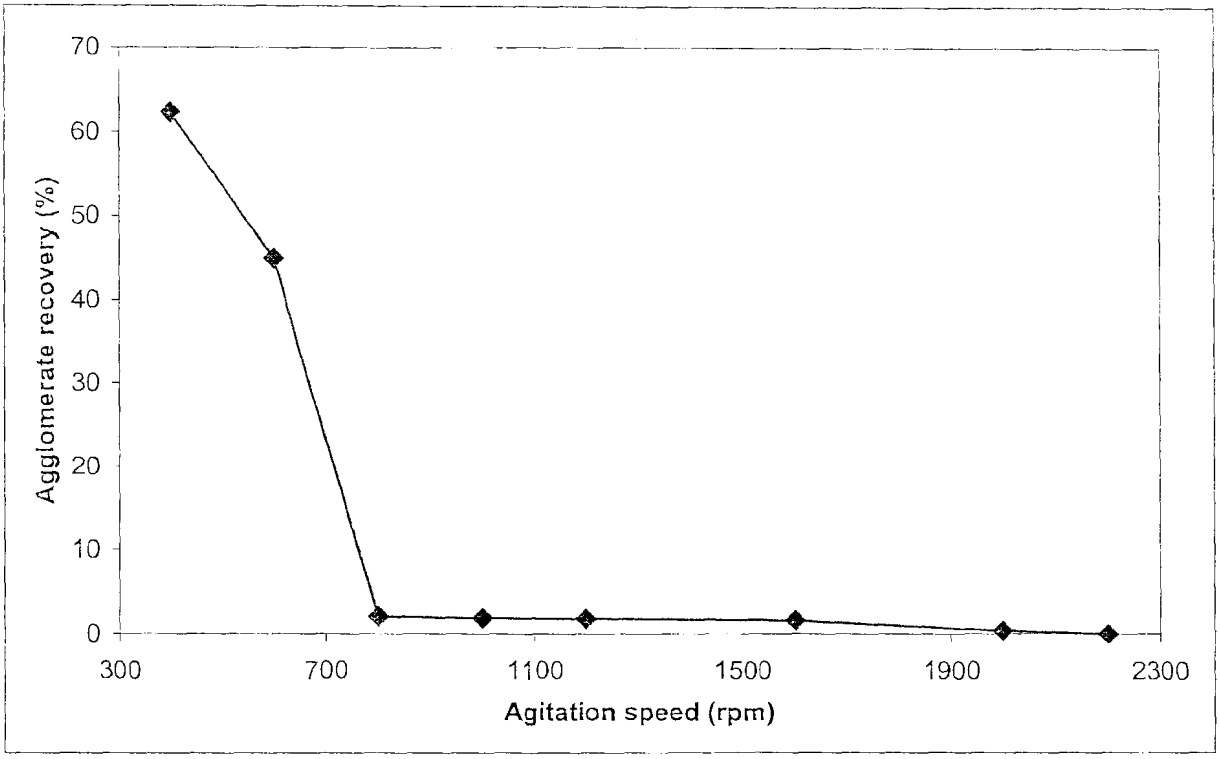

Figure 3.4: A plot of agitation speed against agglomerate recovery.

3.5.2 Agglomeration time

The effect of agglomeration time on the agglomeration recovery is shown in figure 3.5. As it can be seen in figure 3.5, the agglomeration recovery reached its maximum value (66.30 %) at 300 seconds agglomeration time. At very low agglomeration time, the agglomeration recovery was low due to both the insufficient dispersion of bridging liquid in the suspension and insufficient contact between particles. Increasing the agglomeration time resulted in the formation of more compact agglomerates due to an increase in the particle–particle, particle–microagglomerate or microagglomerate–microagglomerate contact. Therefore, the strength of the agglomerates against mechanical forces and the agglomeration recovery increased. The agglomeration recovery did not change at very high agglomeration time because of the formation of very compact agglomerates. However, agglomerates agglomerated for longer were more spherically shaped.

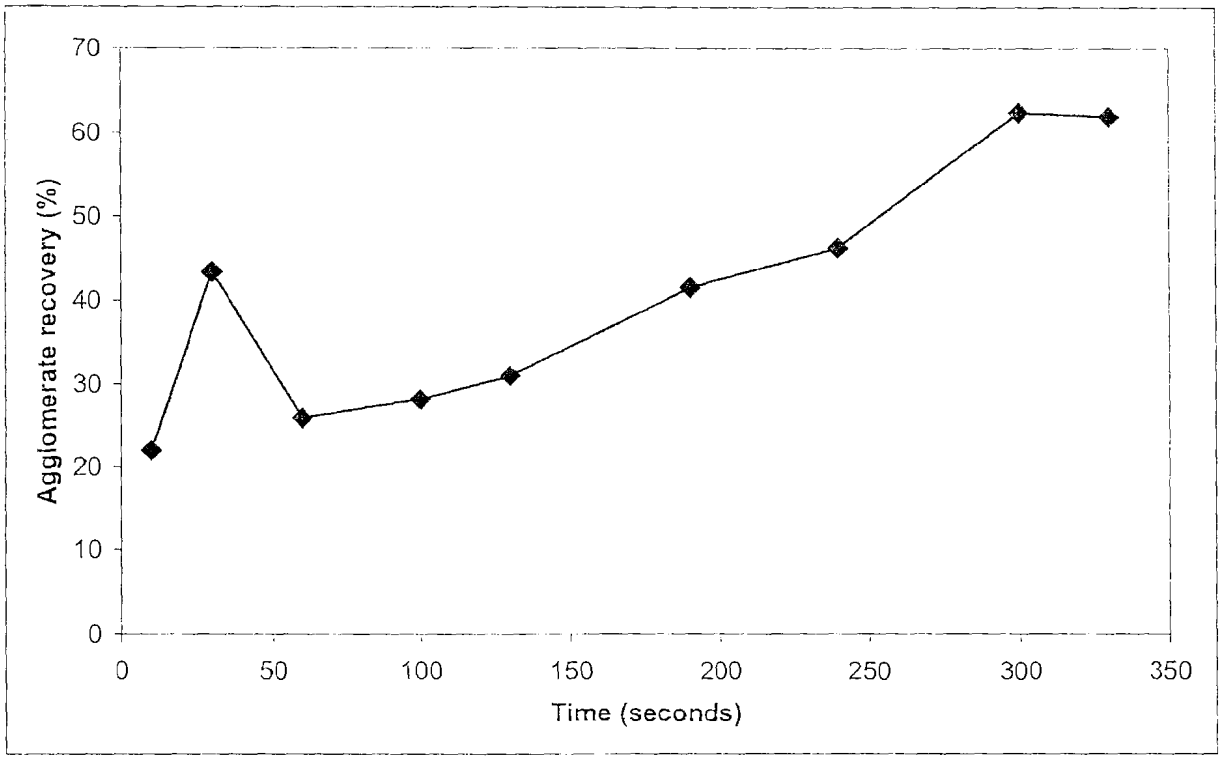

Figure 3.5: A plot of agglomerate recovery versus agglomeration time.

3.5.3 Bridging liquid concentration

It was observed that although agglomerate recovery increased if the bridging liquid concentration increased, the agglomerates were large and had gel-like properties. The gel formation may be a result of the solubilizing (in slight acidic media) properties of chitosan at higher acetic acid concentrations. The surface of the particles in lesser concentrations of the bridging liquid was wetted and solubilized slightly, contributing to minute interparticle bridge formation. It may be possible to form chitosan agglomerates with lesser amount of binder as a result of this.

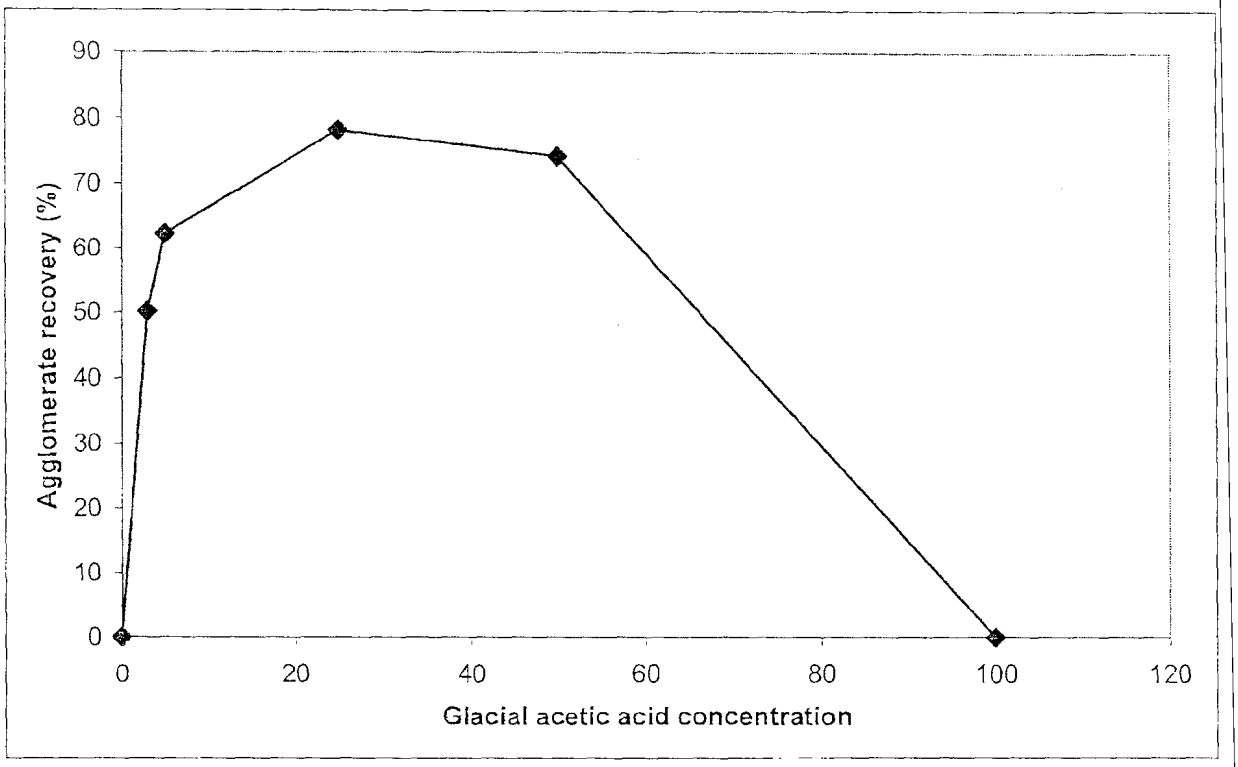

Figure 3.6: A plot of agglomerate recovery against acetic acid concentration.

3.5.4 Bridging liquid volume

As shown in figure 3.7, the agglomeration recovery increased up to 10 ml/3 g of bridging liquid. It did not change reasonably for volumes above 10 ml per 3 g powder. At low amount of bridging liquid, agglomeration recovery was low due to the insufficient wetting of the powder mixture particles by the 5% acetic acid concentration. In this case, most of the voids between particles were filled with aqueous medium. As the amount of the bridging liquid was increased, the voids between particles filled with aqueous medium were coated with an increasing amount of 5% acetic acid solution. Consequently, compact and spherical agglomerates were formed. In the higher amount of acetic acid (>10 ml/3 g), powder particles were dispersed in the bridging liquid and the spherical shape of agglomerates turned into pasty lumps and the agglomerates deviated from spherical shape.

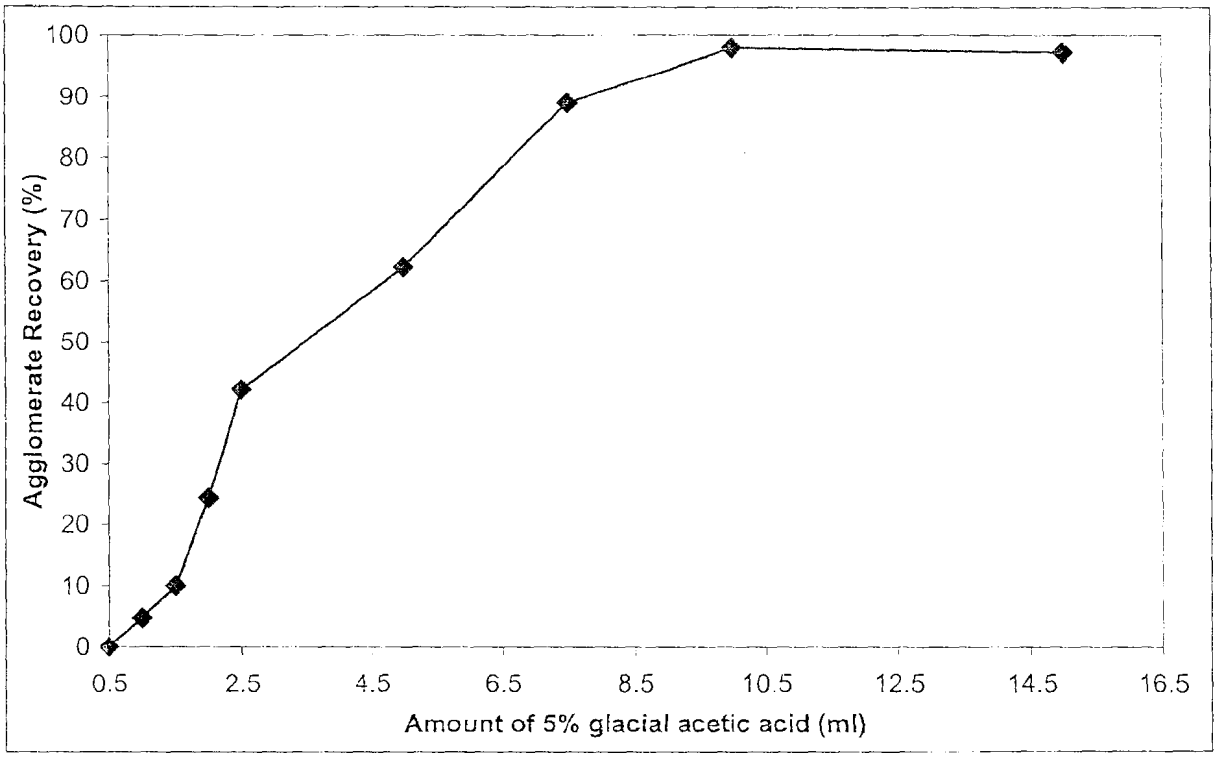

Figure 3.7: A plot of agglomerate recovery versus bridging liquid volume.

3.5.5 Summary

The recovery of chitosan agglomerates was investigated by using spherical agglomeration. For this purpose, effects of operating parameters were investigated. Informed trial and error experimentation were used in the development of a desirable shaped chitosan particle. In the experiments, effects of operating parameters such as; pH, stirring speed, amount of polyvinylpyrrolidone as a collector, and acetic as a bridging liquid, suspension and agglomeration time were investigated to obtain optimum conditions. Graphs indicated that no trends were present and that it could be suggested that agglomerate recovery was the result of the interaction of certain factors and factor levels.

3.6 CONCLUSION

Chitosan lacked the micrometric properties a pharmaceutical excipient intended for direct compression had to comprise prior to spherical agglomeration.

The spherical agglomeration method, as an alternative technique for size enlarging particle design, produced spherical chitosan agglomerates which were able to be directly compressed

unlike dry chitosan powder. Chitosan powder failed to be compressed into 9 mm diameter tablets with the use of a Cadmach® eccentric press at a maximum upper punch setting of 50. However, it was experienced that chitosan and Kollidon® K30, mixed in the ratio 7 : 3, produced tablets with a hardness of greater than 100 Newton, but with no improvement in the flow of the powder mixture, which resulted in tablets varying in mass too much. Only the agglomerates had free flowing properties in contrast with the chitosan and Kollidon® mixture (the addition of binder had no effect on the shape of the chitosan particles), and the produced particles were totally dust free.

The technique for the production of a directly compressible chitosan powder was developed and its parameters were evaluated. Chapter 4 deals with the applicability of spherically agglomerated, directly compressible form of chitosan, with the incorporation of a tracer drug.

4. CHAPTER 4

THE APPLICABILITY OF SPHERICALLY AGGLOMERATED CHITOSAN FORMULATIONS

4.1 INTRODUCTION

The previous chapter determined, by means of a parametrical analysis, the mechanisms and factors that provided spherically agglomerated chitosan particles with enhanced micrometric properties. The products resulting from the spherical agglomeration size enlargement technique could be predicted to some extent and, in the event of future experiments be controlled. The process utilized uncomplicated equipment compared to other size enlargement techniques, altering chitosan powder into a dust free, compressible and free flowing powder.

This chapter aims to:

- establish whether chitosan and a tracer drug, agglomerated spherically as an alternative technique to wet granulation, can be produced in fewer steps, and in tablet form. (Prolonged release p-HCl is commercially available in capsule form). The dissolution behaviour of the tracer should reveal properties imparted to the formulations by chitosan, as well as the properties imparted by the manner in which the formulation powder was formed.
- evaluate the applicability of spherically agglomerated chitosan in prolonged release and directly compressed p-HCl tablet formulations.
- determine an optimum formulation with the most similar dissolution profile compared to Inderal® LA 80 mg.

4.2 PHYSICAL EVALUATION OF POWDER MIXTURES, AGGLOMERATES AND TABLETS

Propranolol hydrochloride (P-HCl) was chosen to act as a tracer drug based on the fact that the drug has theoretically the solubility properties to be spherically agglomerated in conjunction with chitosan and Kollidon® K25. It was concluded during a trial study, based on a factorial design (similar to section 3.4) that p-HCl colored with BASF powder dye adhered to the chitosan agglomerates during agglomeration, indicating a possibility that p-HCl could be integrated in the agglomerates. All the formulations were weighed and mixed in a Turbula® mixer for 5 minutes at 69 revolutions per minute prior to the powder assessments tests to ensure a proper distribution of powder particles.

Various formulations were agglomerated and provided agglomerates with similar physical features. Three different mixture formulations (table 4.1) were agglomerated in accordance with the protocols described in section 2.2.

Table 4.1: Formulations.

	Chitosan (% w/w)	P-HCl (% w/w)	Kollidon®K25(%w/w)
Formula 1	39	39	22
Formula 2	36	36	28
Formula 3	33.3	33.3	33.3

The optimum conditions and factor levels obtained from the previous chapter, together with a factorial designed trial study on the factors contributing to the agglomeration of a chitosan and p-HCl mixture, motivated the formulation of the mixtures utilized in this chapter. The conditions are summarized in table 4.2.

Table 4.2: Conditions and factor levels employed for spherical agglomeration experiments.

Condition	Factor level
Agitation speed	400 rpm
Bridging liquid volume	3 ml
Bridging liquid concentration	5% v/v
Binder / Coating agent	Kollidon® K25
Suspension concentration	3 g/100 cm^3

The experimental design is given in table 4.3.

Table 4.3: Experimental design.

	Time (minutes)		
	10	15	20
Formula 1	X	X	X
Formula 2	X	X	X
Formula 3	X	X	X

4.2.1 Assessment of powder properties

Powder properties were assessed to determine the micrometric differences between the powders prior to and after spherical agglomeration. Table 4.4 summarizes the data obtained from the powder evaluations. (N/d = no data.)

Table 4.4: Powder properties.

Property	Chitosan	P-HCl	SAC	Formula 1*	$SA_{Formula\ 1}$
Tapped density ($g.cm^{-3}$)	0.231	0.501	0.233	0.429	0.444
Untapped bulk density ($g.cm^{-3}$)	0.177	0.429	0.170	0.330	0.340
Hausner ratio	1.307	1.167	1.367	1.300	1.306
Carr index	23.506	14.286	26.852	23.077	23.423
Mean particle size (µm)	208.9	N/d	N/d	N/d	N/d
Angle of repose (°)	23.2	29.6	2.5	21.955	1.92

*N/d = No data. SAC = spherically agglomerated chitosan.*See Table 4.1*

4.2.1.1 *Tapped and untapped bulk density*

The rank order for untapped and tapped bulk density was as follows: p-HCl > formulation 1 > spherically agglomerated chitosan > chitosan. P-HCl is a dense powder, and contributed to the denseness of the spherically agglomerated formulations.

4.2.1.2 *Hausner ratio and Carr's index*

Carr's index and the Hausner ratio previewed the degree of densification which could occur during tabletting. P-HCl displayed the smallest Carr's index of 14.29, a value which is favorable for compressible powders. Theoretically, if p-HCl could be compressed, a relatively large tablet could be compressed for the amount of p-HCl that could fill a tablet die. Carr's indices of the various mixtures and agglomerated powders provided in table 4.4 did not differ except for the fact that only the spherically agglomerated powders could be compressed.

4.2.1.3 *Angle of repose*

An angle of repose test was conducted to measure the differences in powder flow prior to and after agglomeration. The reproducible flow properties obtained from spherically agglomerated powders suggested that the cavity would be filled consistently during each compression cycle, resulting in tablets of uniform weight. The agglomerated formulations had superior flow compared to the fluidity of the formulations not subjected to spherical agglomeration. The angle of repose (figur 4.1) indicated a much smaller angle for the agglomerates containing 33,3%, 36,0% and 39,0% p-HCl (Formula 1,2 and 3) than for the same formulations prior to agglomeration. Compared to the average angle of repose for the dry powders, an improvement of 91.9% in angle reduction was observed, indicating a remarkable improvement in fluidity. The rank order for the angle of repose was as follows: spherically agglomerated powder <<<< powder prior to spherical agglomeration. The angle of repose profiles for chitosan, p-HCl, a mixture and spherical agglomerates of chitosan and p-HCl are presented in figure 4.1.

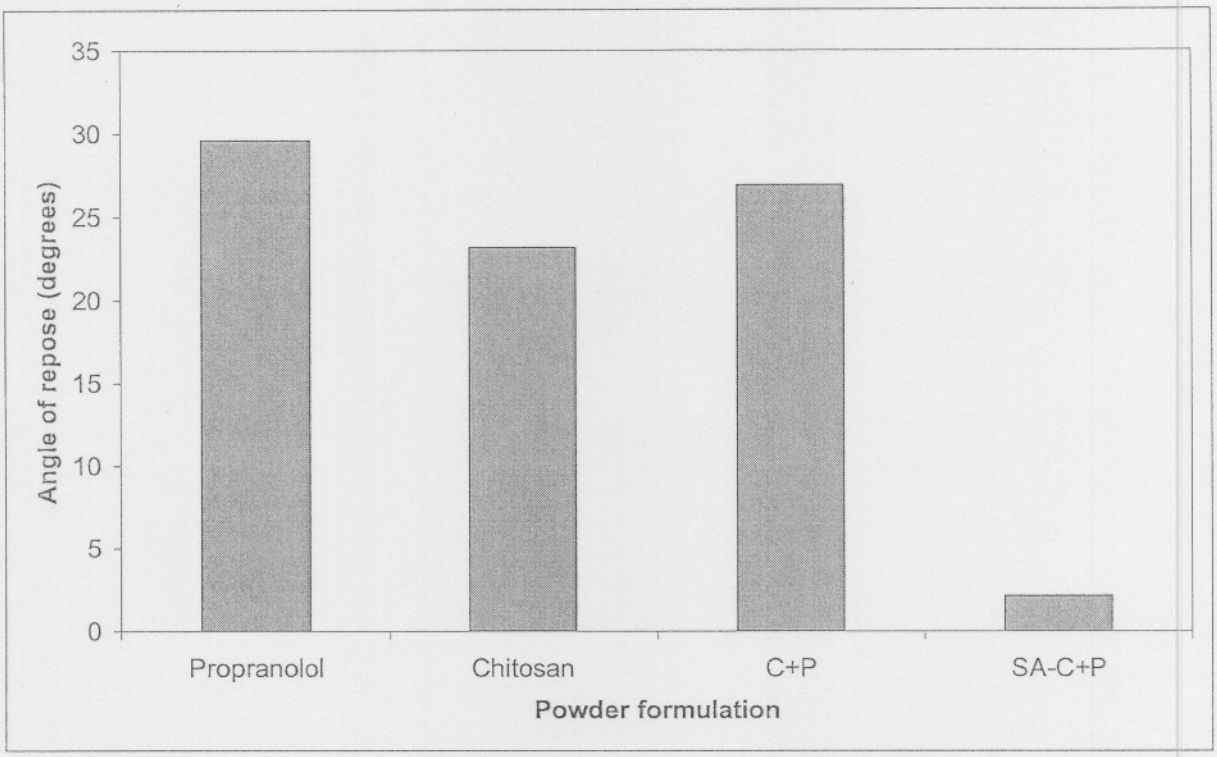

Figure 4.1: The angle of repose profiles for chitosan, p-HCl, a mixture and spherical agglomerates of chitosan and p-HCl. The average angle of repose profiles for the three different powder formulas and nine different agglomerated formulas are displayed. C=chitosan, P= P-HCl, SA=spherically agglomerated.

4.2.1.4 *Visual assessment*

The SEM micrographs indicated that it was possible to incorporate p-HCl in the agglomerates. Figure 4.2 (c) revealed the manner in which p-HCl adhered to chitosan. The p-HCl containing agglomerates did not differ in size and shape from the chitosan agglomerates and had similar fluidity. The addition of p-HCl (figure 4.2 (d)) did not have a detrimental effect on the micrometric properties of the spherical agglomerates.

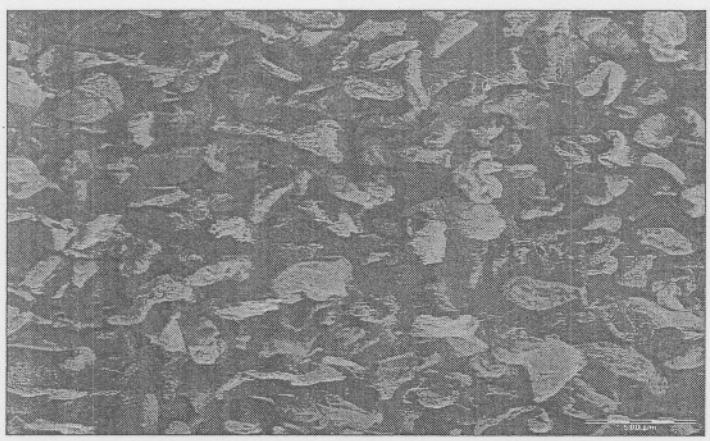

a)

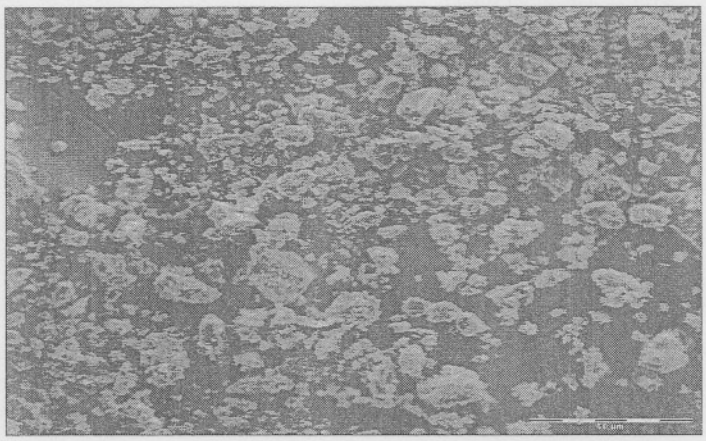

b)

c)

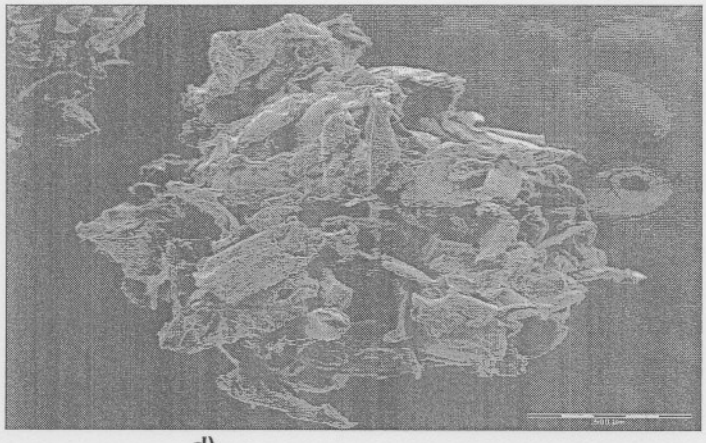

d)

Figure 4.2: SEM micrographs of a) chitosan powder b) P-HCl c) surface of a spherically agglomerated chitosan fibre d) spherically agglomerated formulation of both chitosan and p-HCl. Note the fine particles (P-HCl) on the coated surface of the chitosan fibre.

4.2.2 Tablet evaluation

Tablet dimensions were evaluated to establish the applicability of the process and formulations in terms of tablet weight variation, friability and physical dimensions. The effects of suspension agglomeration times on the tablet properties were analyzed to determine the consequence of different agglomeration times on the physical properties of tablets. Consequently, to identify the optimum formula.

4.2.2.1 *Compactibility*

Tablets were successfully pressed on a Cadmach tablet press (setting 50) without the aid of any lubricants, i.e. magnesium stearate. Neither sticking nor lamination occurred. An average expansion of 0.86% in tablet diameter was observed for all the pressed tablets. The expansion may be the result of the elastic behaviour of chitosan. The tablet surfaces exhibited a satisfactory appearance with no indication of frictional damage on tablet edges. It was found that all the p-HCl mixtures could be compressed at a setting of 50, although only after spherical agglomeration. An additional hardness test was done to measure the strength of the tablets and to determine the whether the tablets could withstand everyday handling.

4.2.2.2 *Weight variation*

The weight variation of tablets is an indirect measurement of powder fluidity. Not more than two of the individual weights (mass) of each of the tablet formulas deviated from the average weight (mass) by more than the percentage deviation shown in table 4.5, and none deviated by more than twice that percentage. This acceptable weight variation proved to be a remarkable finding, since all three formulations failed to be compressed prior to spherical agglomeration, and possessed a wide range of size distribution, as observed with the naked eye.

Table 4.5: British Pharmacopoeia (2002) limits for tablet weight variation.

Average weight of tablet	Percentage deviation
80 mg or less	10
More than 80 mg and less than 250 mg	7.5
250 mg or more	5

Only two tablets (see table 4.6) from twenty randomly picked tablets from each of the formula $1_{10\ minutes}$ and formula $2_{10\ minutes}$ batches deviated from the limit prescribed by the BP (2002). If

one tablet deviated more than twice the standard percentage, a batch was considered a failure. All the formulations complied thus with the BP (2002) limitations. The fact that only formula 1 and 2 had tablets that deviated slightly cannot be explained.

Table 4.6: Tablets formulas complying with the limited percentage deviation prescribed by the BP (2002). The number in parenthesis is the amount of tablets that deviated from set limited percentage deviation.

		[1]AT (minutes)	
	10	15	20
Formula 1	complied (2)	complied (0)	complied (0)
Formula 2	complied (2)	complied (0)	complied (0)
Formula 3	complied (0)	complied (0)	complied (0)

1= Agglomeration time

4.2.2.3 *Density*

Tablet density was determined by tablet weight divided by tablet volume. Tablet density increased as the concentration w/w Kollidon® K25 per formulation increased. Kollidon® K25 has the highest density of the three powders utilized in the tablet formula, explaining the increase in tablet density. The rank order for the tablet densities was as follows: formulation 3>formulation 2>formulation 1. No noteworthy differences between tablet densities from the same batch were experienced, although suspension agglomeration times differed.

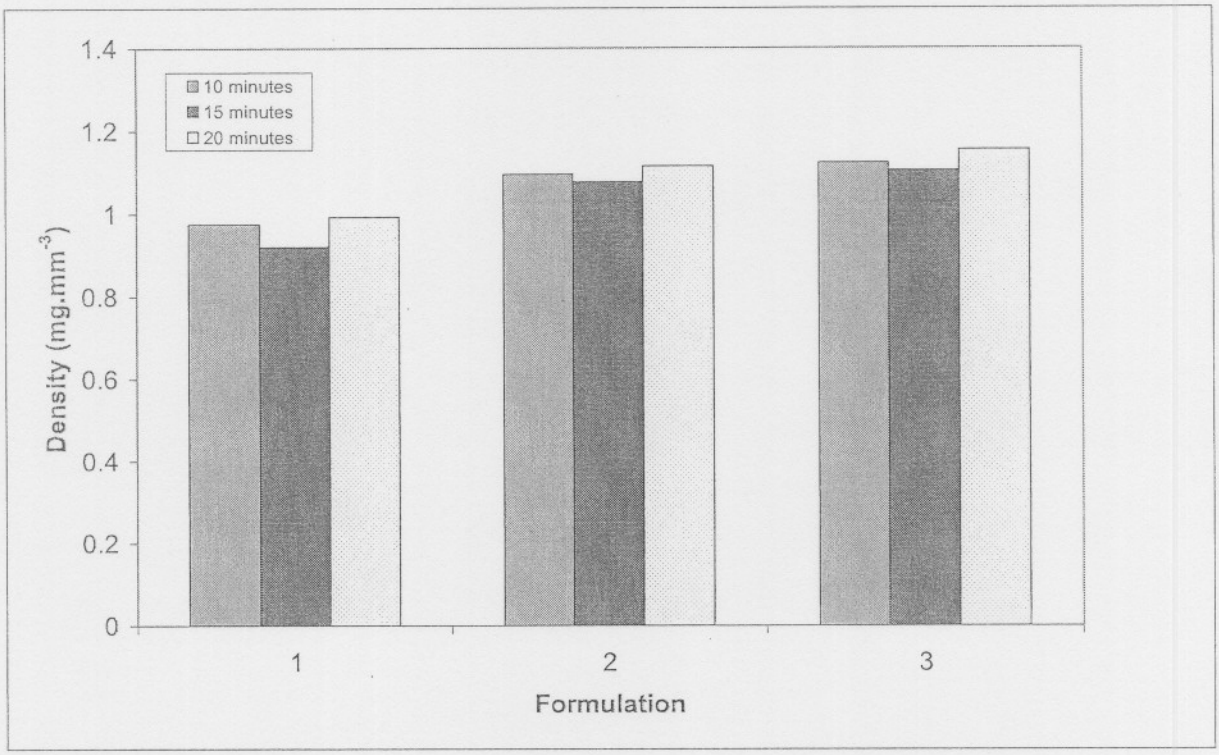

Figure 4.2: Tablet densities of the three different formulations agglomerated for 10, 15 and 20 minutes.

4.2.2.4 *Crushing strength/hardness*

The crushing strength of the tablets decreased from 10 minutes to 15 minutes of suspension agglomeration time and increased again from 15 minutes to 20 minutes of agglomeration time. No explanation can be given for this occurrence.

4.2.2.5 *Tensile strength*

The tensile strength of the agglomerated tablets as a function of suspension agglomeration time is given in figure 4.4 and figure 4.5. The tensile strength of the tablets decreased from 10 minutes to 15 minutes of suspension agglomeration time and increased again from 15 minutes to 20 minutes of agglomeration time. Once again can no explanation be given for this occurrence.

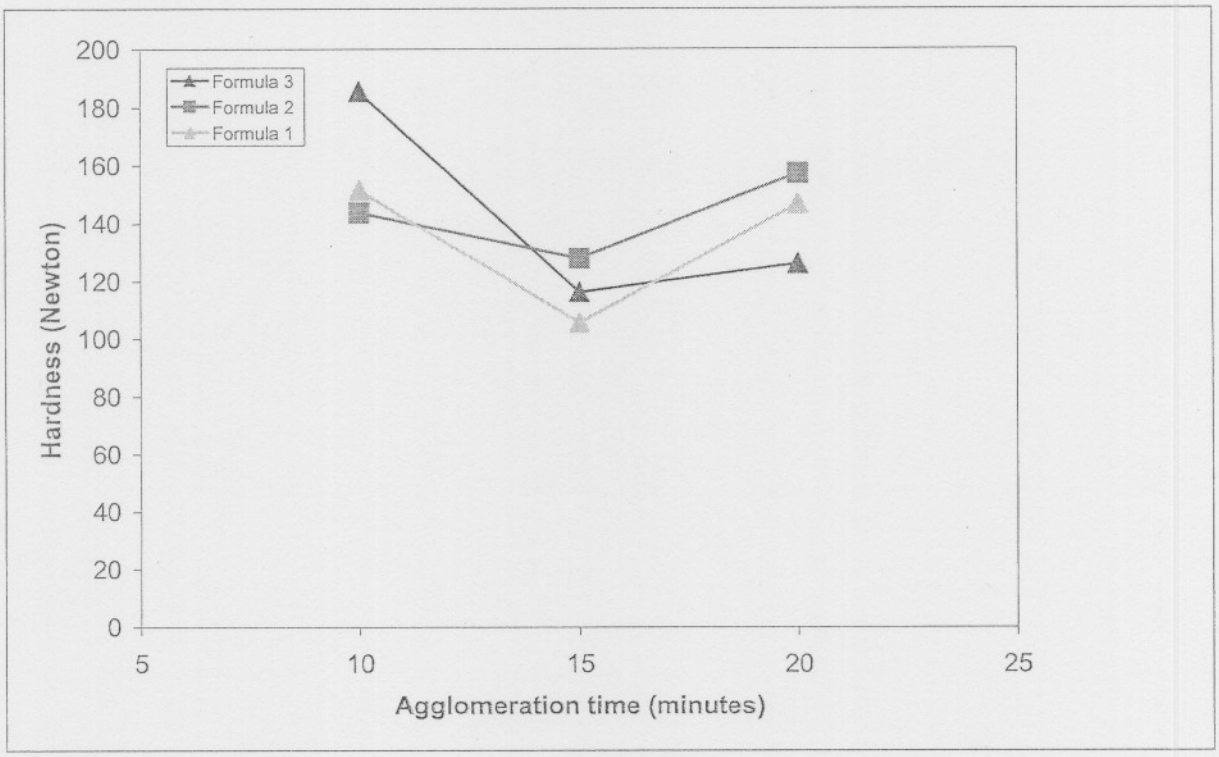

Figure 4.3: The hardness of the agglomerated tablets as a function of suspension agglomeration time.

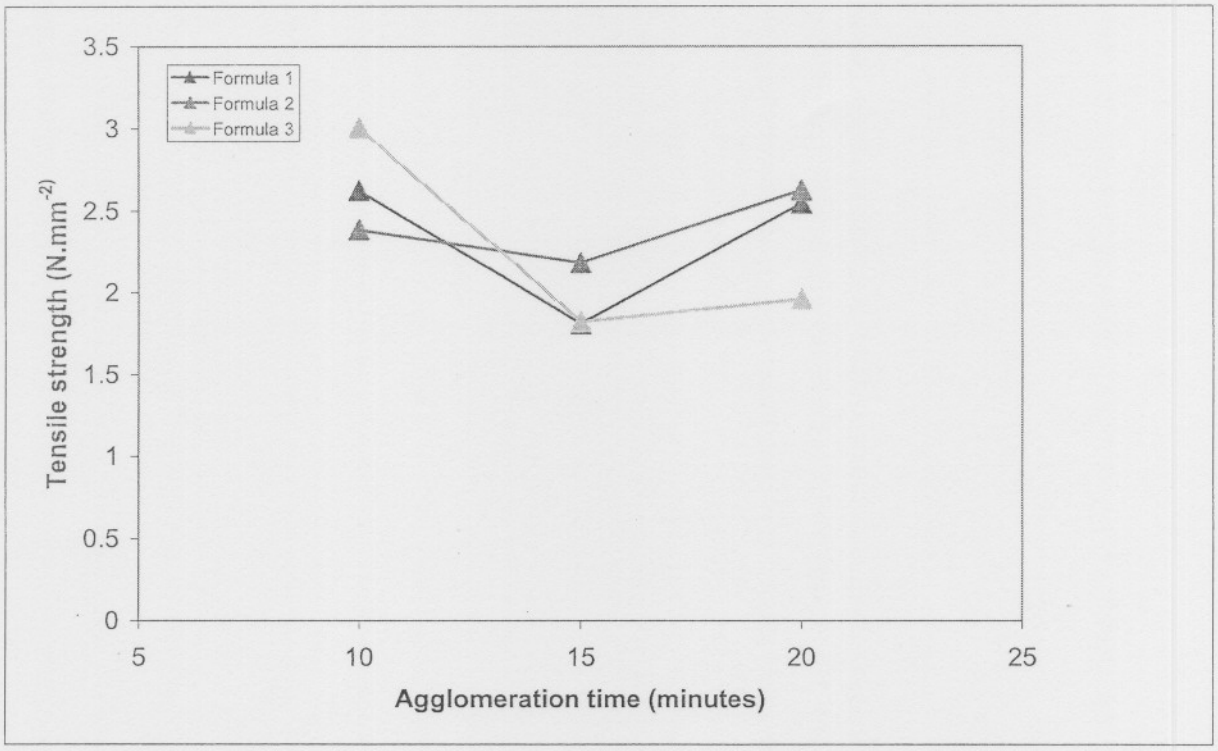

Figure 4.4: The tensile strength of the agglomerated tablets as a function of suspension agglomeration time.

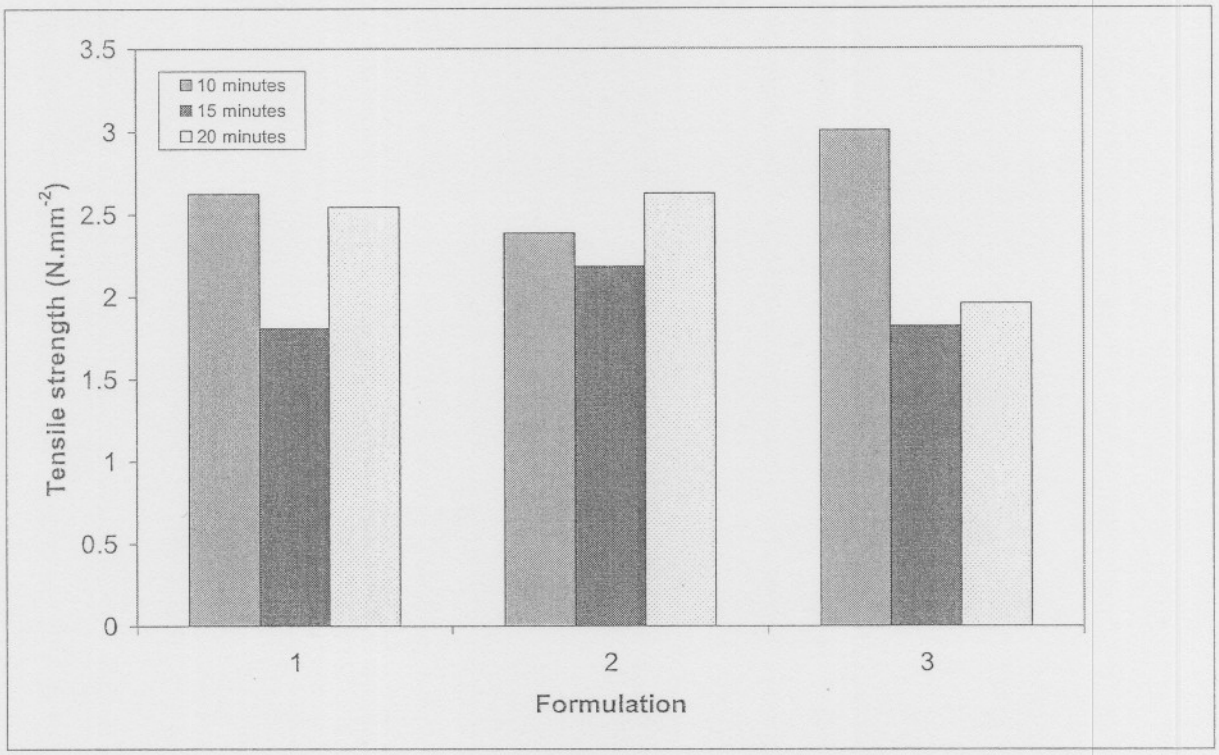

Figure 4.5: The tensile strength of the various formulations at different suspension agglomeration times.

4.2.2.6 *Friability*

A friability test (see 2.3.6) revealed that the tablets obtained from the nine different formulas could withstand normal handling. A negligible loss in weight resulted after being tested for ten minutes with a friabilator machine. The loss in tablet mass due to friability of all formulations was less than 1%. There was no relationship between hardness values and friability observations. Small values in friability imply much less friability during transportation, which is favorable.

4.2.3 X-ray powder diffraction (XRPD)

The XRPD traces of the p-HCl prior to agglomeration and of p-HCl after being exposed to the conditions under which spherical agglomeration occurred were identical with regard to peak position and relative intensity, peak shifting and the presence or lack of peaks in certain regions of °2θ values. The X-ray powder diffractogram of the experiment is illustrated in figure 4.6.

4.2.4 Infrared absorption spectroscopy (IR)

Infrared absorption spectroscopy revealed a peak-by-peak correlation of the IR spectra of p-HCl prior to agglomeration and of p-HCl after being exposed to the conditions under which spherical agglomeration took place. A peak-by-peak correlation is excellent evidence for identity and

proved the process to be stable to ensure drug stability. IR–spectral results of the samples are given in figure 4.7.

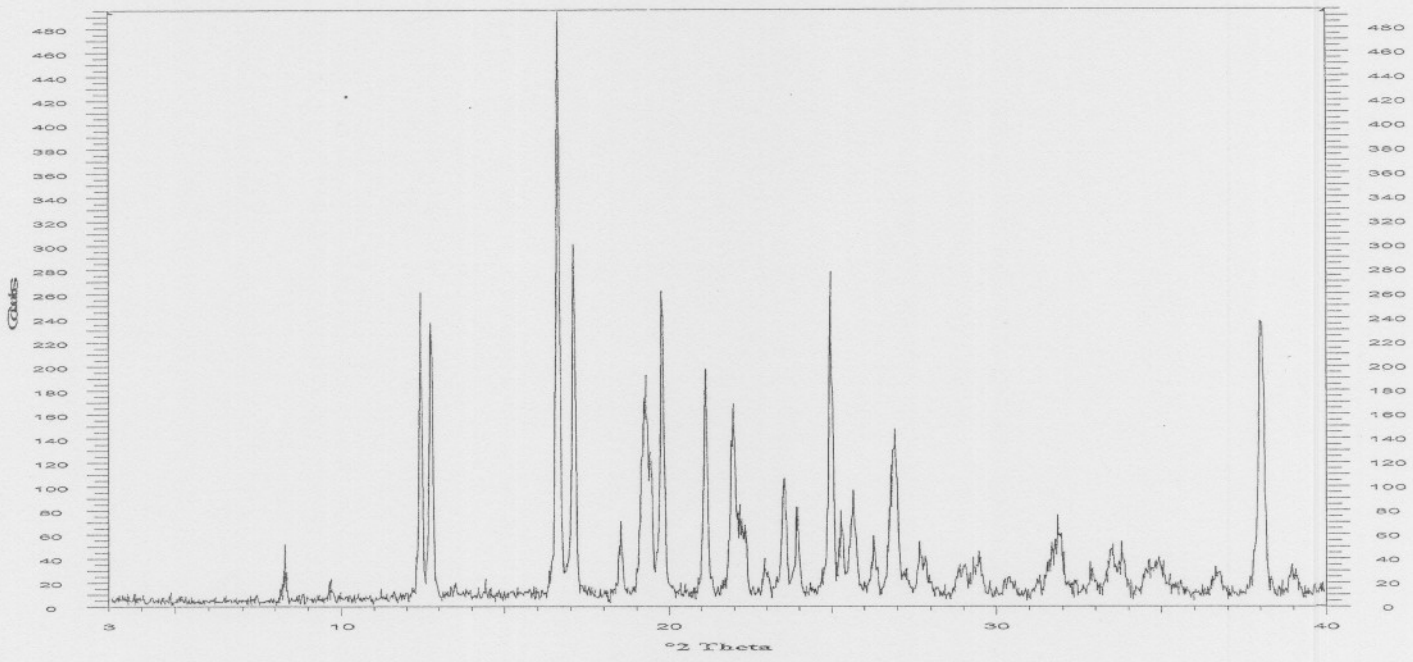

a)

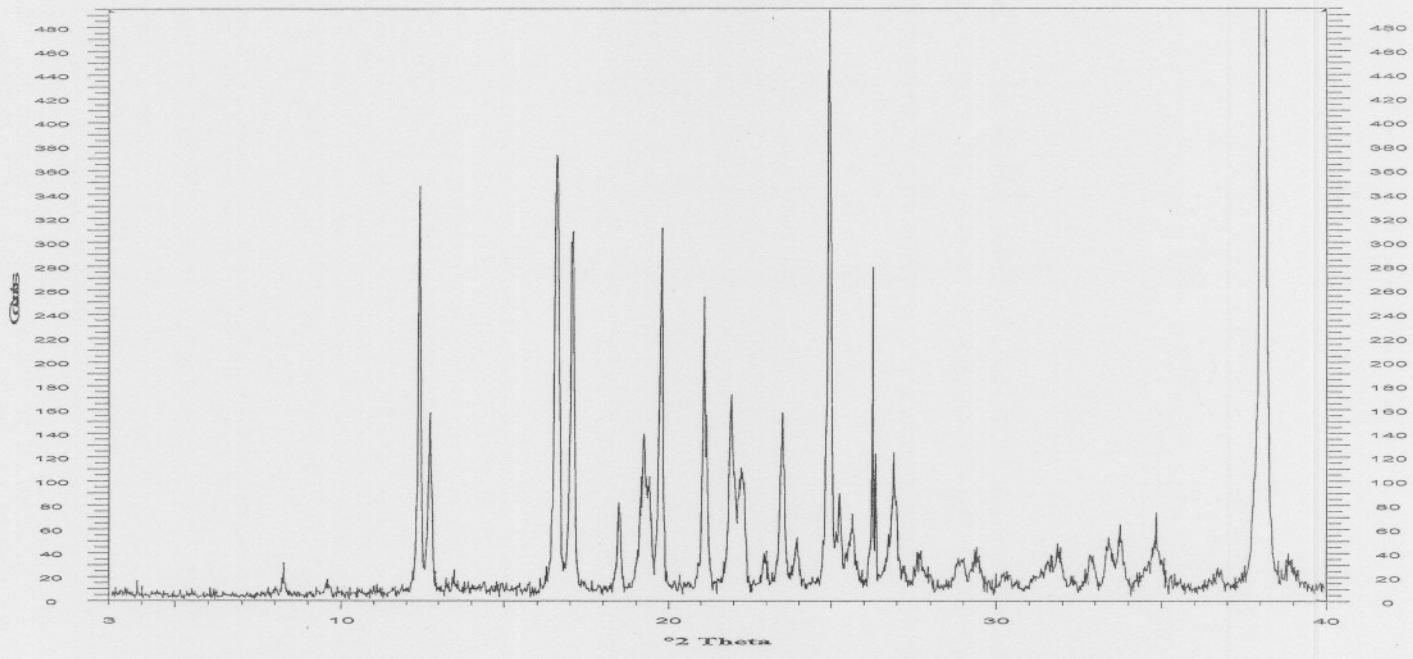

b)

Figure 4.6: The XRPD patterns of a) P-HCl b) Spherically agglomerated p-HCl.

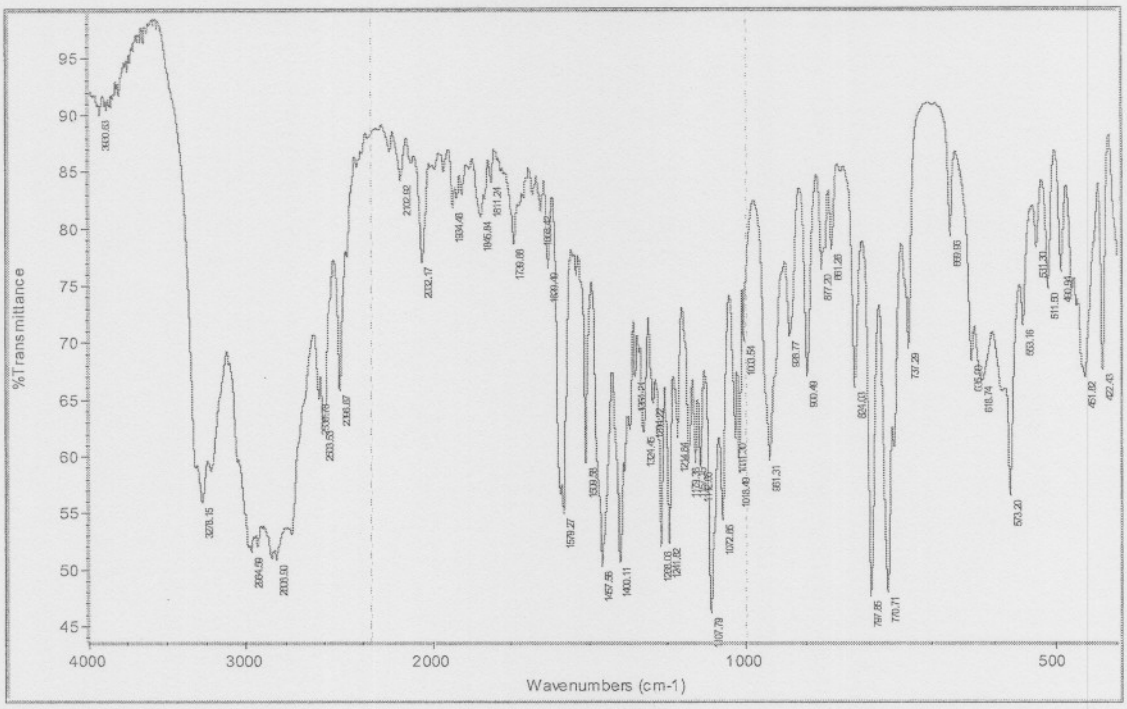

a)

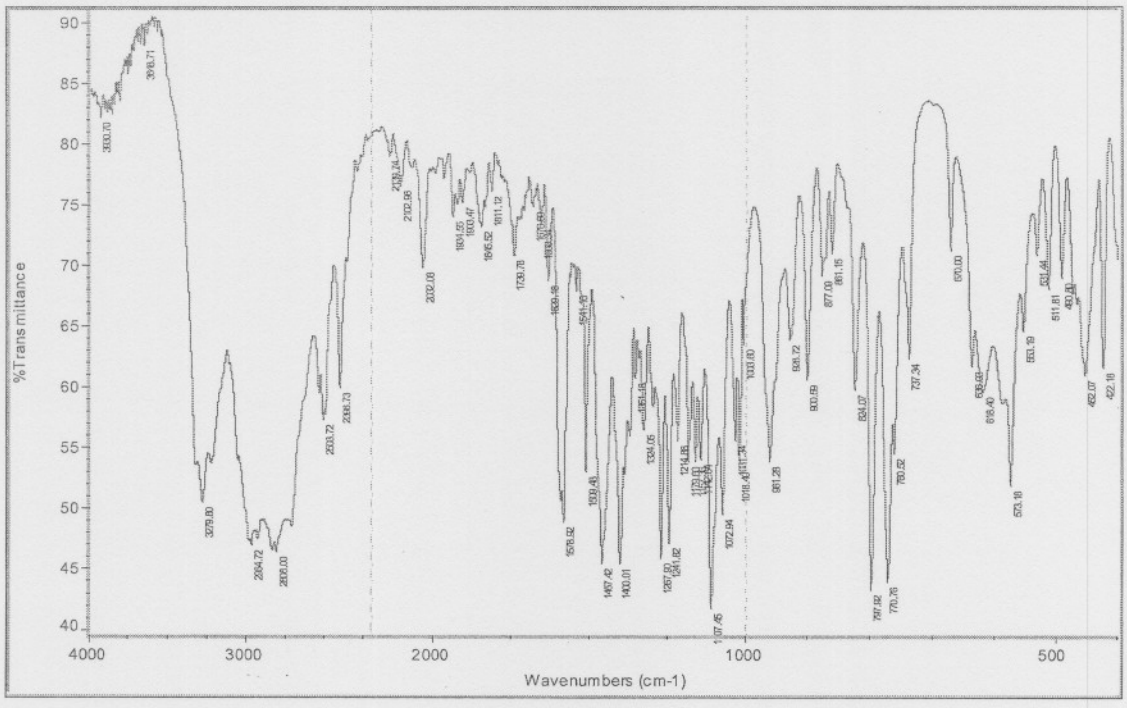

b)

Figure 4.7: IR spectra of a) P-HCl and b) Spherically agglomerated p-HCl

Table 4.7 presents a summary of the physical properties obtained from the various experiments.

Table 4.7: Summary of the physical properties of each batch.

Formula	Agglomeration Time (minutes)	Property	Value
1	10	Tablet density ($mg.mm^{-3}$)	1.095
		Crushing strength (Newton)	143.833
		Tensile strength ($N.mm^{-2}$)	2.385
		Friability (%)	0.000
		Weight variation	Complied
	15	Tablet density ($mg.mm^{-3}$)	1.076
		Crushing strength (Newton)	127.867
		Tensile strength ($N.mm^{-2}$)	2.181
		Friability (%)	0.011
		Weight variation	Complied
	20	Tablet density ($mg.mm^{-3}$)	1.115
		Crushing strength (Newton)	157.167
		Tensile strength ($N.mm^{-2}$)	2.626
		Friability (%)	0.000
		Weight variation	Complied
2	10	Tablet density ($mg.mm^{-3}$)	0.975
		Crushing strength (Newton)	151.333
		Tensile strength ($N.mm^{-2}$)	2.624
		Friability (%)	0.115
		Weight variation	Complied
	15	Tablet density ($mg.mm^{-3}$)	0.920
		Crushing strength (Newton)	105.433
		Tensile strength ($N.mm^{-2}$)	1.809
		Friability (%)	0.004
		Weight variation	Complied
	20	Tablet density ($mg.mm^{-3}$)	0.993
		Crushing strength (Newton)	146.700
		Tensile strength ($N.mm^{-2}$)	2.545
		Friability (%)	0.039
		Weight variation	Complied
3	10	Tablet density ($mg.mm^{-3}$)	1.123
		Crushing strength (Newton)	185.501
		Tensile strength (N.mm-2)	3.004
		Friability (%)	0.003
		Weight variation	Complied
	15	Tablet density ($mg.mm^{-3}$)	1.104
		Crushing strength (Newton)	116.202
		Tensile strength (N.mm-2)	1.820374
		Friability (%)	0.000
		Weight variation	Complied
	20	Tablet density ($mg.mm^{-3}$)	1.154
		Crushing strength (Newton)	126.321
		Tensile strength (N.mm-2)	1.958
		Friability (%)	0.003
		Weight variation	Complied

4.3 DISSOLUTION STUDIES

Dissolution studies were performed on three tablets from each batch according to the protocols described in section 2.4.

4.3.1 The effect of agglomeration time on the dissolution parameters of different formulations

The parameters contributing to the spherical agglomeration of a desirable, compressible chitosan powder structure was established. Successful spherical agglomeration is dependant on the wettability and surface area of the suspended powder or powder mixtures as well. Due to the complex manner by which agglomeration takes place, formulations with different concentrations were prepared to identify a formulation able to deliver a specific dissolution profile similar to that of a commercially available product. Inderal® LA 80 mg is available in capsule form, a more complex dosage form in terms of production complexity than tableting.

The chitosan:p-HCl ratios were 1:1 for formulation 1, 2 and 3, except for a change in Kollidon® % w/w for each tablet batch. Agglomeration time was chosen as a variable due to the fact that the time for agglomeration had probably the smallest amount of influence on agglomerate formation (section 3.5.2). Formulation 1 had the highest quantities of p-HCl and chitosan, whilst formulation 3 had the least amount of p-HCl and chitosan (see table 4.1).

For agglomeration to take place, the chitosan:Kollidon® K25 ratio was optimal at values 7:3. Agglomeration took place as a result of coating, as the SEM micrographs indicated. A specific area had thus to be coated for agglomeration to take place. Agglomeration of chitosan and p-HCl took place for the same ratio to Kollidon® K25 as the ratio for chitosan only and Kollidon® K25 in terms of powder weight. The amount of p-HCl and chitosan was altered to determine the optimal formulation for agglomerates, although the chitosan:p-HCl ratio was kept constant.

4.3.2 Dissolution profiles

The dissolution profiles are given in annexure A. Two parameters are noted that were denoted as normalized. Normalization of data allows comparison of the AUC's (extent of dissolution) and DR_i's (initial rate of dissolution from $t_0 - t_5$) of the various formulations. Equations 4.1 and 4.2 shows the equations utilized to normalize the dissolution parameters:

$$(AUC_n) = \frac{AUC_{formula}}{AUC_{baseline}} \qquad \text{Equation 4.1}$$

Where $(AUC)_n$ = normalized AUC, $AUC_{formula}$ = AUC of formulation and $AUC_{baseline}$ = AUC of reference.

$$(DR_i)_n = \frac{(DR_i)_{formula}}{(DR_i)_{baseline}} \qquad \text{Equation 4.2}$$

Where $(DR_i)_n$ = *normalized* DR_i, $(DR_i)_{formula}$ = DR_i of formulation and $(DR_i)_{baseline}$ = DR_i of reference.

4.3.3 AUC and DR_i

The p-HCl 39% w/w formula had a significant AUC_n value of 0.904 for the first two hours of dissolution in the acidic medium. This AUC_n deviated only 9.06% from the AUC of Inderal® LA and proved to be quite pronounced in 0.1 M HCl, since two hours is the approximate gastric residence time for substances entering the stomach. Note that this formula had the highest percentage of p-HCl (% w/w) per tablet, as well as the maximum amount of chitosan and least amount of binder (chitosan 39% w/w : binder 22% w/w).

Table 4.8: DR_i's of the different formulations.*

	10 minutes		15 minutes		20 minutes	
	pH 1.2	pH 4.5	pH 1.2	pH 4.5	pH 1.2	pH 4.5
Formula 1	0.28	0.51	0.39	0.31	0.34	0.45
Formula 2	0.46	0.35	0.28	0.48	0.38	0.62
Formula 3	0.29	0.49	0.39	0.64	0.40	0.60

*$\mu g.cm^{-3}.min^{-1}$

Table 4.9: AUC_n of the different formulations.

	10 minutes		15 minutes		20 minutes	
	pH 1.2	pH 4.5	pH 1.2	pH 4.5	pH 1.2	pH 4.5
Formula 1	1.30	2.495	1.51	2.766	1.45	2.755
Formula 2	1.73	2.755	1.36	2.413	1.55	2.822
Formula 3	1.37	2.354	1.54	2.761	1.61	2.713

4.3.3.1 *The ratio of the percentage w/w to DR_i (PDI)*

A % w/w and DR_i index was constructed to determine the effect of the different ratios on the initial dissolution rate of p-HCl and to establish the joint effect of specific concentrations of spherically agglomerated chitosan and p-HCl on dissolution rate (figure 4.8).

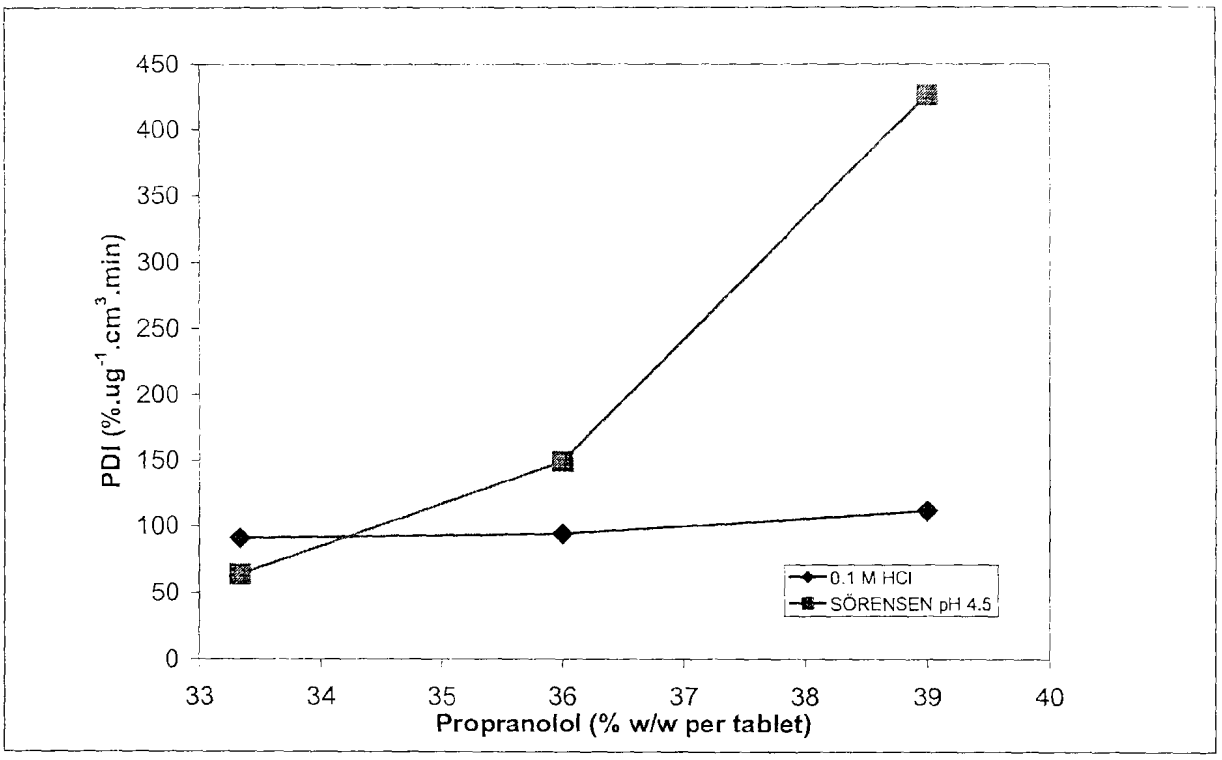

Figure 4.8: The PDI as a function of percentage p-HCl per tablet.

Tablets theoretically contained 33.3%, 36% and 39% p-HCl and chitosan per tablet. The

percentage p-HCl per tablet was divided by its initial dissolution rate to supply the % w/w and DR_i index for comparison with other tablets with different formulations (equation 4.3):

$$PDI = \frac{\%w/w}{DR_i} \qquad \text{Equation 4.3}$$

A high value obtained from the index is an indication of a relative slow initial dissolution rate for the specific concentration p-HCl present in the tablet formulation. It is interesting to note that the plot showed higher values for higher concentrations of p-HCl per tablet in both 0.1 M HCl and Sörensen buffer.

Additionally, a plot of the % w/w and DRi index against the % w/w Kollidon® K25 and chitosan revealed the same interesting results (figure 4.9). The index values decreased as the % w/w of chitosan and Kollidon® K25 increased. The DR_i of each tablet formula for the amount of p-HCl increased relative to a decrease in the amount of p-HCl per tablet. This may suggest that micro agglomerates of p-HCl were also prepared with higher concentrations of p-HCl per mixture and that larger p-HCl agglomerates were formed with even higher p-HCl concentrations.

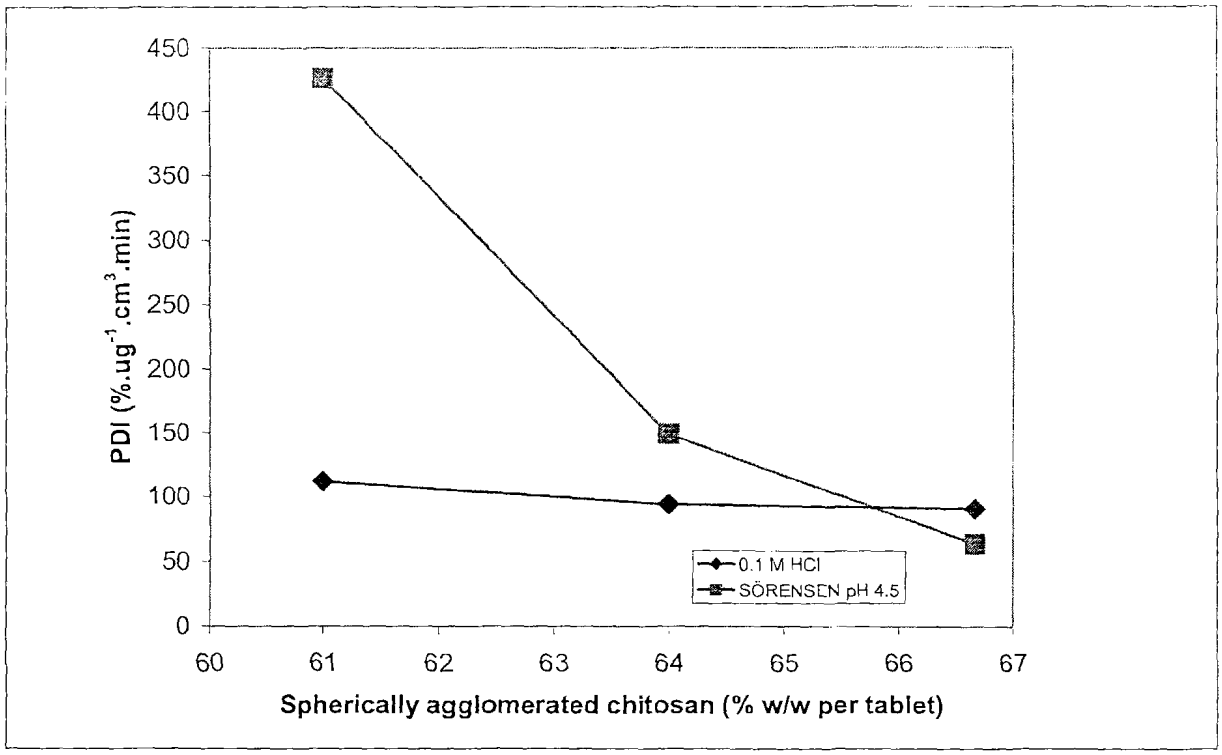

Figure 4.9: The PDI as a function of percentage spherically agglomerated chitosan per tablet.

It may also suggest that a high percentage of spherically aggiomerated chitosan contributed to a desirable decrease in p-HCl initial dissolution rate in both the dissolution mediums. Formulations containing high concentration polymers have exhibited slow release rate due to gelation formed around tablets (Krajewska 2005:305). Chitosan is a polymer and gelation was almost certainly present during dissolution. The effect of gelation of chitosan around p-HCl particles was probably greater for higher concentrations of p-HCl and chitosan per tablet than for lower concentrations per tablet. The most desirable formulation for prolonged release purposes would perhaps be the formulations containing the higher concentrations of p-HCl and chitosan.

4.3.4 Mathematical comparison of dissolution profiles

The f2-values were determined according to the protocols described in section 2.4.6.2. Table 4.10 and 4.11 displays the f2-values obtained from the experiments. The 39% w/w p-HCl spherically agglomerated tablet formula had an f2-value of 51.49 compared to the commercially available product. An f2-value of more than 50 indicates a similarity of a dissolution profile.

Table 4.10: F2-values in 0.1 M HCl (pH 1.2).

	Time (minutes)		
	10	15	20
Formula 1	**51.44819**	41.92821	41.21418
Formula 2	36.62637	47.65935	41.61051
Formula 3	49.54701	41.61051	43.79324

% Relative standard deviation (RSD) = 10.72

Formulation $1_{10\ minutes}$ displayed the most similar dissolution profile to Inderal® LA 80 in 0.1 M HCl and Formulation $3_{10\ minutes}$ had the most similarity towards the commercial dosage form in the Sörensen buffer (pH 4.5). The effect of gelation of spherically agglomerated chitosan and micro p-HCl agglomerates probably played a role in the variation in f2-values across the range of different tablet batches. The f2-values in 0.1 M HCl had less relative standard deviation than the f2-values obtained in Sörensen buffer (pH 4.5). This may be due to the fact that the degree of swelling of spherically agglomerated chitosan in Sörensen buffer (pH 4.5) probably was not as great or constant as in 0.1 M HCl. P-HCl is a weak base and may have had difficulty being wetted by the Sörensen buffer (pH 4.5).

Table 4.11: F2–values in Sörensen buffer (pH 4.5).

	Time (minutes)		
	10	15	20
Formula 1	23.06322	15.13821	17.78815
Formula 2	17.17822	25.74029	20.92599
Formula 3	**28.00826**	20.04657	23.78102

% RSD = 19.85

4.3.5 F2–values as a function of crushing strength

There were no pronounced trends amongst the crushing strength and agglomeration time of the tablets and the type of formulation. The f2-values of all the batches were plotted against crushing strength. It seems that the f2-value in both 0.1 M HCl (figure 4.10) and Sörensen buffer pH 4.5 (figure 4.11) increased as the crushing strength increased.

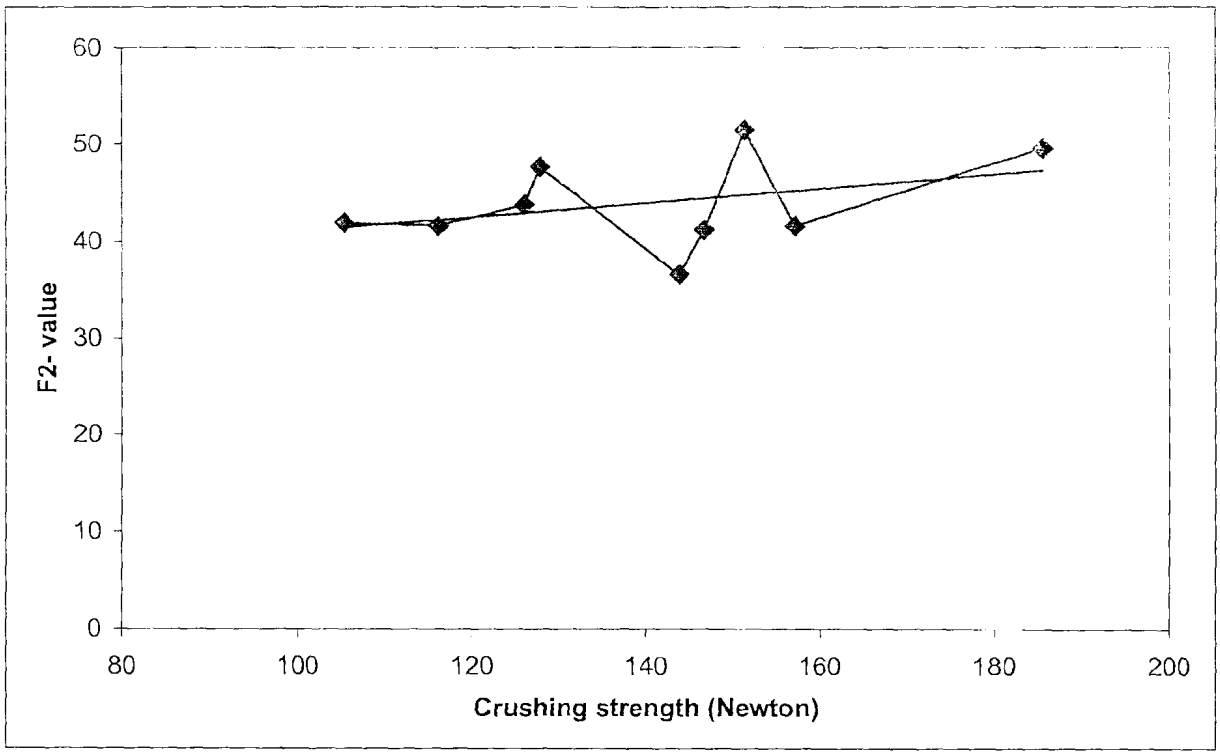

Figure 4.10: F2–values plotted against crushing strength (0.1 M HCl pH 1.2).

This increase in f2-value as a function of crushing strength indicated that tablets with greater hardness had more similarity towards the dissolution profile of Inderal® LA 80. Numerous authors have indicated a decrease in drug dissolution with an increase in compression force. It might thus be possible to achieve a higher f2-value if the upper punch setting could be increased to a setting higher than 50. In addition, a greater ratio of p-HCl per formulation would deliver an even greater f2-value, since initial dissolution rate decreased with an increase in the amount of p-HCl and spherically agglomerated chitosan present per formulation.

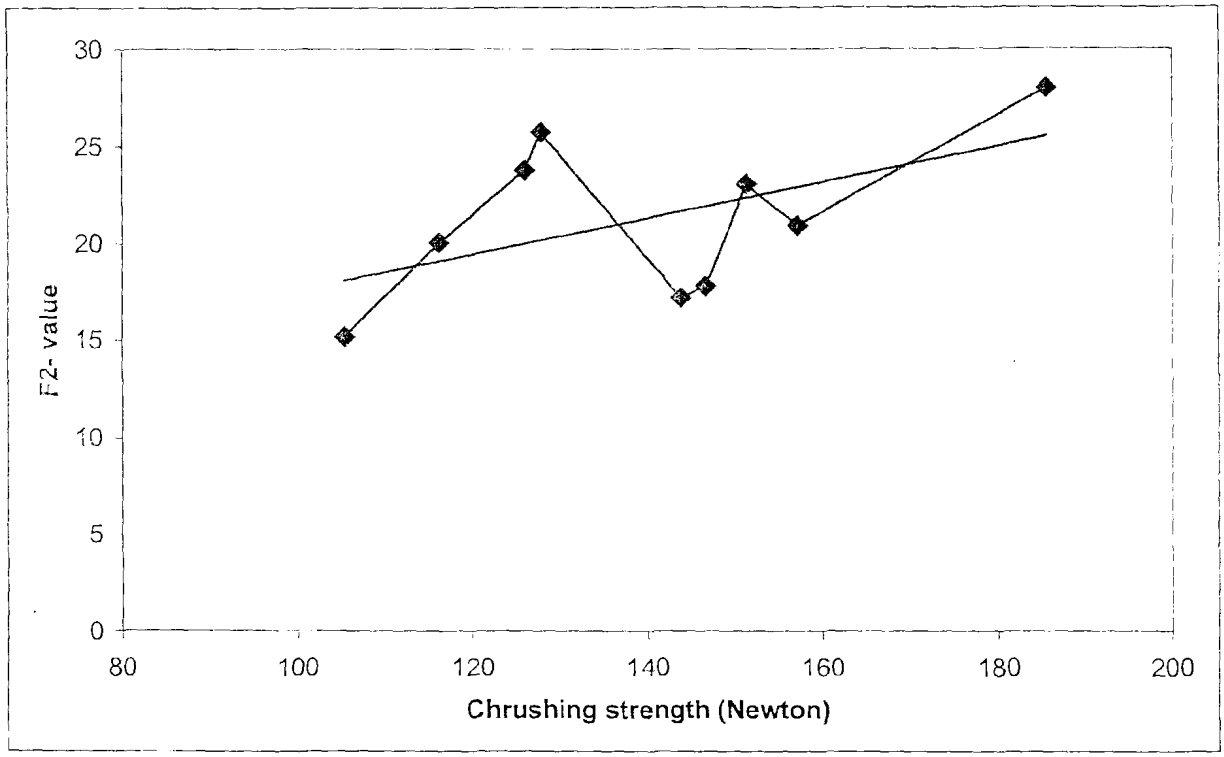

Figure 4.11: A plot of the F2–values against crushing strength (Sörensen buffer pH 4.5).

4.3.6 Dissolution profiles of Inderal® LA 80 mg and most similar tablet formulas

The dissolution profiles of Inderal® LA 80 mg and the tablet formula were not exactly the same, but illustrated the potential for spherically agglomerated chitosan in sustained release tablet formulations. Dissolution profiles of Inderal® LA 80 mg and formulation $1_{10\ minutes}$ in 0.1 M HCl (pH 1.2) are presented in figure 4.12.

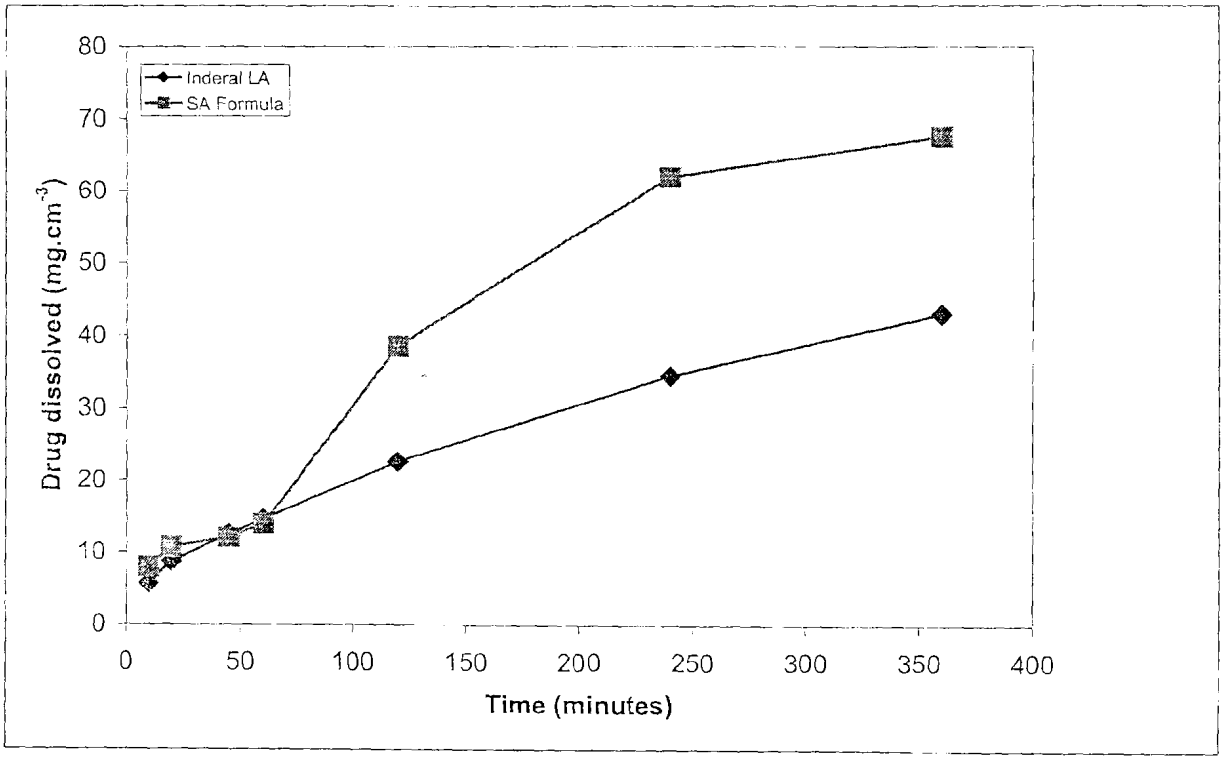

Figure 4.12: Dissolution profiles of Inderal® LA 80mg and formulation $1_{10\ minutes}$ in 0.1 M HCl pH 1.2. (SA = spherically agglomerated).

Dissolution profiles of Inderal® LA 80 mg and formulation $3_{10\ minutes}$ in Sörensen buffer (pH 4.5) are presented in figure 4.13.

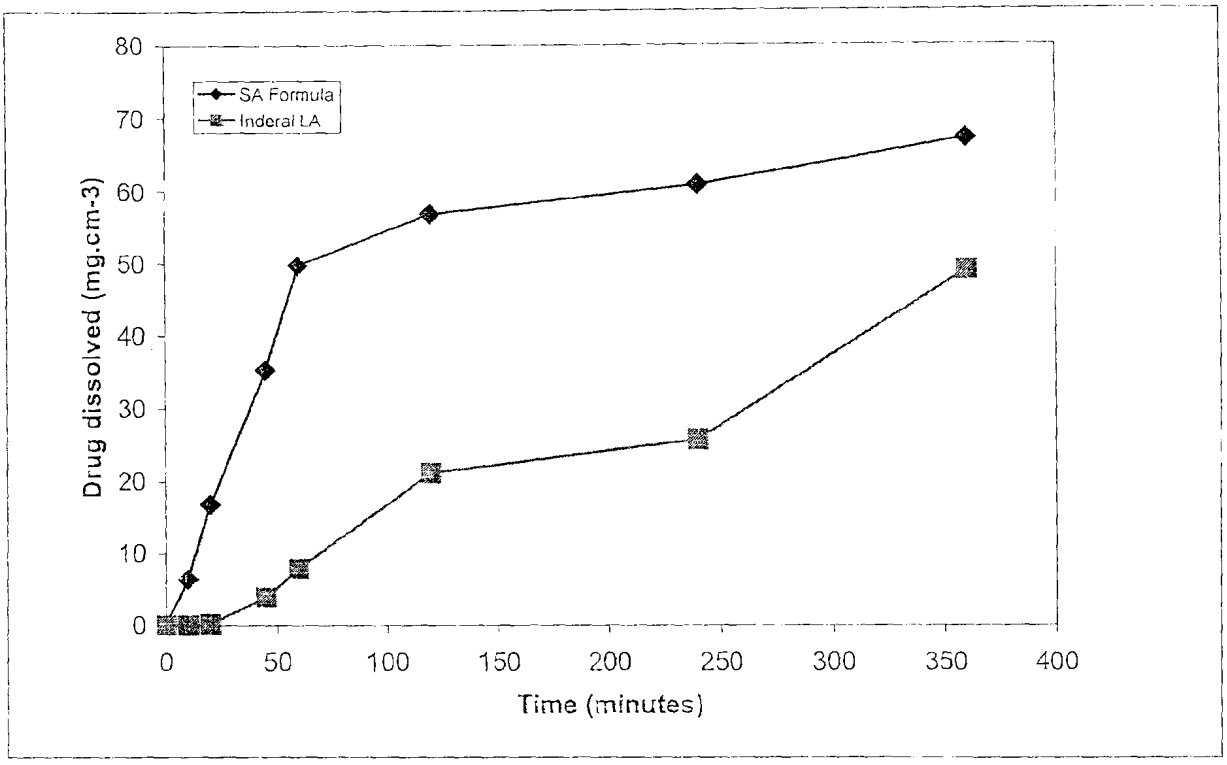

Figure 4.13: Dissolution profiles of Inderal® LA 80mg and formulation $3_{10\ minutes}$ in Sörensen buffer pH 4.5. (SA = spherically agglomerated).

4.3.7 Summary

The effect of suspension agglomeration time seemed negligible. Figures 4.14, 4.15 and 4.16 indicate the average dissolution parameters obtained from the three formulations without the suspension agglomeration time taken into effect.

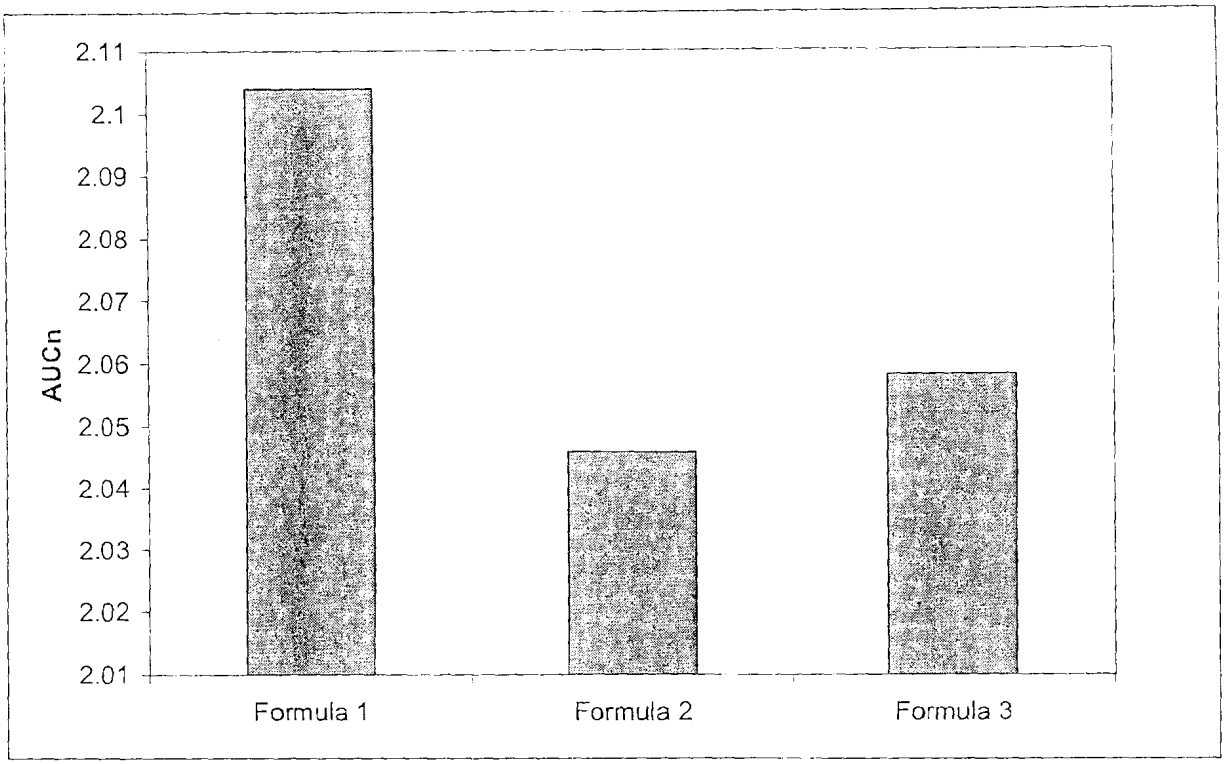

Figure 4.14: AUC_n values for the three different formulations. (Formula $1_{39\%\ P\text{-}HCl\ w/w}$ / Formula $2_{36\%\ P\text{-}HCl\ w/w}$ / Formula $3_{33.3\%\ P\text{-}HCl\ w/w}$).

Table 4.12 reveales two optimum formulas. Formula 1 displayed the most dissolution profile similarity towards Inderal® LA capsules in terms of AUC_n and DR_i (formula 1>formula 2> formula 3). However, the chitosan:p-HCl:Kollidon® K25 (ratio = 1:1:1) tablets displayed more mathematical similarity towards Inderal® LA capsules than formula 1 and 2 (formula 3> formula 1 > formula 2).

Table 4.12: Optimization table. * Average of the 10, 15 and 20 minute agglomeration time batches in both 0.1 M HCl and Sörensen buffer pH 4.5

	*AUC_n	*$(DR_i)_n$	*AUC_n + *$(DR_i)_n$	*F2 average
Formula 1	2.1039	**1.417022**	**3.520922**	31.76336
Formula 2	**2.045974**	1.783163	3.829137	31.62345
Formula 3	2.05829	2.076443	4.134733	**34.46443**

Table 4.13 is a summary of the dissolution parameters of the optimum formulations in the respective dissolution mediums. Formula 1 and formula 3 was viewed as the optimum formulations in 0.1 M HCl pH 1.2 and Sörensen buffer pH 4.5 respectively.

Table 4.13: Dissolution parameters of the optimum formulations in the respective dissolution mediums.

	Formula 1	Inderal® LA	Formula 3	Inderal® LA
	0.1 M HCl pH 1.2	0.1 M HCl pH 1.2	Sörensen buffer pH 4.5	Sörensen buffer pH 4.5
$(DR_i)_n$	1.46	1	1.91	1
F2	51.45	<50<100	28.01	<50<100
AUC_n	1.30	1	2.35	1

Figure 4.15 shows the f2-averages for the different formulations. Formula 3 had the highest average f2-value in both dissolution media.

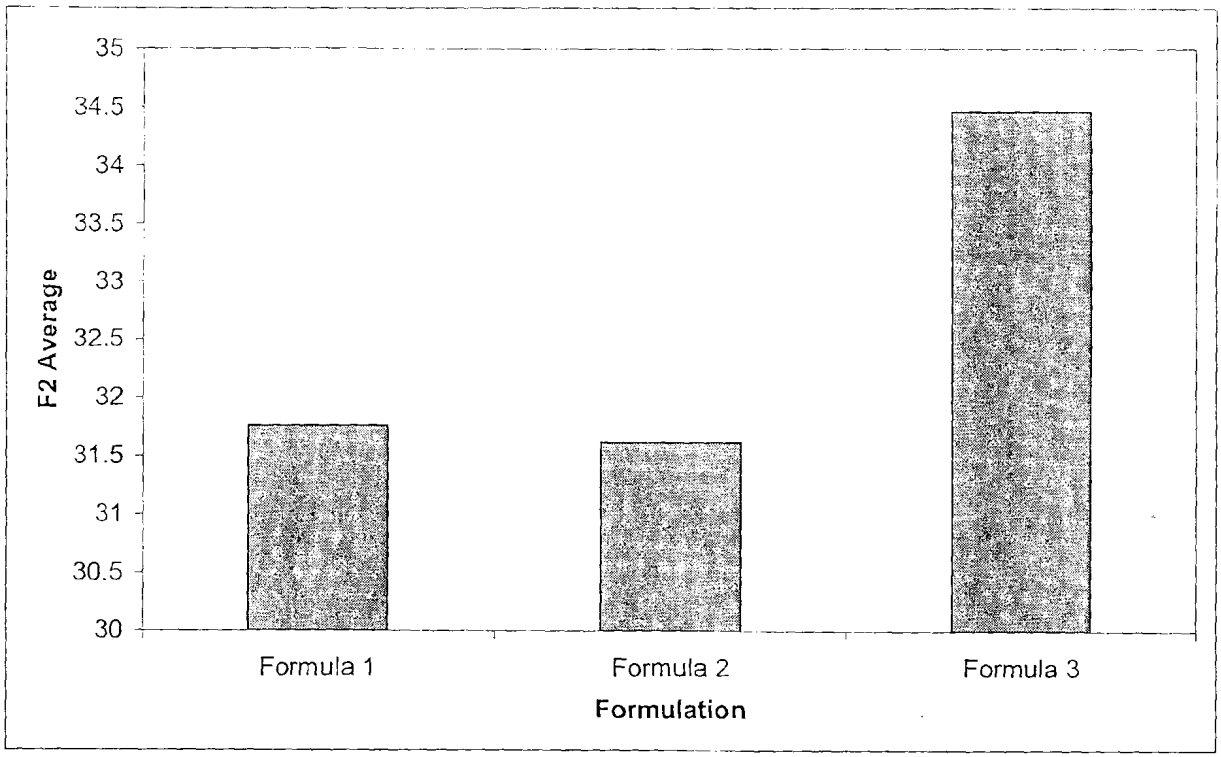

Figure 4.15: F2 averages for the three different formulations. (Formula $1_{39\%\ P\text{-}HCl\ w/w}$ / Formula $2_{36\%\ P\text{-}HCl\ w/w}$ / Formula $3_{33.3\%\ P\text{-}HCl\ w/w}$).

Table 4.14: Summary of the dissolution parameters for each batch.

Agglomeration time (minutes)	Formula	Parameter	0.1M HCl	Sörensen buffer
10	1	(DR_i) $\mu g.cm^{-3}.min^{-1}$	0.29	0.51
		(AUC) $\mu g.cm^{-3}.min$	14228.13	20550.25
		f2	51.45	23.06
		AUC_n	1.30	2.50
	2	(DR_i) $\mu g.cm^{-3}.min^{-1}$	0.48	0..35
		(AUC) $\mu g.cm^{-3}.min$	18931.53	22694.29
		f2	36.63	17.18
		AUC_n	1.73	2.76
	3	(DR_i) $\mu g.cm^{-3}.min^{-1}$	0.29	0.49
		(AUC) $\mu g.cm^{-3}.min$	14972.46	19390.71
		f2	49.55	28.01
		AUC_n	1.37	2.35
15	1	(DR_i) $\mu g.cm^{-3}.min^{-1}$	0.42	0.31
		(AUC) $\mu g.cm^{-3}.min$	16536.30	22778.59
		f2	41.93	15.14
		AUC_n	1.51	2.77
	2	(DR_i) $\mu g.cm^{-3}.min^{-1}$	0.30	0.48
		(AUC) $\mu g.cm^{-3}.min$	14846.59	19873.00
		f2	47.66	25.74
		AUC_n	1.36	2.41
	3	(DR_i) $\mu g.cm^{-3}.min^{-1}$	0.41	0.64
		(AUC) $\mu g.cm^{-3}.min$	16915.03	22740.22
		f2	41.61	20.05
		AUC_n	1.54	2.76
20	1	(DR_i) $\mu g.cm^{-3}.min^{-1}$	0.37	0.45
		(AUC) $\mu g.cm^{-3}.min$	15879.19	22691.72
		f2	41.21	17.79
		AUC_n	1.45	2.76
	2	(DR_i) $\mu g.cm^{-3}.min^{-1}$	0.41	0.62
		(AUC) $\mu g.cm^{-3}.min$	16952.14	23241.79
		f2	41.61	20.93
		AUC_n	1.55	2.82
	3	(DR_i) $\mu g.cm^{-3}.min^{-1}$	0.42	0.60
		(AUC) $\mu g.cm^{-3}.min$	17622.21	22342.39
		f2	43.79	23.78
		AUC_n	1.61	2.71

Figure 4.16 shows an almost linear increase in $(DR_i)_n$ to a decrease in % w/w p-HCl per tablet. This may be attributed to possible micro p-HCl agglomerates formed with higher concentration of the drug during the agglomeration process leading to matrix diffusion type prolonged release.

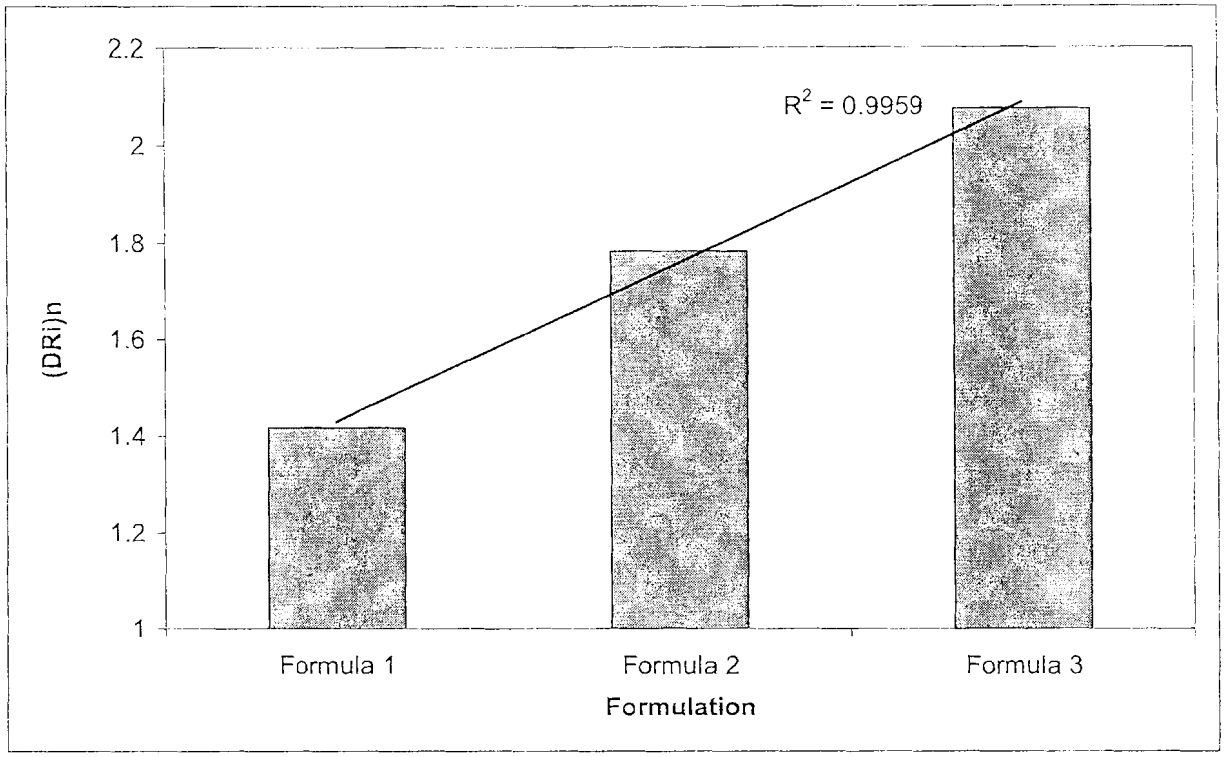

Figure 4.16: Initial rate of drug release (normalized) for the three different formulas. (Formula $1_{39\%\ P\text{-}HCl\ w/w}$ / Formula $2_{36\%\ P\text{-}HCl\ w/w}$ / Formula $3_{33.3\%\ P\text{-}HCl\ w/w}$).

If taken into account that the dissolution tests took place in both 0.1 M HCl and Sörensen buffer pH 4.5, formula 3 would be chosen as the optimum formula, based on two criterions. Formulation 3 displayed optimal dissolution similarities towards Inderal® LA capsules calculated from the Moore and Flanner equation. Moore *et al.* (1996:64) indicated that the f2-value delivers a more precise estimation of dissolution profile similarity than the AUC_n method.

4.4 CONCLUSION

Spherically agglomerated chitosan was compressed successfully and used in tablet formulations without any tableting excipients other than Kollidon® K25, an excipient that proved essential in the agglomeration step. No glidants were necessary, as the powder flowed freely into the tablet die. In addition, the formulations required no lubrication in view of the fact that the tablets underwent no friction during compression. The tablets were hard, and had minimum friability and acceptable weight variation. P-HCl is an extremely poor flowing powder and could only be compressed with chitosan after being spherically agglomerated with chitosan. P-HCl

was stable during and after spherical agglomeration. The process proved stable, given the results obtained from the X-ray powder diffraction and infrared absorption spectroscopy.

P-HCl is highly soluble in weak acidic mediums which presented the challenge of formulating a prolonged release delivery system in tablet form. The mathematical comparisons of some of the dissolution profiles of the p-HCl tablets and Inderal® LA in simulated gastric media presented acceptable f2-values and good area under graph correlations. The initial drug dissolution rates of all the tablet formulas and Inderal® LA capsules were highly comparable, considering that gastric residence time is about two hours. The formulations containing p-HCl were coated with chitosan without using spray drying or capsules, proving the economical advantages of the spherical agglomeration technique and chitosan as pharmaceutical excipient.

The tablet and the Inderal® LA capsules dissolution profiles in Sörensen buffer pH 4.5 presented less similarity, as the f2, *AUCn* and *DRi* values indicated. It may however be possible to obtain more dissolution profile similarity between the tablet formulas and the commercial product if the tablets could be compressed with a greater upper punch setting than used in this study.

Gel formation by chitosan at pH values between 1 and 2, as in the stomach, would make chitosan interesting to study *in vitro* as an excipient for the development of a slow release oral dosage form.

Following in chapter 5 is the determination of the drug release mechanisms of propranolol hydrochloride from spherically agglomerated chitosan tablets

5. CHAPTER 5

DETERMINING THE DRUG RELEASE MECHANISM OF PROPRANOLOL HYDROCHLORIDE FROM SPHERICALLY AGGLOMERATED CHITOSAN TABLETS

5.1 INTRODUCTION

When designing extended-release dosage forms, the solubility characteristics of the active must be taken into account as these can strongly influence the overall release profile of a drug. In fact, the solubility and the dissolution rate of p-HCl at acidic pH values are very high, making it difficult to control the release of p-HCl in the stomach. In addition, it is necessary to ensure the dissolution of the drug on the intestinal medium.

The release mechanism of p-HCl was determined from the dissolution profiles of spherically agglomerated chitosan tablets throughout this chapter. Chitosan is known for its solubility in weak acidic mediums, and as a polymer, solubilizing p-HCl during dissolution in simulated gastric media. Agglomerates were produced subjected to the conditions described in table 5.1 and tablets were pressed on a Cadmach eccentric press at setting 50.

Table 5.1: Agglomeration conditions.

Chitosan	39% w/w
P-HCl	39% w/w
Kollidon K25	22% w/w
Suspension concentration	3 g/100 cm^3
Agitation speed	400 rpm
Agglomeration time	10 minutes

The tablets were tested in enzyme-free 0.1M HCl, simulated gastric juice with pH 1.2, in accordance with the method described in chapter 2.

The zero order model, first order model and matrix models are available to describe a drug release mechanism. The dissolution data obtained from the experiments were examined to determine the type of release mechanism of p-HCl obtained from compressed spherical chitosan agglomerates. The variables attained from each of the models were plotted. Linearity was determined from the calculation of the correlation coefficient. The model of drug release will provide some information on the structure of the agglomerates and the potential utilization of

spherically agglomerated chitosan for controlled release dosage forms. The evaluation of the dissolution profiles against the various drug release models are described in this chapter.

5.2 ZERO ORDER RELEASE

A linear relationship between the amount of drug released and time is an indication of zero order drug release. The experimental dissolution data is given in annexure B. (Table (d)) and is graphically represented in Figure 5.1. The correlation coefficient, r, = 0.9678

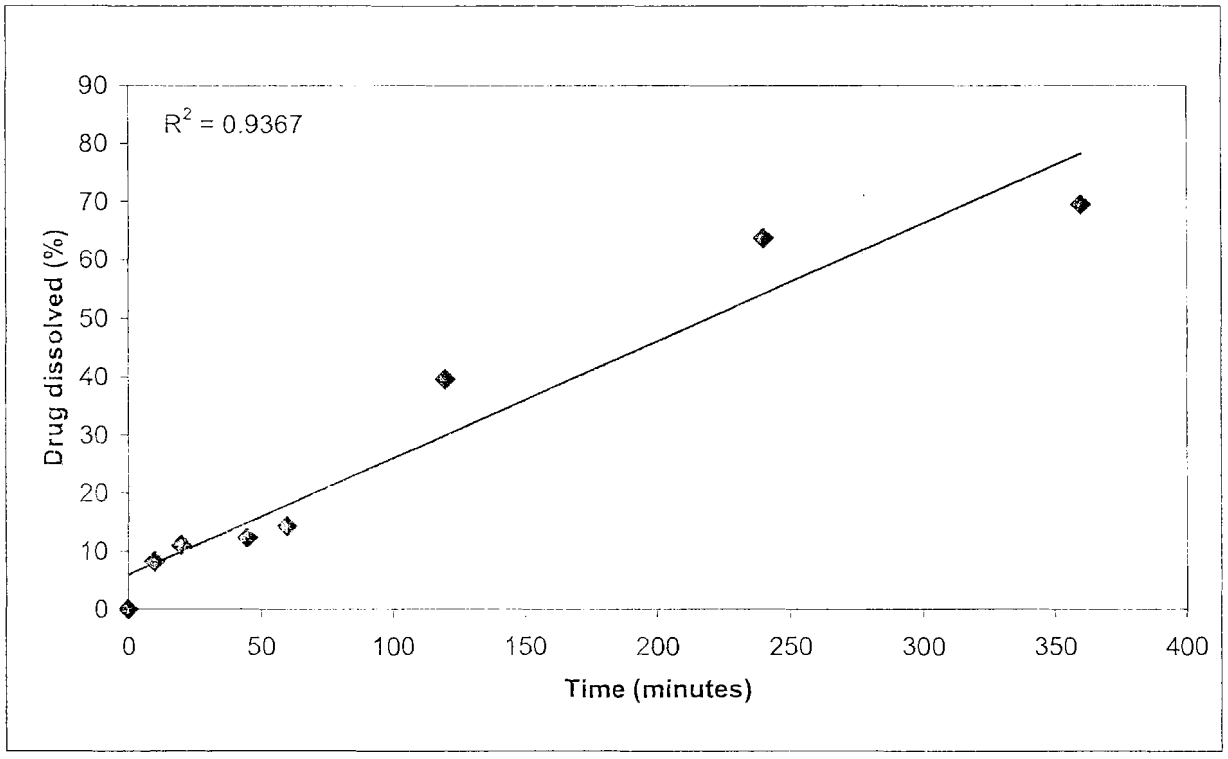

Figure 5.1: Dissolution profile of p-HCl from spherically agglomerated chitosan tablets.

5.3 FIRST ORDER RELEASE

According to the equation describing first order kinetics:

$$\log W = \log W_0 + kt/2.303 \qquad \text{Equation 5.1}$$

Where:

W	=	remaining drug concentration
W_0	=	initial amount of drug present
k	=	first order rate constant
t	=	time

A linear relationship between the logarithm of the amount of drug remaining and time would indicate first order drug release. The experimental dissolution data is given in annexure B (table (a)) and is graphically represented in figure 5.2. The correlation coefficient, r, = 0.9843

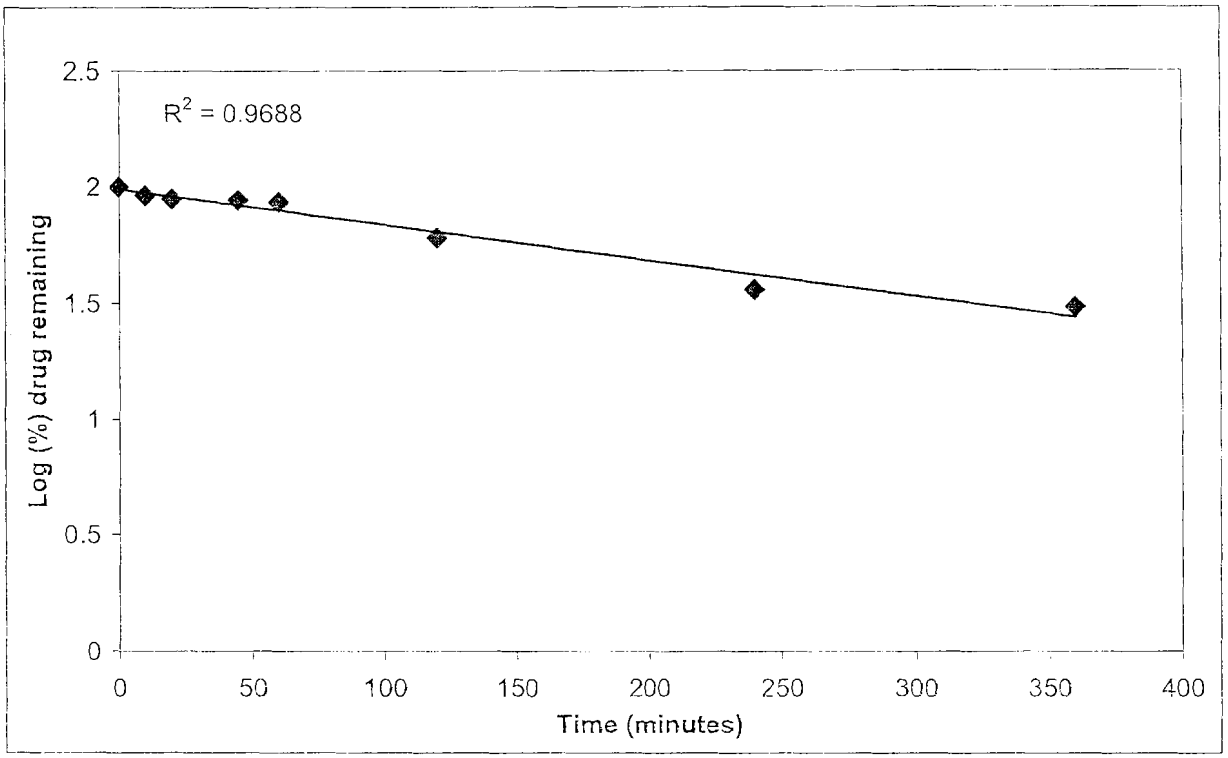

Figure 5.2: A plot of the logarithm of the percentage drug remaining against time.

An additional test to verify first order release was done to establish a linear relationship between the rate of drug release and the amount of drug released (Donbrow & Benita, 1982:548). The rate of drug release dQ'/dt, according to equation 5.1 can be derived to:

$$dQ'/dt = kW_0 - kQ' \qquad \text{Equation 5.2}$$

The rate of drug release was calculated from the experimental dissolution data given in annexure B (table (b)) and is graphically represented in figure 5.3. The correlation coefficient, r, = 0.5528.

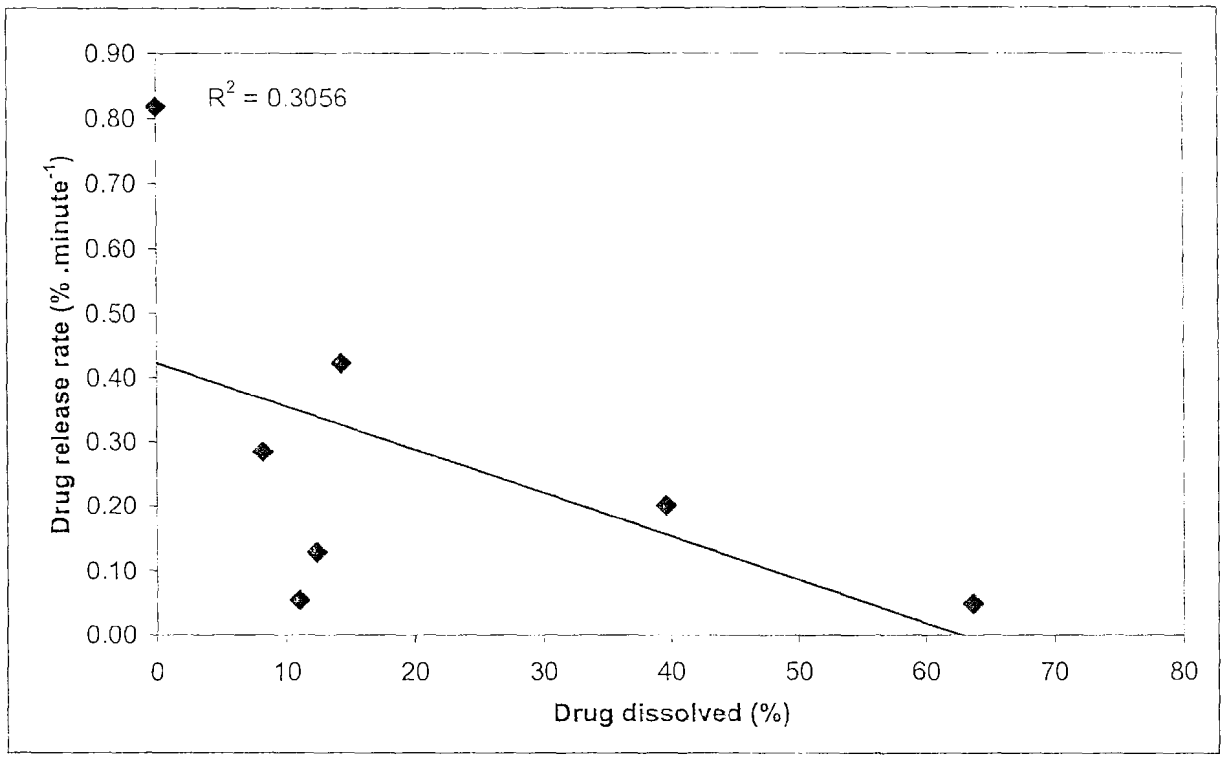

Figure 5.3: A plot of the rate of drug release against the percentage of drug dissolved.

5.4 MATRIX: DISSOLUTION

According to the law of the cube roots, a linear relationship would exist between $W_0^{1/3} - W^{1/3}$ and time if drug release is subjected to the dissolution of drug particles in the dissolution medium (Ritchel & Udeshi, 1987:739). The experimental dissolution data is given in the annexure B (table (c)) and is graphically represented in figure 5.4. The correlation coefficient, r, = 0.8143.

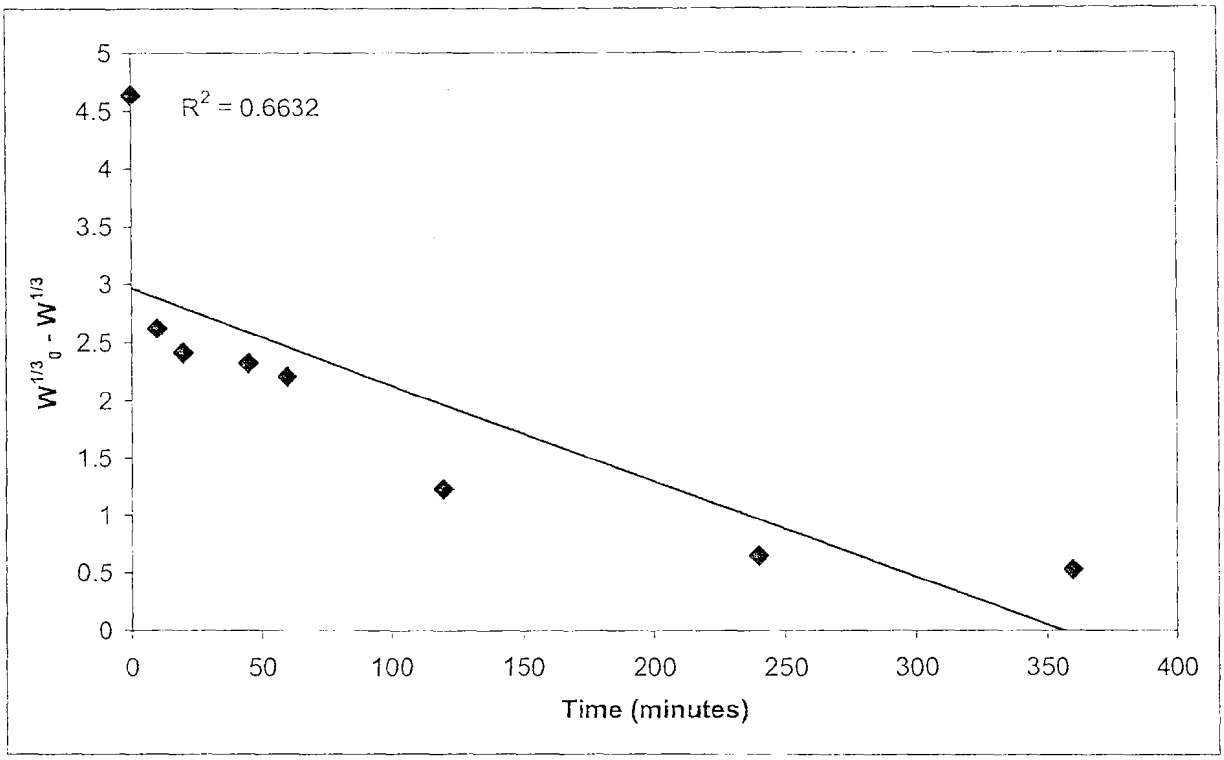

Figure 5.4: $W_0^{1/3} - W^{1/3}$ *against time.*

5.5 MATRIX: DIFFUSION.

The Higuchi equation (1963:1145) explains the drug release, dependent on diffusion, out of an inert matrix. The Higuchi equation can be transformed to equation 5.3 (Schwartz *et al*, 1968:275):

$$Q' = KSt^{1/2} \qquad \text{Equation 5.3}$$

A linear relationship would exist between the percentage of drug dissolved and the square root of time if the drug release is subjected diffusion from an inert matrix. The experimental dissolution data is given in annexure B (table (e)) and is graphically represented in figure 5.5. The correlation coefficient, r, = 0.9713.

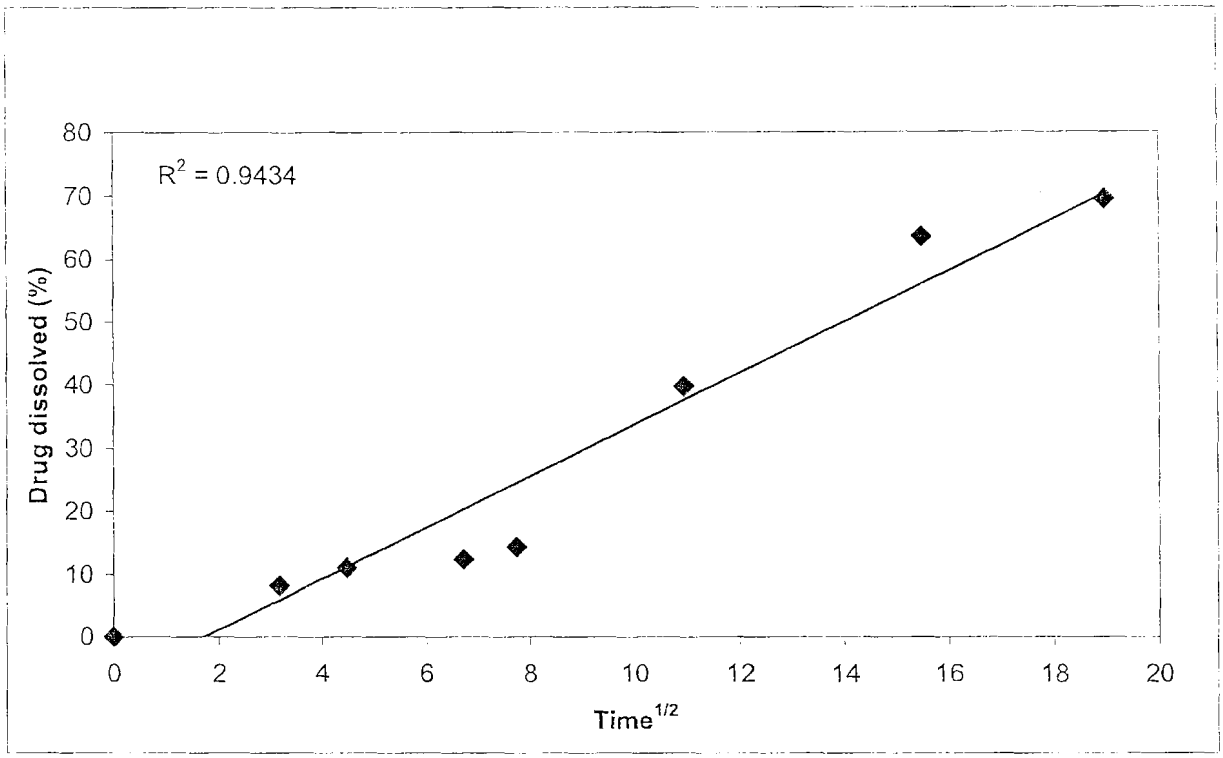

Figure 5.5: The percentage of drug dissolved versus the square root of time.

Equation 5.3 can logarithmically be presented as equation 5.4:

$$\log Q' = \log K + \frac{1}{2}\log t \qquad \text{Equation 5.4}$$

to provide an additional test for drug diffusion derived from a matrix. A graphic representation of log Q' against log t from the experimental dissolution data is given in annexure B (table (f)). The data is graphically represented in figure 5.6. The correlation coefficient, r, = 0.9577.

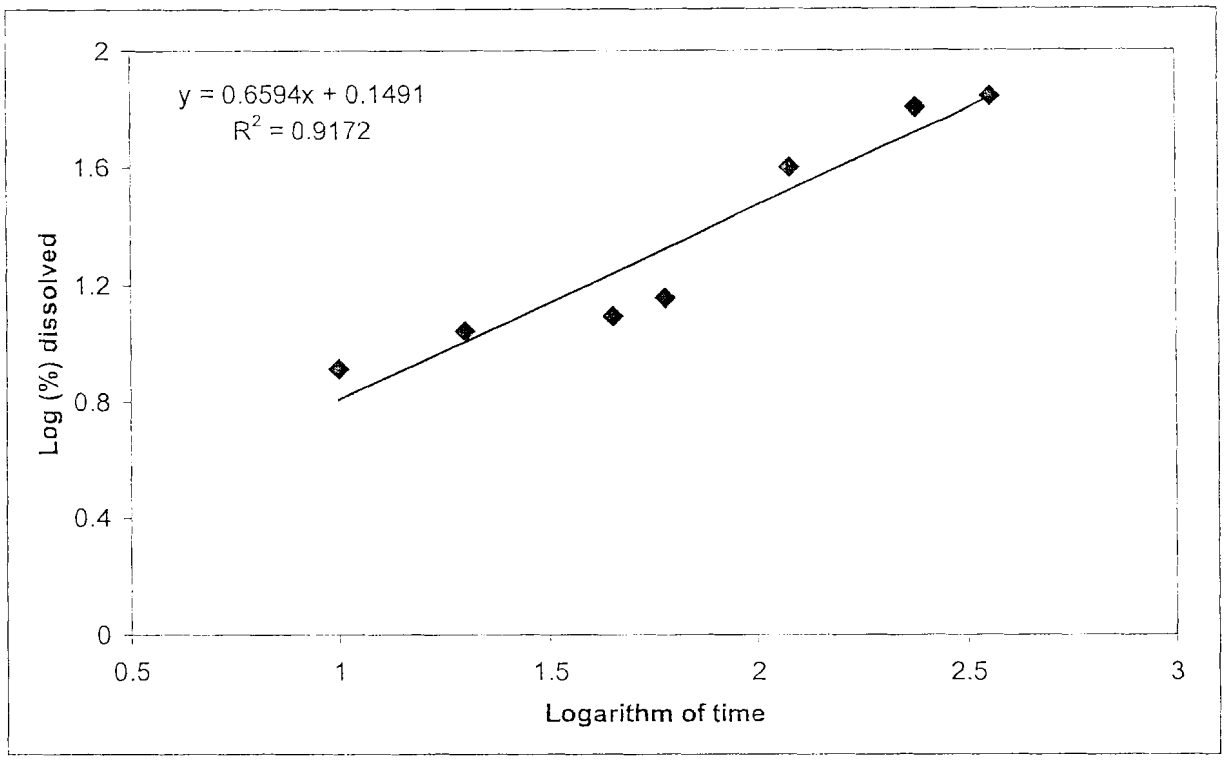

Figure 5.6: The logarithm of percentage of drug dissolved versus the logarithm of time.

5.6 CONCLUSION

The R^2-values are summarized in table 5.2. An almost linear dependency for zero order drug release is observed from figure 5.1 for the percentage of drug released against time (R^2 = 0.937). The rapid drug release for a highly water soluble, basic drug was sustained in 0.1M HCl dissolution medium.

The linearity between the logarithm of the amount of drug remaining and time was investigated to determine whether drug release was subjected to first order kinetics. The R^2 obtained from the dissolution data was 0.9688. The linearity of the release profile of a drug diffusing from an inert matrix was tested (R^2 = 0.943). It is clear that there is a legitimate linear relationship for both first order kinetics and the matrix model. It could not be said with certainty whether the drug release from spherically agglomerated chitosan tablets was in agreement with first order kinetics or the matrix model.

Additional tests were done to differentiate the two models from each other (Donbrow & Benita, 1982:79). For first order release the rate of drug release is proportionate to the percentage of

drug dissolved. No linearity was present between the rate of release and the percentage of drug released (R^2 = 0.306).

Table 5.2: Summary of R^2-values.

Release model	R^2	Data points
Zero order		
%diss / time	0.937	8
First order		
ln(100-Q)/ time	0.969	8
dq/dt /%	0.306	7
Matrix: diffusion		
%diss/$t^{1/2}$	0.943	8
Log Q/ log time	0.917	7
Matrix: dissolution		
Law of the cube roots	0.651	8

A test was conducted to establish whether drug dissolution were the rate limiting factor in the dissolution medium, according to the law of the cube roots. No linear relationship existed between $W_0^{1/3} - W^{1/3}$ and time (R^2 = 0.651). Thus, the dissolution of p-HCl is not the release rate limiting factor from the spherically agglomerated chitosan tablets.

The correlation coefficients were generally high for the tests conducted to identify matrix models subjected to diffusion release. A linear correlation is present between the percentage of drug released and the square root of time (R^2 = 0.943). Additionally, a linear relationship was found between the logarithm of the amount of drug released and the logarithm of time (R^2 = 0.917). With a slope of 0.659, it can be concluded that drug release took place passing through a porous system and as a result of a combination of diffusion through a polymer and diffusion through pores in the system (Peppas, 1985:111).

It can be concluded that the release of p-HCl from spherically agglomerated chitosan tablets is in accordance with the matrix model where diffusion is the rate limiting factor, with an almost desirable linear dependency for zero order drug release.

6. CHAPTER 6

SUMMARY

Chitosan, derived from the most abundant natural polymer available next to cellulose, lacked the micrometric properties a pharmaceutical excipient intended for direct compression had to comprise prior to spherical agglomeration. A technique for the production of a directly compressible chitosan powder was developed. The parameters contributing to successful spherical agglomeration were evaluated and the influences of the various factors on agglomeration were described. Optimum formulations were designed.

The spherical agglomeration method, an alternative technique for size enlargement particle design, produced spherical chitosan agglomerates which were able to be directly compressed, unlike chitosan powder. Chitosan powder failed to be compressed into 9 mm diameter tablets with the use of a Cadmach® eccentric press at a maximum upper punch setting of 50. However, it was experienced that chitosan and Kollidon® K25, mixed in the ratio 7:3, produced tablets with a hardness of greater than 100 Newton, but with no improvement in the flow of the powder mixture, which resulted in tablet batches with unacceptable weight variations. Only the agglomerates had free flowing and dust free properties, in contrast with the chitosan and Kollidon® K25 mixture (the addition of binder had obviously no effect on the shape of the chitosan particles).

Spherically agglomerated chitosan had enhanced micrometric properties and was compressed successfully. It was used in tablet formulations without any tableting excipients other than Kollidon® K25, an excipient that proved essential in the agglomeration step.

P-HCl is an extremely poor flowing powder and could only be compressed with chitosan after being spherically agglomerated with chitosan. No glidants were necessary, as the powder flowed freely into the tablet die. The formulations required no lubrication in view of the fact that the tablets underwent no friction during compression. The tablets had crushing strengths of greater than 100 Newton, together with minimum friability to withstand every day handling. In addition the tablets had acceptable weight variation within the limits prescribed by the British Pharmacopoeia.

P-HCl was stable during and after spherical agglomeration. The process proved stable, given the results obtained from the X-ray powder diffraction and infrared absorption spectroscopy.

P-HCl is highly soluble in weak acidic mediums which presented the challenge of formulating a prolonged release delivery system in tablet form. The mathematical comparisons of some of the dissolution profiles of the p-HCl tablets and Inderal® LA in simulated gastric media presented acceptable f2-values and good area under graph correlations. The initial drug dissolution rates of all the tablet formulas and Inderal® LA capsules were highly comparable, considering that gastric residence time is about two hours. The formulations containing p-HCl were coated with chitosan without using spray drying or capsules, accentuating the economical advantages of the spherical agglomeration technique and chitosan as pharmaceutical excipient.

The mathematical comparisons of the tablet dissolution profiles and the Inderal® LA capsules in Sörensen buffer pH 4.5 presented less similarity, as the f2, *AUCn* and *DRi* values indicated. It may however be possible to obtain more dissolution profile similarity between the tablet formulas and the commercial product if the tablets could be compressed with a greater upper punch setting than used in this study.

Various tests were done to establish the type of drug release from the tablet formulas. The correlation coefficients were acceptable for the tests conducted to identify matrix models subjected to diffusion release. A linear correlation is present between the percentage of drug released and the square root of time (R^2 = 0.943). Additionally, a linear relationship was found between the logarithm of the amount of drug released and the logarithm of time (R^2 = 0.917). With a slope of 0.659, it can be concluded that drug release took place passing through a porous system and as a result of a combination of diffusion through a polymer and diffusion through pores in the system (Peppas, 1985:111).

It can be concluded that the release of p-HCl from spherically agglomerated chitosan tablets is in accordance with the matrix model where diffusion is the rate limiting factor, with an almost desirable linear dependency for zero order drug release.

The combination of the effects of spherically agglomerated chitosan and the spherical agglomeration technique proved to be economical, safe and effective. To reduce the amount of binder utilized during agglomeration would be a desirable future prospect.

7. REFERENCES

BP (BRITISH PHARMACOPOEIA). 2002. London:HMSO. Appendix XII G. Uniformity of Weight .(Mass) [CD-ROM.]

BRUCK, S.D. 1983. Pharmacological basis of controlled drug delivery. (*In* Bruck, S.D., ed. Controlled drug delivery. Vol.1. Basic concepts. Boca Raton, Fla : CRC Press. p. 1-13.)

BUYS, G.M. 1988. Die toepassing van olie-agglomerasie vir die regulering van die dissolusiesnelheid van geneesmiddels. Potchefstroom : PU vir CHO. (Verhandeling – M.Sc.). 137 p.

BRITS, M. 2003. Crystal polymorphism and pseudopolymorphism of venlafaxine hydrochloride. Potchefstroom : PU for CHE. (Thesis – M.Sc.). 213 p.

CHOW, A.H.L. & LEUNG, W.M. 1996. A study of the mechanisms of wet spherical agglomeration of pharmaceutical powders. *Drug development and industrial pharmacy*, 22:357-371.

DONBROW, M. & BENITA, S. 1982. Release kinetics of sparingly soluble drugs from ethyl cellulose-walled microcapsules: salicylamide microcapsules: salicylamide microcapsules. *Journal of pharmacy and pharmacology,* 34:547-551.

ENNIS, B.J. 1996. Agglomeration and size enlargement. *Powder technology*, 88:203-225.

EUROTHERM. 2003. The tablet coating process. [Web:] http://www.eurotherm.com/library/industry/pharma/an_tabletcoating.pdf [Date of access: 11 March 2003].

GÅSERØD, O., JOLLIFFE, I.G., HAMPSON, F.C., DETTMAR, P.W. & SKJÅK-BRÆK, G. 1998. The enhancement of the bioadhesive properties of calcium alginate gel beads by coating with chitosan. *International journal of pharmaceutics,* 175:237-246.

HIGUCHI, T. 1963. Mechanism of sustained-action medication: theoretical analysis of rate of release of solid drugs dispersed in solid matrices. *Journal of pharmaceutical sciences,* 52:1145-1149.

IVESON, S.M., LITSTER, J.D., HAPGOOD, K. & ENNIS, B.J. 2001. Nucleation, growth and breakage phenomena in agitated wet granulation processes: a review. *Powder technology,* 117:3–39.

KAWASHIMA, Y. & CAPES, C.E. 1974. An experimental study of the kinetics of spherical agglomeration in a stirred vessel. *Powder technology,* 10:85-92.

KAWASHIMA, Y. & CAPES, C.E. 1980. Some experiments on the effect of contact angle in agglomeration from liquids. *Industrial and engineering chemistry fundamentals*, 19:312-314.

KAWASHIMA, Y., FURUKAWA, K. & TAKENAKA, H. 1981. The physicochemical parameters determining the size of agglomerate prepared by the wet spherical agglomeration technique. *Powder technology,* 30:211-216.

KAWASHIMA, Y., IMAI, M., TAKEUCHI, H., YAMAMOTO, H., KAMIYA, K. & HINO, T. 2002. Improved flowability and compactibility of spherically agglomerated crystals of ascorbic acid for direct tableting designed by spherical crystallization process. *Powder technology.* 130:283-289.

KAWASHIMA, Y., NAITO, M., LIN, S.Y. & TAKENAKA, H. 1983. An experimental study of the kinetics of the spherical crystallization of aylline sodium theophylline monohydrate. *Powder technology,* 34:255-260.

KAWASHIMA, Y., OHNO, H. & TAKENAKA, H. 1981b. Preparation of spherical matrixes of prolonged – release drugs from liquid suspension. *Journal of pharmaceutical sciences*, 70:913-916.

KAWASHIMA, Y., TAKAGI H. & TAKENAKA, H. 1981c. Wet spherical agglomeration of binary mixtures. Part II. Mechanism and kinetics of agglomeration and the crushing strength. *Chemical and pharmaceutical bulletin,* 29:1403-1409.

KELEB, E.I., VERMEIRE, A., VERVAET, C. & REMON, J.P. 2004. Twin screw granulation as a simple and efficient tool for continuous wet granulation. *International journal of pharmaceutics,* 273:183–194.

KNIGHT, P. 2004. Challenges in granulation technology. *Powder technology*, 140:156-162.

KOIZUMI, T., RITTHIDEJ, G.C. & PHAECHAMUD, T. 2001. Mechanistic modelling of drug release from chitosan coated tablets.2000. *Journal of controlled release,* 70:277–284.

KRAJEWSKA, B. 2005. Membrane-based processes performed with use of chitin/chitosan materials. *Separation and purification technology*, 41:305-312.

KYDONIEUS, A.F. 1980. Fundamental concepts of controlled release. (*In* Kydonieus, A.F., *Ed.* Controlled-release technologies: methods, theory, and applications. Vol.1. Boca Raton, Fla: CRC Press. p. 1-19.)

LEE, V.H. & ROBINSON, J.R. 1978. Methods to achieve sustained drug delivery – the physical approach: oral and parental dosage forms. (*In* Robinson, J.R., *ed.* Sustained and controlled release drug delivery systems. New York:Marcel Dekker. p.123-209.)

LEHR, C.M., BOUWSTRA, J.A., SCHACHT, E.H. & JUNGINGER, H.E. 1992. In vitro evaluation of mucoadhesive properties of chitosan and some other natural polymers. *International journal of pharmaceutics*, 78:43 - 48.

MACLEOD, G.S., FELL, J.T., COLLETT, J.H., SHARMA, H.L. & SMITH, A.M. 1999. Selective drug delivery to the colon using pectin:chitosan:hydroxypropyl methylcellulose film coated table. *International journal of pharmaceutics,* 187:251-257.

MEADES, F.W. & SPARKS, B.D. 1983. Effect of agglomerate pore structure on efficiency of solid-liquid separation by an agglomeration technique: use of a model system. *Separation science and technology,* 18:341-362.

MOORE, J.W. & FLANNER, H.H. 1996. Mathematical comparison of dissolution profiles. *Pharmaceutical technology,* 20:64-74.

NORTJÈ, J.H. 1992. Die invloed van verskillende grade PVP op die saampersbaarheid van parasetamol. Potchefstroom: PU vir CHO. (Verhandeling – M.Sc.). 155p.

OTTO, D.P. 2002. Optimisation of tablet and drug release properties of directly compressible Emcompress® formulations. Potchefstroom: PU for CHE. (Dissertation – M.Sc.). 169p.

PARROT, E.L. 1981. Compression. (*In* Lieberman, H.A. & Lachman, L., *eds.* Pharmaceutical dosage forms: tablets. Vol.2. New York : Marcel Dekker. p.153-184.)

PEPPAS, N.A. 1985. Analysis of fickian and non-fickian drug release from polymers. *Pharmaceutica acta helvetiae,* 60:110-111.

PIETSCH, W. 2003. An interdisciplinary approach to size enlargement by agglomeration. *Powder technology,*130:8-13.

PRUDAT-CHRISTIAENS, C., ARNAUD, P., ALLAIN, P. & CHAUMEIL, J.C. 1996. Aminophylline bioadhesive tablets attempted by wet granulation. *International journal of pharmaceutics*, 141:109-116.

RAVI KUMAR, M.N.V. 2000. A review of chitin and chitosan applications. *Reactive & functional polymers,* 46:1–27.

REGE, P.J., BLOCK, L.H. & SHUKLA, D.J.1999. Chitinosans as tableting excipients for modified release delivery systems. *International journal of pharmaceutics,* 181:49–60.

REGE, P.J., GARMISE, R.J., BLOCK, L.H. 2003. Spray-dried chitinosans Part I: preparation and characterization. *International journal of pharmaceutics,* 252:41–51.

RITCHEL, W.A. & UDESHI, R. 1987. Drug release mechanisms from matrix and barrier coated tablets prepared with acrylic resin, with and without addition of channeling agents. *Die Pharmazeutische Industrie*, 49:734-739.

ROSSETTI, D. & SIMONS, S.J.R. 2003. A microscale investigation of liquid bridges in the spherical agglomeration process. *Powder technology*, 130:49-55.

SÄKKINEN, M., LINNA, A., OJALA, S., JURJENSON, H., VESKI, P. & MARVOLA, M. 2002. In vivo evaluation of matrix granules containing microcrystalline chitosan as a gel-forming excipient. *International journal of pharmaceutics,* 250:227-237.

SASTRY, K.V.S. & FUERSTENAU, D.W. 1973. Mechanisms of agglomerate growth in green pelletization. *Powder technology*, 7:97-105.

SCHWARTZ, J.B., SIMONELLI, A.P. & HIGUCHI, W.I. 1968. Drug release from wax matrixes I. analysis of data with first-order kinetics and with the diffusion controlled model. *Journal of pharmaceutical sciences,* 57:274-277.

ŞENEL, S. & MCCLURE, S.J. 2004. Potential applications of chitosan in veterinary medicine. *Advanced drug delivery reviews*, 56:1467–1480.

SHEPARD, R., READER, S. & FALSHAW, A. 1997. Chitosan functional properties. *Glycoconjugate journal,* 14:535-542.

SILVERSTEIN, R.M., BASSELER, G.C. & MORRIL, T.C. 1991. Spectrometric identification of organic compounds. 5th ed. New York : Wiley. 419 p.

SÖNMEZ, İ. & CEBECCI, Y. 2003. A study on spherical oil agglomeration of barite suspensions. *International journal of mineral processing,* 71:225-232.

STANIFORTH, J. 2000. Powder flow. (*In* Aulton, M.E., *ed.* Pharmaceutics: the science of dosage form design. 2nd ed. London : Churchill Livingstone, p. 600-615.)

THEEUWES, F. 1975. Elementary osmotic pump. *Journal of pharmaceutical sciences*, 64:1987-1991.

THEEUWES, F. 1984. Oral dosage form design: status and goals of oral osmotic systems technology. *Pharmacy international,* 5:293-296.

WILLIAMS, A.C., COOPER, V.B., THOMAS, L., GRIFFITH, L.J., PETTS, C.R. & BOOTH, S.W. 2004. Evaluation of drug physical form during granulation, tabletting and storage. *International journal of pharmaceutics*, 275:29-39.

8. ANNEXURES

8.1 ANNEXURE A: THE APPLICABILITY OF SPHERICALLY AGGLOMERATED CHITOSAN FORMULATIONS

FORMULATIONS TESTED IN 0.1 M HCL (pH ~ 1.2).
FORMULA 1: Agglomeration time 10 minutes.

Table A1.1: Dissolution data of three repetitions

Time (min)	[1]C1	C2	C3	Average	*s*	*%RSD*
0	0.000	0.000	0.000	0.000	0.000	0.000
10	6.560	3.969	3.088	4.538	1.805	39.758
20	7.320	6.580	6.368	6.755	0.500	7.397
45	7.635	7.838	8.562	8.011	0.488	6.085
60	7.999	9.607	9.248	8.951	0.844	9.426
120	37.587	32.881	38.526	36.331	3.025	8.326
240	55.627	54.927	56.927	55.826	1.015	1.818
360	59.508	60.230	60.241	59.993	0.420	0.700
[2]DR	0.278	0.254	0.302	0.278	0.024	8.662
[3]AUC	14274.85	13836.12	14573.43	14228.13	370.87	2.607

[1]*Corrected sample concentration ($\mu g.cm^{-3}$)*
[2]*DR_i = initial dissolution rate ($\mu g.cm^{-3}.min^{-1}$)*
[3]*AUC = area under curve ($\mu g.min.cm^{-3}$)*

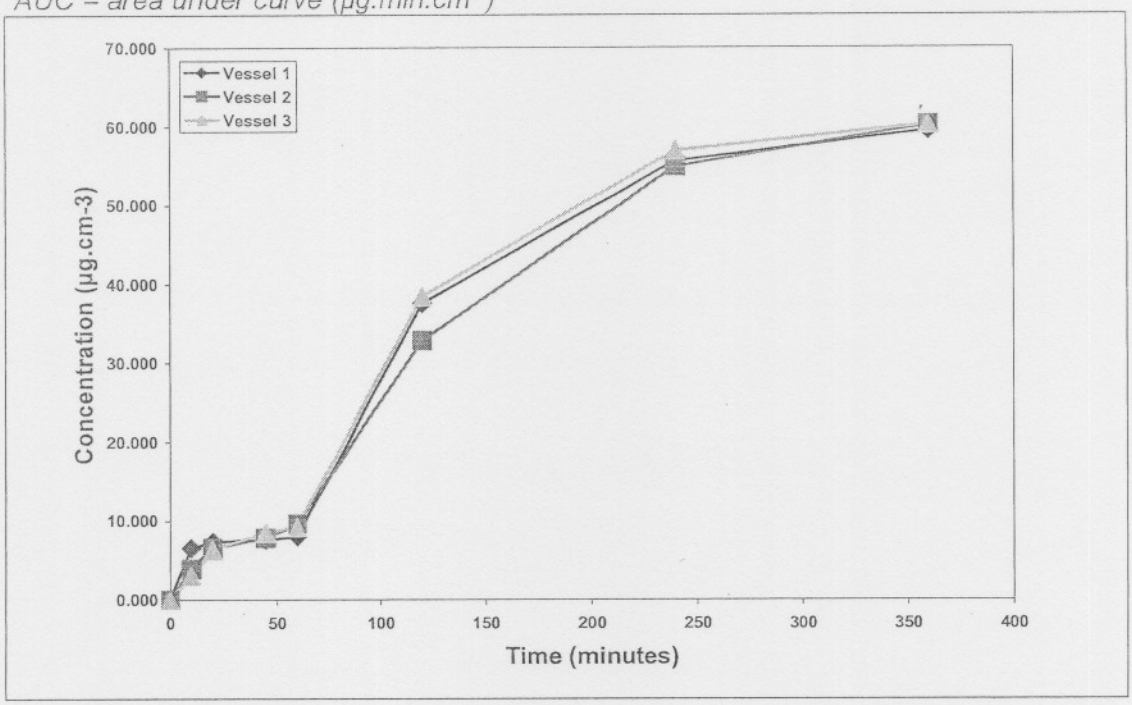

Figure A1.1: Dissolution profiles of individual stations.

FORMULATIONS TESTED IN 0.1 M HCL (pH ~ 1.2).
FORMULA 1: Agglomeration time 15 minutes.

Table A1.2: Dissolution data of three repetitions

Time (min)	[1]C1	C2	C3	Average	*s*	*%RSD*
0	0.000	0.000	0.000	0.000	0.000	0.000
10	3.969	3.710	4.642	4.107	0.481	11.722
20	3.834	2.900	3.838	3.523	0.540	15.335
45	6.424	6.419	6.786	6.542	0.211	3.224
60	8.303	8.252	8.616	8.390	0.197	2.352
120	46.708	50.749	49.974	49.143	2.145	4.364
240	62.361	65.337	66.006	64.568	1.940	3.005
360	62.292	63.448	65.110	63.616	1.417	2.227
[2]DR	0.368	0.403	0.393	0.388	0.018	4.659
[3]AUC	15971.16	16740.36	16897.38	16536.30	495.682	2.998

[1]*Corrected sample concentration ($\mu g.cm^{-3}$)*
[2]*DR_i = initial dissolution rate ($\mu g.cm^{-3}.min^{-1}$)*
[3]*AUC = area under curve ($\mu g.min.cm^{-3}$)*

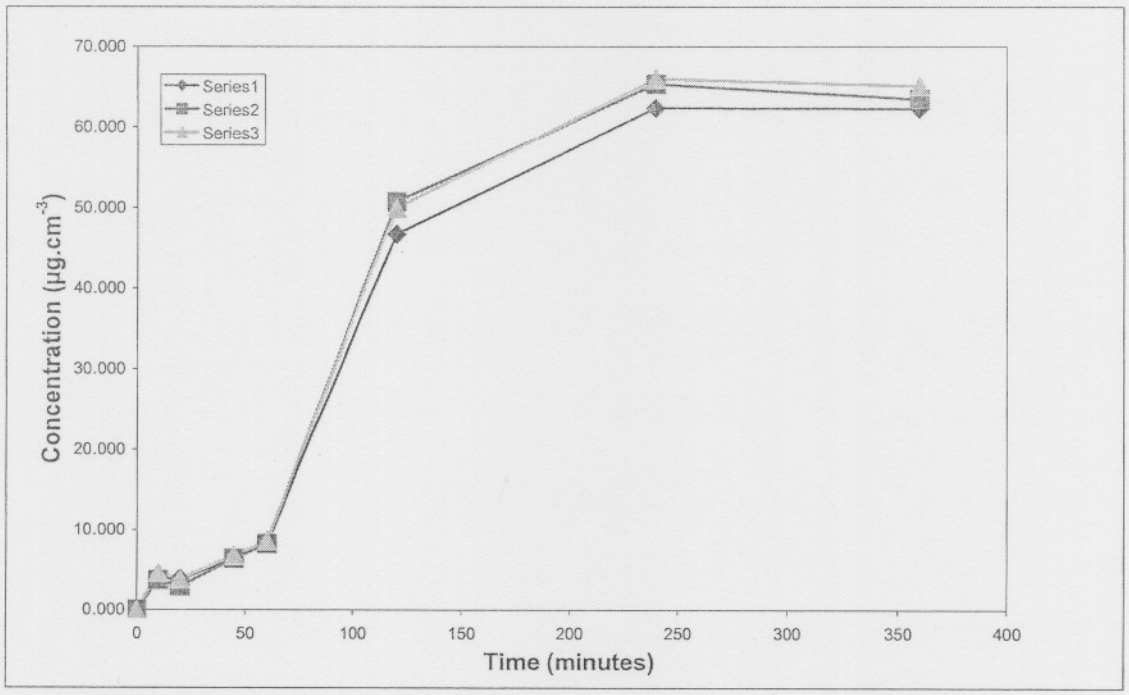

Figure A1.2: Dissolution profiles of individual stations.

FORMULATIONS TESTED IN 0.1 M HCL (pH ~ 1.2).
FORMULA 1: Agglomeration time 20 minutes.

Table A1.3: Dissolution data of three repetitions

Time (min)	[1]C1	C2	C3	Average	s	%RSD
0	0.000	0.000	0.000	0.000	0.000	0.000
10	2.725	2.777	2.363	2.622	0.226	8.614
20	3.775	4.035	3.825	3.878	0.138	3.549
45	6.113	6.580	6.216	6.303	0.246	3.897
60	7.887	8.304	7.888	8.026	0.241	2.998
120	45.099	39.972	43.441	42.837	2.616	6.108
240	63.544	63.153	64.778	63.825	0.848	1.329
360	64.164	64.058	63.963	64.062	0.100	0.156
[2]DR	0.359	0.318	0.347	0.341	0.021	6.162
[3]AUC	16045.35	15560.67	16031.56	15879.19	275.93	1.738

[1] *Corrected sample concentration ($\mu g.cm^{-3}$)*
[2] *DR_i = initial dissolution rate ($\mu g.cm^{-3}.min^{-1}$)*
[3] *AUC = area under curve ($\mu g.min.cm^{-3}$)*

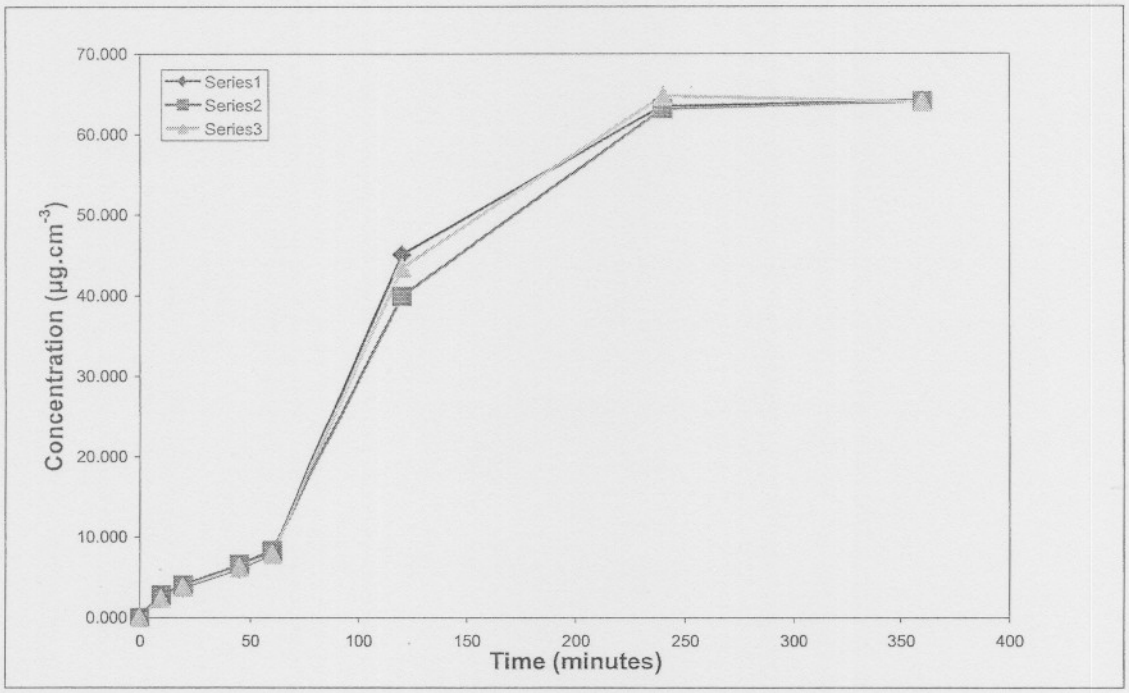

Figure A1.3 :Dissolution profiles of individual stations.

FORMULATIONS TESTED IN 0.1 M HCL (pH ~ 1.2).
FORMULA 2: Agglomeration time 10 minutes.

Table A1.4: Dissolution data of three repetitions

Time (min)	[1]C1	C2	C3	Average	s	%RSD
0	0.000	0.000	0.000	0.000	0.000	0.000
10	5.679	8.166	8.321	7.389	1.483	20.069
20	6.382	9.868	10.231	8.827	2.125	24.074
45	9.650	10.447	10.656	10.251	0.531	5.177
60	12.518	12.471	13.508	12.832	0.586	4.564
120	54.451	70.409	55.389	60.083	8.955	14.904
240	68.829	71.405	69.611	69.948	1.321	1.888
360	69.426	70.735	70.622	70.261	0.725	1.032
[2]DR	0.427	0.538	0.419	0.461	0.067	14.483
[3]AUC	18156.53	20080.42	18557.63	18931.53	1014.98	5.361

[1]*Corrected sample concentration ($\mu g.cm^{-3}$)*
[2]*DR_i = initial dissolution rate ($\mu g.cm^{-3}.min^{-1}$)*
[3]*AUC = area under curve ($\mu g.min.cm^{-3}$)*

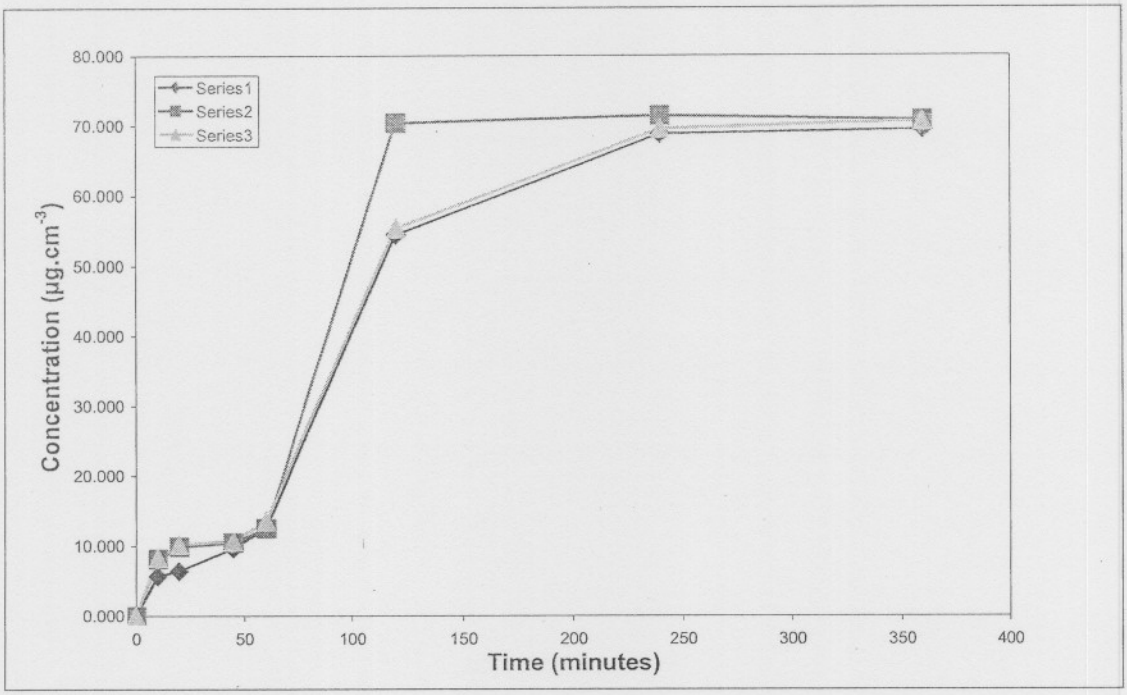

Figure A1.4: Dissolution profiles of individual stations.

FORMULATIONS TESTED IN 0.1 M HCL (pH ~ 1.2).
FORMULA 2: Agglomeration time 15 minutes.

Table A1.5: Dissolution data of three repetitions

Time (min)	[1]C1	C2	C3	Average	*s*	*%RSD*
0	0.000	0.000	0.000	0.000	0.000	0.000
10	4.435	3.606	3.503	3.848	0.511	13.284
20	4.355	4.143	4.764	4.420	0.316	7.144
45	6.789	6.425	7.206	6.807	0.391	5.739
60	8.772	8.200	9.085	8.685	0.449	5.168
120	32.306	38.365	37.852	36.174	3.360	9.288
240	58.810	61.279	61.431	60.507	1.471	2.432
360	62.687	62.182	62.753	62.541	0.312	0.499
[2]DR	0.251	0.302	0.298	0.284	0.028	9.974
[3]AUC	14311.2	15081.78	15146.79	14846.59	464.80	3.131

[1]Corrected sample concentration ($\mu g.cm^{-3}$)
[2]DR_i = initial dissolution rate ($\mu g.cm^{-3}.min^{-1}$)
[3]AUC = area under curve ($\mu g.min.cm^{-3}$)

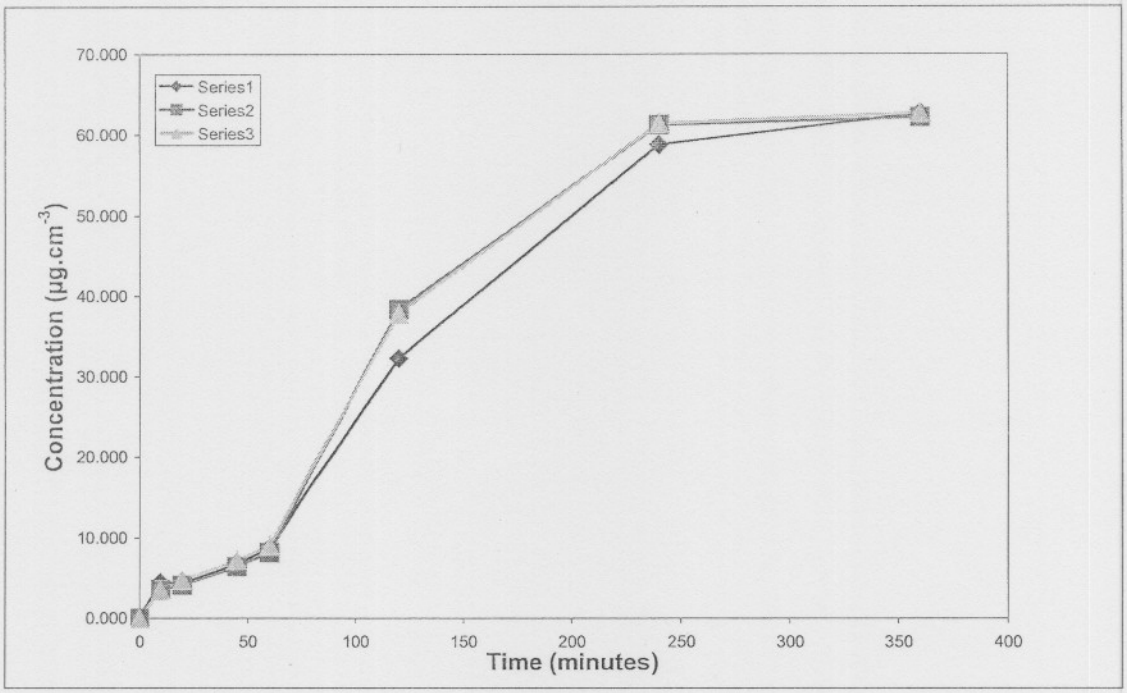

Figure A1.5: Dissolution profiles of individual stations.

FORMULATIONS TESTED IN 0.1 M HCL (pH ~ 1.2).
FORMULA 2: Agglomeration time 20 minutes.

Table A1.6: Dissolution data of three repetitions

Time (min)	[1]C1	C2	C3	Average	s	%RSD
0	0.000	0.000	0.000	0.000	0.000	0.000
10	3.658	4.021	3.451	3.709	0.288	7.776
20	5.076	5.078	4.712	4.955	0.211	4.251
45	7.933	7.363	7.517	7.604	0.295	3.878
60	10.125	9.345	9.398	9.622	0.436	4.532
120	50.085	48.579	47.335	48.666	1.377	2.830
240	63.883	67.760	67.598	66.413	2.193	3.303
360	65.305	67.037	65.948	66.096	0.875	1.324
[2]DR	0.397	0.382	0.375	0.385	0.011	2.903
[3]AUC	16755.67	17152.26	16948.49	16952.14	198.32	1.170

[1]Corrected sample concentration ($\mu g.cm^{-3}$)
[2]DR_i = initial dissolution rate ($\mu g.cm^{-3}.min^{-1}$)
[3]AUC = area under curve ($\mu g.min.cm^{-3}$)

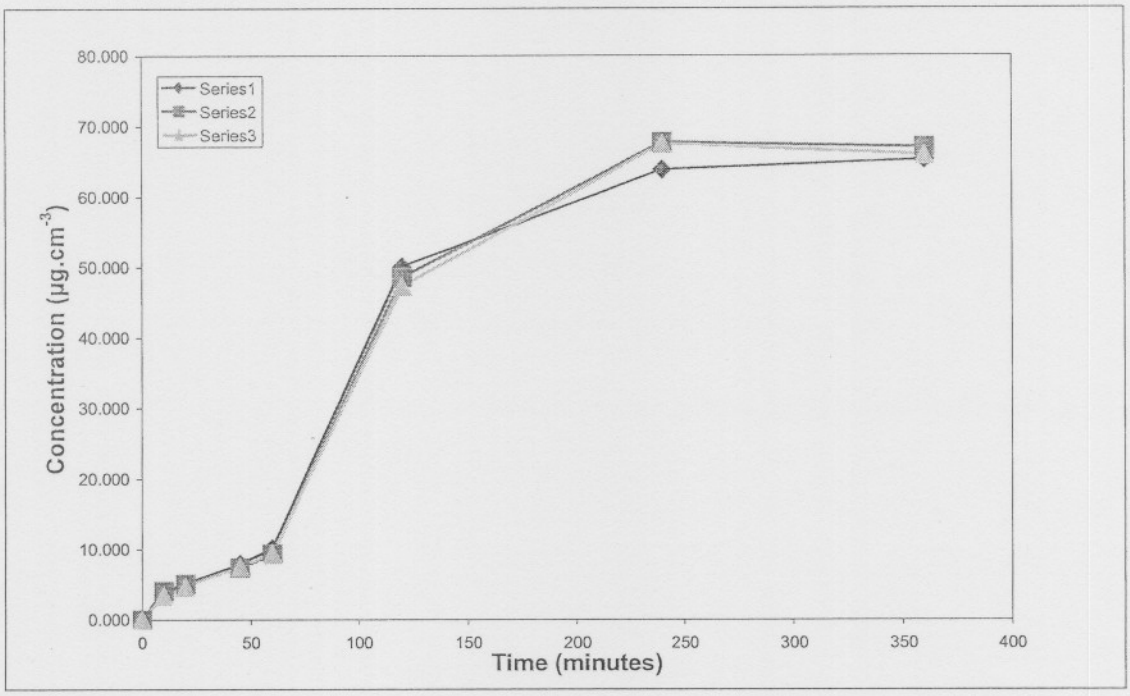

Figure A1.6: Dissolution profiles of individual stations.

FORMULATIONS TESTED IN 0.1 M HCL (pH ~ 1.2).
FORMULA 3: Agglomeration time 10 minutes.

Table A1.7: Dissolution data of three repetitions

Time (min)	[1]C1	C2	C3	Average	*s*	*%RSD*
0	0.000	0.000	0.000	0.000	0.000	0.000
10	7.078	6.301	6.041	6.473	0.539	8.331
20	5.406	5.194	8.250	6.283	1.706	27.158
45	12.598	9.177	8.210	9.995	2.306	23.068
60	12.275	11.376	10.386	11.345	0.945	8.331
120	40.097	33.149	40.294	37.846	4.069	10.752
240	59.786	58.037	59.424	59.082	0.923	1.562
360	61.397	61.335	61.084	61.271	0.166	0.271
[2]DR	0.310	0.255	0.304	0.290	0.030	10.411
[3]AUC	15344.49	14392.06	15180.83	14972.46	509.26	3.401

[1]*Corrected sample concentration ($\mu g.cm^{-3}$)*
[2]*DR_i = initial dissolution rate ($\mu g.cm^{-3}.min^{-1}$)*
[3]*AUC = area under curve ($\mu g.min.cm^{-3}$)*

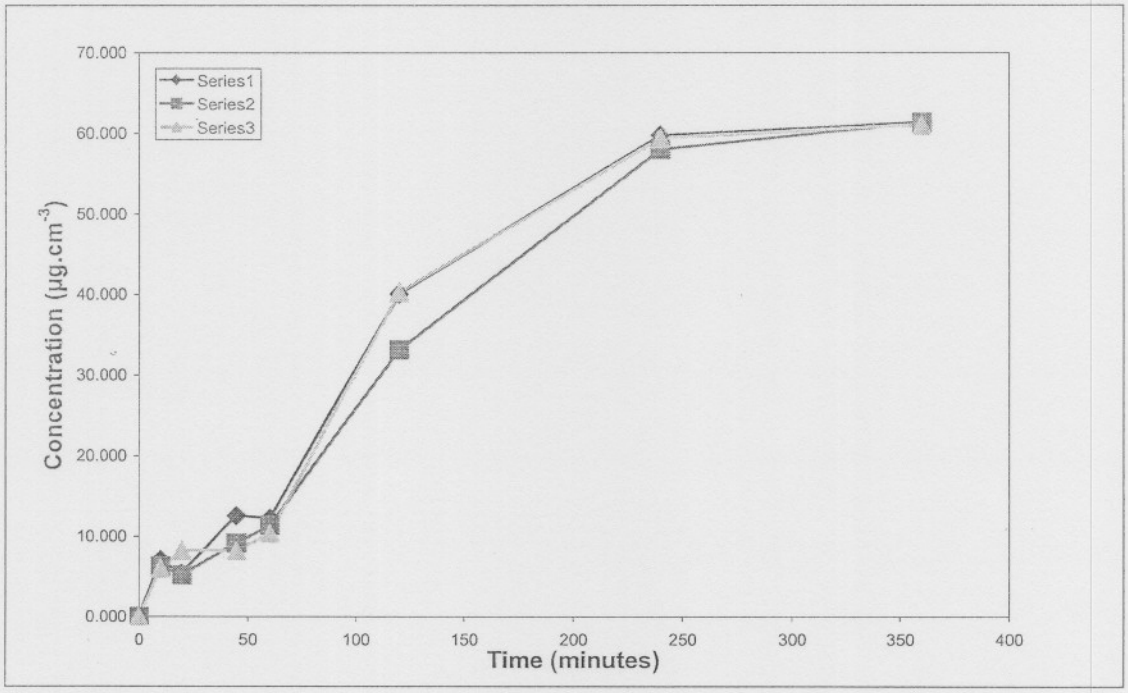

Figure A1.7: Dissolution profiles of individual stations.

FORMULATIONS TESTED IN 0.1 M HCL (pH ~ 1.2).
FORMULA 3: Agglomeration time 15 minutes.

Table A1.8: Dissolution data of three repetitions

Time (min)	[1]C1	C2	C3	Average	*s*	*%RSD*
0	0.000	0.000	0.000	0.000	0.000	0.000
10	3.762	3.554	4.073	3.796	0.261	6.870
20	5.076	4.920	5.544	5.180	0.325	6.274
45	7.674	8.088	8.609	8.123	0.469	5.769
60	9.709	10.541	10.958	10.402	0.636	6.111
120	46.197	47.704	52.318	48.739	3.189	6.543
240	66.037	64.336	67.781	66.051	1.723	2.608
360	65.214	64.738	66.104	65.351	0.693	1.061
[2]DR	0.365	0.379	0.414	0.386	0.025	6.560
[3]AUC	16639.05	16576.6	17529.44	16915.03	533.01	3.151

[1]*Corrected sample concentration ($\mu g.cm^{-3}$)*
[2]*DR_i = initial dissolution rate ($\mu g.cm^{-3}.min^{-1}$)*
[3]*AUC = area under curve ($\mu g.min.cm^{-3}$)*

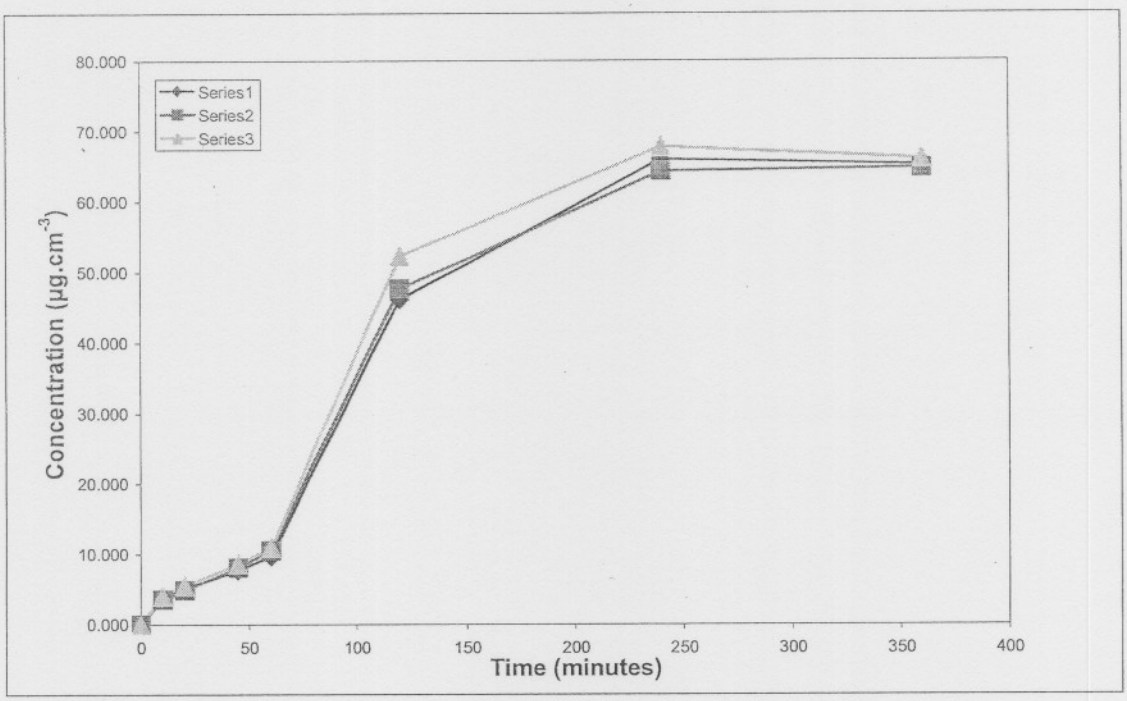

Figure A1.8: Dissolution profiles of individual stations.

FORMULATIONS TESTED IN 0.1 M HCL (pH ~ 1.2).
FORMULA 3: Agglomeration time 20 minutes.

Table A1.9: Dissolution data of three repetitions

Time (min)	[1]C1	C2	C3	Average	*s*	*%RSD*
0	0.000	0.000	0.000	0.000	0.000	0.000
10	4.383	4.383	4.073	4.279	0.179	4.194
20	6.323	5.753	5.959	6.011	0.289	4.801
45	9.961	8.973	9.493	9.475	0.494	5.214
60	15.991	11.685	13.657	13.777	2.156	15.645
120	52.761	48.851	47.514	49.708	2.726	5.484
240	70.478	68.021	66.666	68.388	1.932	2.825
360	69.280	68.282	66.823	68.128	1.235	1.813
[2]DR	0.424	0.386	0.380	0.397	0.024	6.051
[3]AUC	18315.91	17418.12	17132.62	17622.21	617.48	3.504

[1]*Corrected sample concentration ($\mu g.cm^{-3}$)*
[2]*DR_i = initial dissolution rate ($\mu g.cm^{-3}.min^{-1}$)*
[3]*AUC = area under curve ($\mu g.min.cm^{-3}$)*

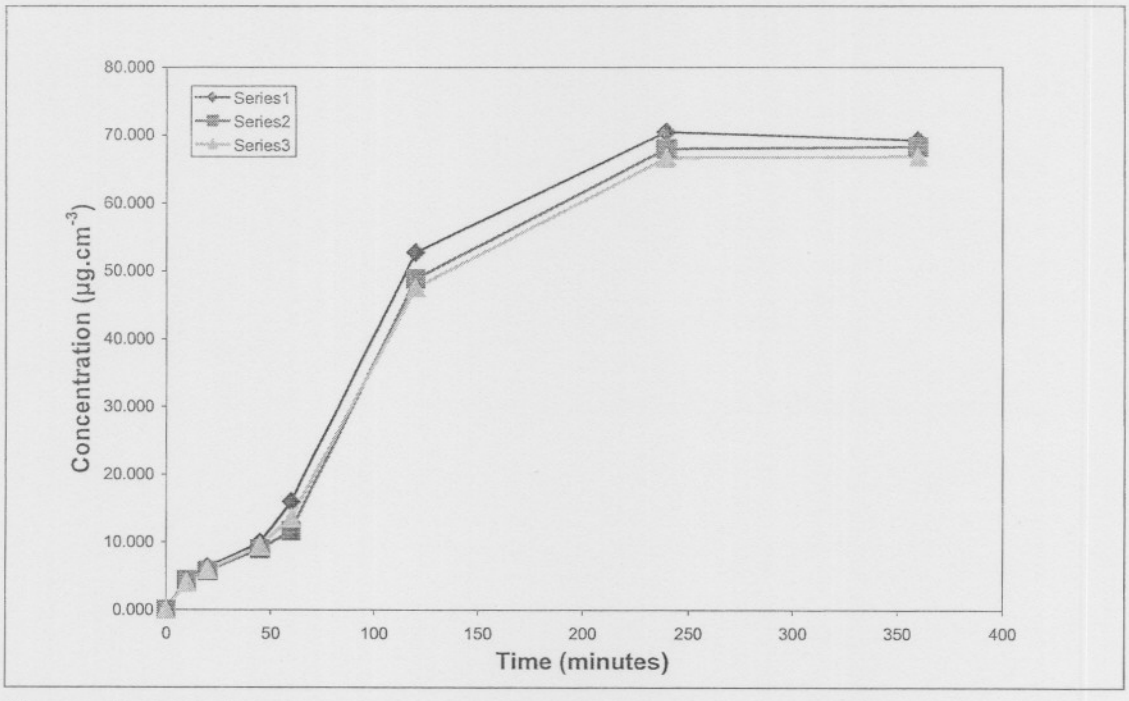

Figure A1.9: Dissolution profiles of individual stations.

FORMULATIONS TESTED IN 0.1 M HCL (pH ~ 1.2).
Inderal® LA 80 mg

Table A1.10: Dissolution data of three repetitions

Time	R 1	R 2	R 3	Average	[1]Cave	s	%RSD
0	0.000	0.000	0.000	0.000	0.000	0.000	0.000
10	0.046	0.021	0.022	0.029	6.616	0.014	47.709
20	0.096	0.1	0.054	0.083	9.366	0.025	30.578
45	0.188	0.145	0.126	0.153	14.436	0.031	20.761
60	0.24	0.147	0.184	0.190	17.321	0.046	24.600
120	0.389	0.263	0.357	0.336	25.551	0.065	19.472
240	0.626	0.454	0.577	0.552	38.591	0.088	16.043
360	0.787	0.595	0.736	0.706	47.510	0.099	14.086
[2]DR_i	0.195						
[3]AUC	10949.45						

[1]*Corrected sample average concentration ($\mu g.cm^{-3}$)*
[2]*DR_i = initial dissolution rate ($\mu g.cm^{-3}.min^{-1}$)*
[3]*AUC = area under curve ($\mu g.min.cm^{-3}$)*

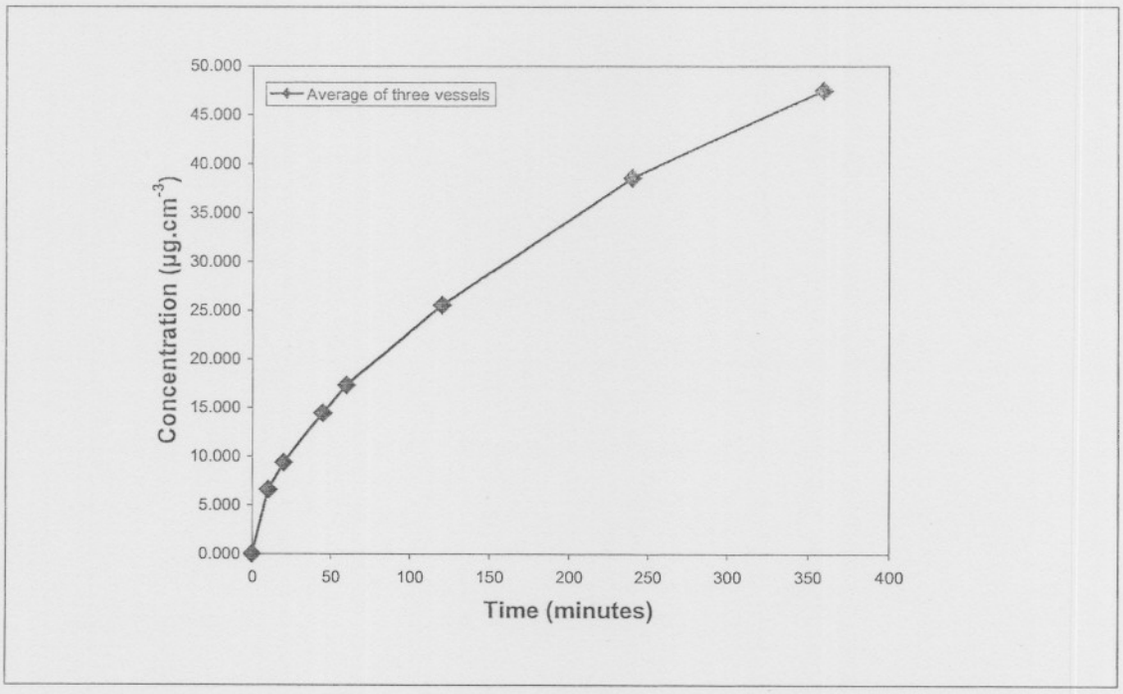

Figure A1.10: Dissolution profiles of individual stations.

FORMULATIONS TESTED IN SÖRENSEN BUFFER (pH ~ 4.5).
FORMULA 1: Agglomeration time 10 minutes.

Table A2.1: Dissolution data for three repetitions.

Time (min)	[1]C1	C2	C3	Average	*s*	*%RSD*
0	0.000	0.000	0.000	0.000	0.000	0.000
10	6.560	3.969	3.088	4.538	1.805	39.758
20	7.320	6.580	6.368	6.755	0.500	7.397
45	7.635	7.838	8.562	8.011	0.488	6.085
60	7.999	9.607	9.248	8.951	0.844	9.426
120	37.587	32.881	38.526	36.331	3.025	8.326
240	55.627	54.927	56.927	55.826	1.015	1.818
360	59.508	60.230	60.241	59.993	0.420	0.700
[2]DR_i	0.278	0.254	0.302	0.278	0.024	8.662
[3]AUC	14274.85	13836.12	14573.43	14228.13	370.87	2.607

[1]*Corrected sample concentration ($\mu g.cm^{-3}$)*
[2]*DR_i = initial dissolution rate ($\mu g.cm^{-3}.min^{-1}$)*
[3]*AUC = area under curve ($\mu g.min.cm^{-3}$)*

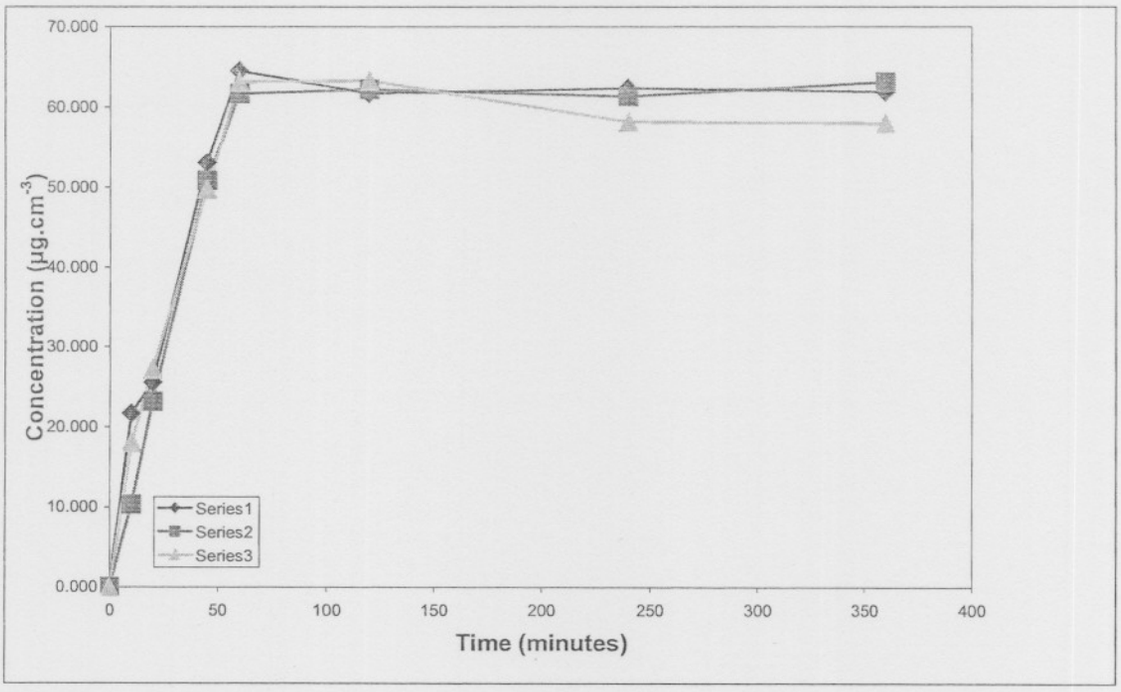

Figure A2.1: Dissolution profiles of individual stations.

FORMULATIONS TESTED IN SÖRENSEN BUFFER (pH ~ 4.5).
FORMULA 1: Agglomeration time 15 minutes.

Table A2.2: Dissolution data for three repetitions.

Time (min)	[1]C1	C2	C3	Average	s	%RSD
0	0.000	0.000	0.000	0.000	0.000	0.000
10	3.969	3.710	4.642	4.107	0.481	11.722
20	3.834	2.900	3.838	3.523	0.540	15.335
45	6.424	6.419	6.786	6.542	0.211	3.224
60	8.303	8.252	8.616	8.390	0.197	2.352
120	46.708	50.749	49.974	49.143	2.145	4.364
240	62.361	65.337	66.006	64.568	1.940	3.005
360	62.292	63.448	65.110	63.616	1.417	2.227
[2]DR_i	0.368	0.403	0.393	0.388	0.018	4.659
[3]AUC	15971.16	16740.36	16897.38	16536.31	495.68	2.998

[1]*Corrected sample concentration ($\mu g.cm^{-3}$)*
[2]*DR_i = initial dissolution rate ($\mu g.cm^{-3}.min^{-1}$)*
[3]*AUC = area under curve ($\mu g.min.cm^{-3}$)*

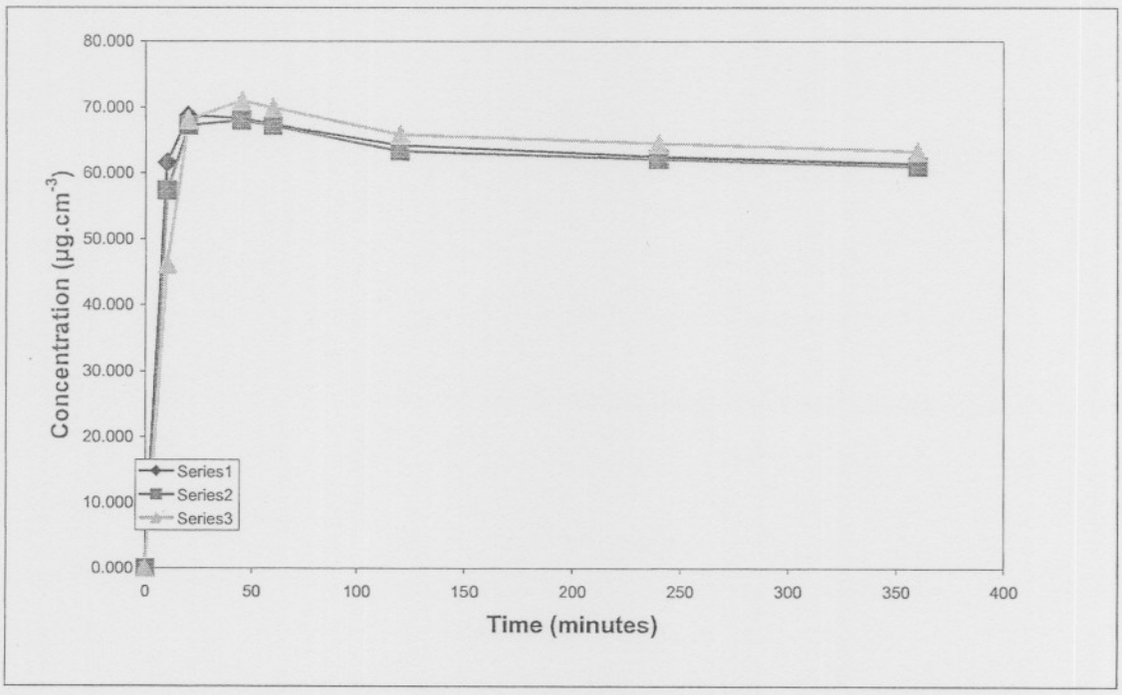

Figure A2.2: Dissolution profiles of individual stations.

FORMULATIONS TESTED IN SÖRENSEN BUFFER (pH ~ 4.5).
FORMULA 1: Agglomeration time 20 minutes.

Table A2.3: Dissolution data for three repetitions.

Time (min)	[1]C1	C2	C3	Average	*s*	*%RSD*
0	0.000	0.000	0.000	0.000	0.000	0.000
10	2.725	2.777	2.363	2.621	0.226	8.614
20	3.775	4.035	3.825	3.878	0.138	3.549
45	6.113	6.580	6.216	6.303	0.246	3.897
60	7.887	8.304	7.888	8.026	0.241	2.998
120	45.099	39.972	43.441	42.837	2.616	6.108
240	63.544	63.153	64.778	63.825	0.848	1.329
360	64.164	64.058	63.963	64.061	0.100	0.156
[2]DR_i	0.359	0.318	0.347	0.341	0.021	6.163
[3]AUC	16045.35	15560.67	16031.56	15879.19	275.94	1.738

[1]*Corrected sample concentration ($\mu g.cm^{-3}$)*
[2]*DR_i = initial dissolution rate ($\mu g.cm^{-3}.min^{-1}$)*
[3]*AUC = area under curve ($\mu g.min.cm^{-3}$)*

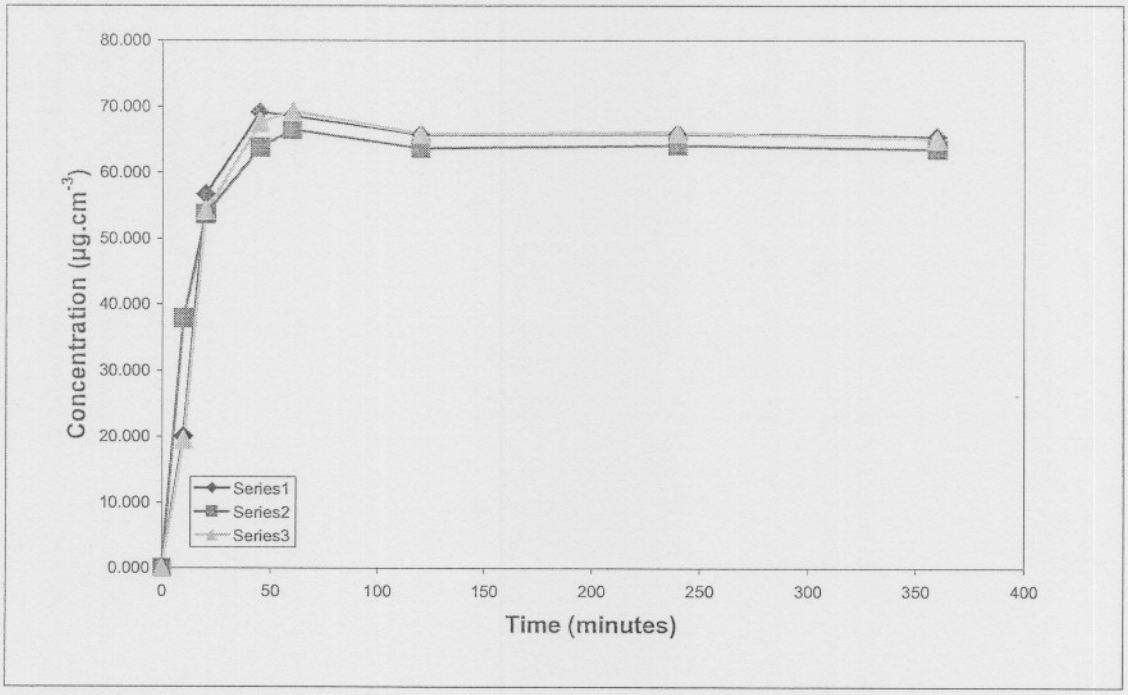

Figure A2.3: Dissolution profiles of individual stations.

FORMULATIONS TESTED IN SÖRENSEN BUFFER (pH ~ 4.5).
FORMULA 2: Agglomeration time 10 minutes.

Table A2.4: Dissolution data for three repetitions.

Time (min)	[1]C1	C2	C3	Average	*s*	*%RSD*
0	0.000	0.000	0.000	0.000	0.000	0.000
10	5.679	8.166	8.321	7.388	1.483	20.069
20	6.382	9.868	10.231	8.827	2.125	24.074
45	9.650	10.447	10.656	10.251	0.531	5.177
60	12.518	12.471	13.508	12.832	0.586	4.564
120	54.451	70.409	55.389	60.083	8.955	14.904
240	68.829	71.405	69.611	69.948	1.321	1.888
360	69.426	70.735	70.622	70.260	0.725	1.032
[2]DR_i	0.427	0.538	0.419	0.461	0.067	14.483
[3]AUC	18156.53	20080.42	18557.63	18931.53	1014.98	5.361

[1]*Corrected sample concentration ($\mu g.cm^{-3}$)*
[2]*DR_i = initial dissolution rate ($\mu g.cm^{-3}.min^{-1}$)*
[3]*AUC = area under curve ($\mu g.min.cm^{-3}$)*

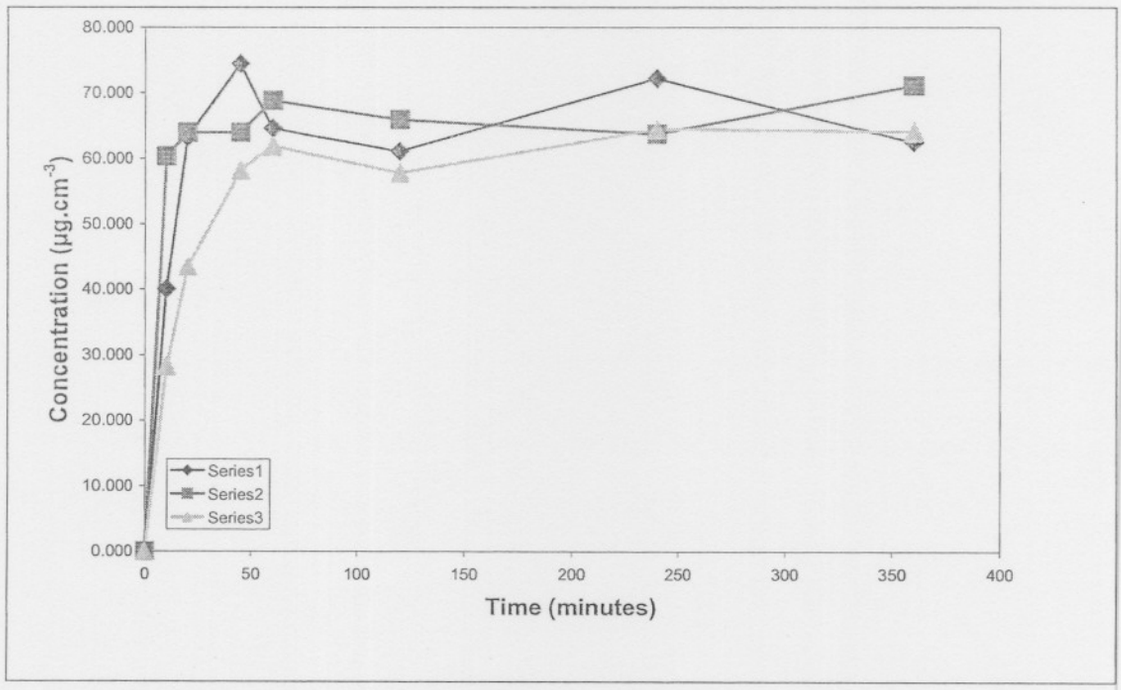

Figure A2.4: Dissolution profiles of individual stations.

FORMULATIONS TESTED IN SÖRENSEN BUFFER (pH ~ 4.5).
FORMULA 2: Agglomeration time 15 minutes.

Table A2.5: Dissolution data for three repetitions.

Time (min)	[1]C1	C2	C3	Average	*s*	*%RSD*
0	0.000	0.000	0.000	0.000	0.000	0.000
10	4.435	3.606	3.503	3.848	0.511	13.284
20	4.355	4.143	4.764	4.420	0.316	7.144
45	6.789	6.425	7.206	6.806	0.391	5.739
60	8.772	8.200	9.085	8.685	0.449	5.168
120	32.306	38.365	37.852	36.174	3.360	9.288
240	58.810	61.279	61.431	60.506	1.471	2.432
360	62.687	62.182	62.753	62.540	0.312	0.499
[2]DR_i	0.251	0.302	0.298	0.284	0.028	9.974
[3]AUC	14311.2	15081.78	15146.79	14846.59	464.80	3.131

[1]*Corrected sample concentration ($\mu g.cm^{-3}$)*
[2]*DR_i = initial dissolution rate ($\mu g.cm^{-3}.min^{-1}$)*
[3]*AUC = area under curve ($\mu g.min.cm^{-3}$)*

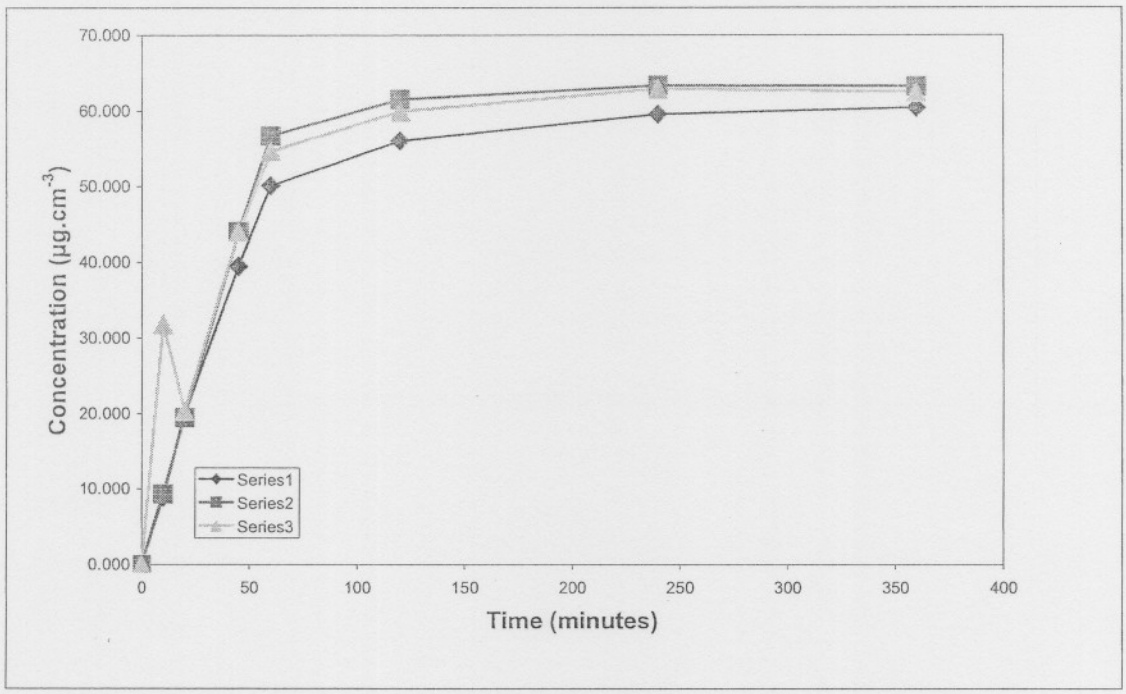

Figure A2.5: Dissolution profiles of individual stations.

FORMULATIONS TESTED IN SÖRENSEN BUFFER (pH ~ 4.5).
FORMULA 2: Agglomeration time 20 minutes.

Table A2.6: Dissolution data for three repetitions.

Time (min)	[1]C1	C2	C3	Average	*s*	*%RSD*
0	0.000	0.000	0.000	0.000	0.000	0.000
10	3.658	4.021	3.451	3.709	0.288	7.776
20	5.076	5.078	4.712	4.955	0.211	4.251
45	7.933	7.363	7.517	7.604	0.295	3.878
60	10.125	9.345	9.398	9.622	0.436	4.532
120	50.085	48.579	47.335	48.666	1.377	2.830
240	63.883	67.760	67.598	66.413	2.193	3.303
360	65.305	67.037	65.948	66.096	0.875	1.324
[2]DR_i	0.397	0.382	0.375	0.385	0.011	2.903
[3]AUC	16755.67	17152.26	16948.49	16952.14	198.32	1.170

[1]*Corrected sample concentration ($\mu g.cm^{-3}$)*
[2]*DR_i = initial dissolution rate ($\mu g.cm^{-3}.min^{-1}$)*
[3]*AUC = area under curve ($\mu g.min.cm^{-3}$)*

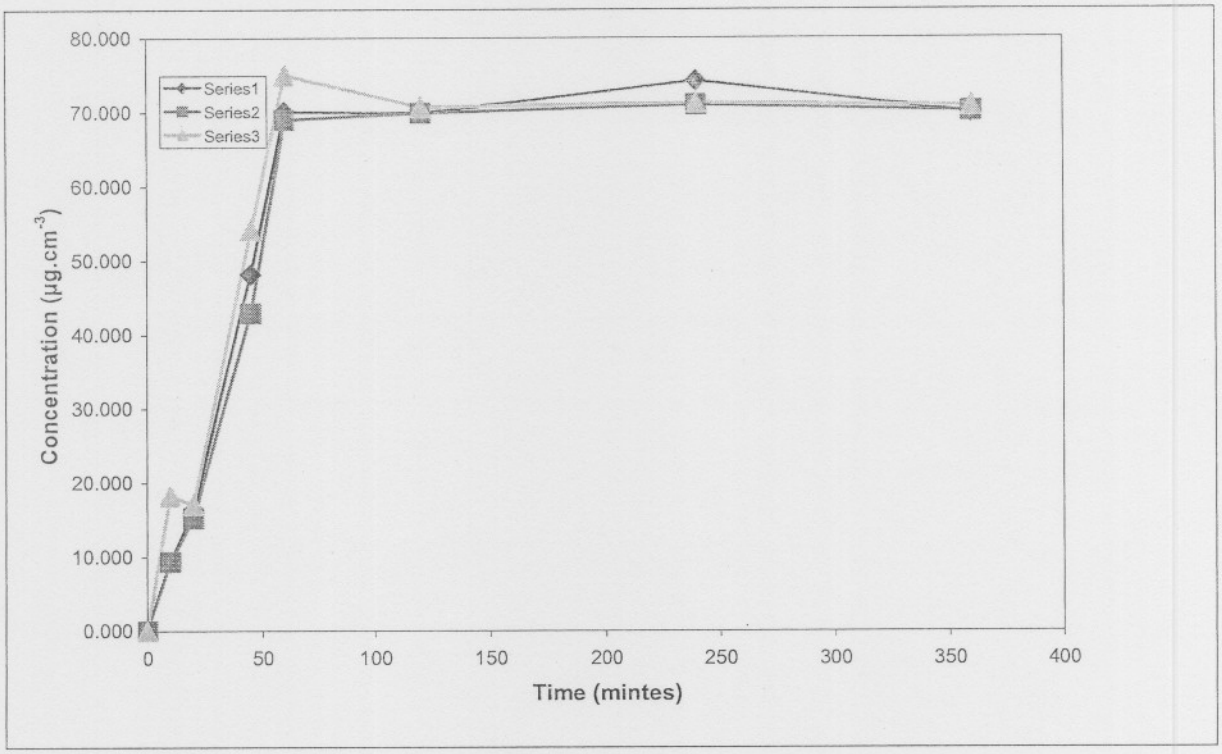

Figure A2.6: Dissolution profiles of individual stations.

FORMULATIONS TESTED IN SÖRENSEN BUFFER (pH ~ 4.5).
FORMULA 3: Agglomeration time 10 minutes.

Table A2.7: Dissolution data for three repetitions.

Time (min)	[1]C1	C2	C3	Average	*s*	*%RSD*
0	0.000	0.000	0.000	0.000	0.000	0.000
10	7.078	6.301	6.041	6.473	0.539	8.331
20	5.406	5.194	8.250	6.283	1.706	27.158
45	12.598	9.177	8.210	9.995	2.306	23.068
60	12.275	11.376	10.386	11.345	0.945	8.331
120	40.097	33.149	40.294	37.846	4.069	10.752
240	59.786	58.037	59.424	59.082	0.923	1.562
360	61.397	61.335	61.084	61.271	0.166	0.271
[2]DR_i	0.310	0.255	0.304	0.290	0.030	10.411
[3]AUC	15344.49	14392.06	15180.83	14972.46	509.26	3.401

[1]*Corrected sample concentration ($\mu g.cm^{-3}$)*
[2]*DR_i = initial dissolution rate ($\mu g.cm^{-3}.min^{-1}$)*
[3]*AUC = area under curve ($\mu g.min.cm^{-3}$)*

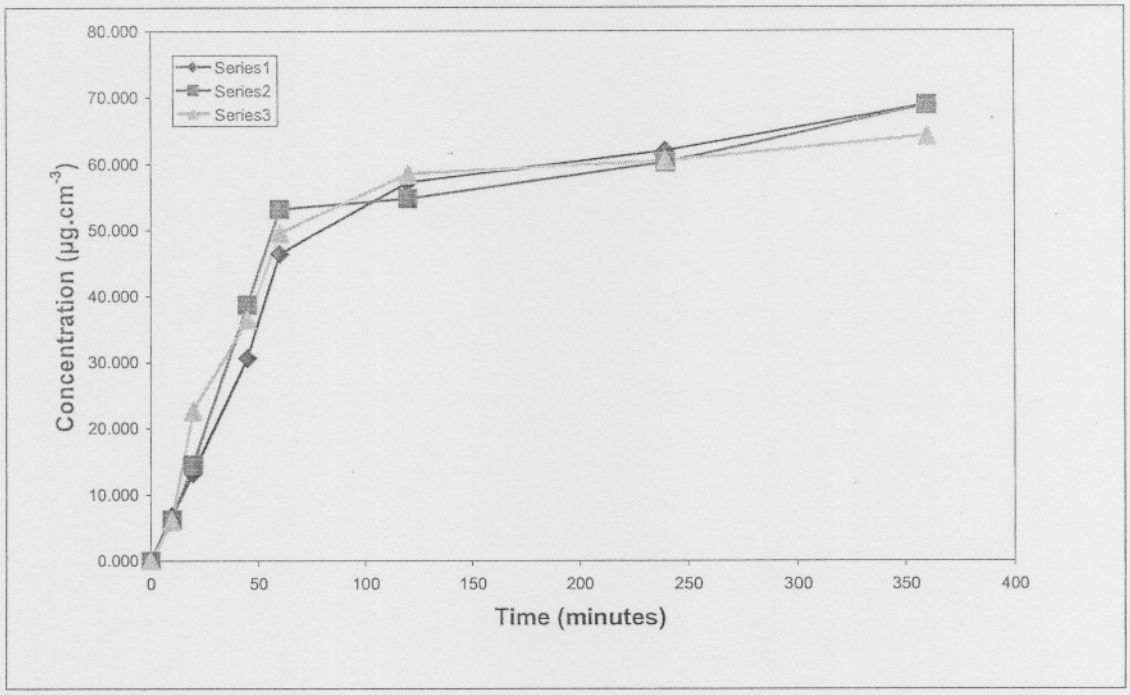

Figure A2.7: Dissolution profiles of individual stations.

FORMULATIONS TESTED IN SÖRENSEN BUFFER (pH ~ 4.5).
FORMULA 3: Agglomeration time 15 minutes.

Table A2.8: Dissolution data for three repetitions.

Time (min)	[1]C1	C2	C3	Average	*s*	*%RSD*
0	0.000	0.000	0.000	0.000	0.000	0.000
10	3.762	3.554	4.073	3.796	0.261	6.870
20	5.076	4.920	5.544	5.180	0.325	6.274
45	7.674	8.088	8.609	8.123	0.469	5.769
60	9.709	10.541	10.958	10.402	0.636	6.111
120	46.197	47.704	52.318	48.739	3.189	6.543
240	66.037	64.336	67.781	66.051	1.723	2.608
360	65.214	64.738	66.104	65.351	0.693	1.061
[2]DR_i	0.365	0.380	0.414	0.386	0.025	6.560
[3]AUC	16639.05	16576.6	17529.44	16915.03	533.01	3.151

[1]*Corrected sample concentration ($\mu g.cm^{-3}$)*
[2]*DR_i = initial dissolution rate ($\mu g.cm^{-3}.min^{-1}$)*
[3]*AUC = area under curve ($\mu g.min.cm^{-3}$)*

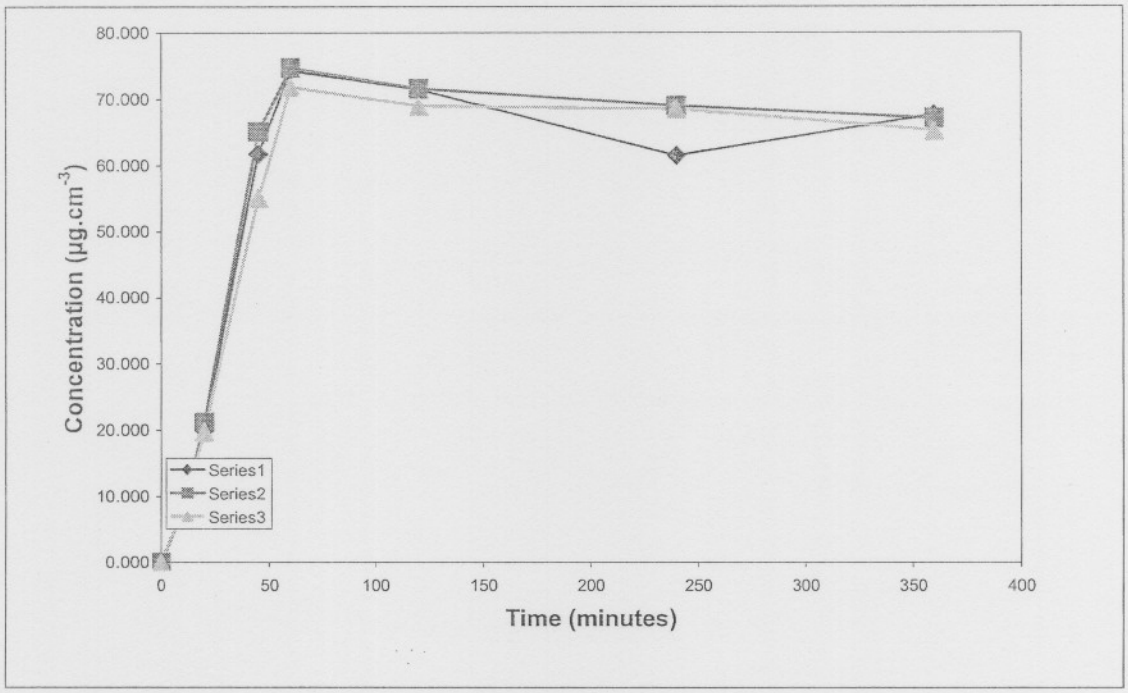

Figure A2.8: Dissolution profiles of individual stations.

FORMULATIONS TESTED IN SÖRENSEN BUFFER (pH ~ 4.5).
FORMULA 3: Agglomeration time 20 minutes.

Table A2.9: Dissolution data for three repetitions.

Time (min)	[1]C1	C2	C3	Average	*s*	*%RSD*
0	0.000	0.000	0.000	0.000	0.000	0.000
10	4.383	4.383	4.073	4.279	0.179	4.194
20	6.323	5.753	5.959	6.011	0.289	4.801
45	9.961	8.973	9.493	9.475	0.494	5.214
60	15.991	11.685	13.657	13.777	2.156	15.645
120	52.761	48.851	47.514	49.708	2.726	5.484
240	70.478	68.021	66.666	68.388	1.932	2.825
360	69.280	68.282	66.823	68.128	1.235	1.813
[2]DR_i	0.424	0.386	0.380	0.397	0.024	6.051
[3]AUC	18315.91	17418.12	17132.62	17622.21	617.48	3.504

[1]*Corrected sample concentration ($\mu g.cm^{-3}$)*
[2]*DR_i = initial dissolution rate ($\mu g.cm^{-3}.min^{-1}$)*
[3]*AUC = area under curve ($\mu g.min.cm^{-3}$)*

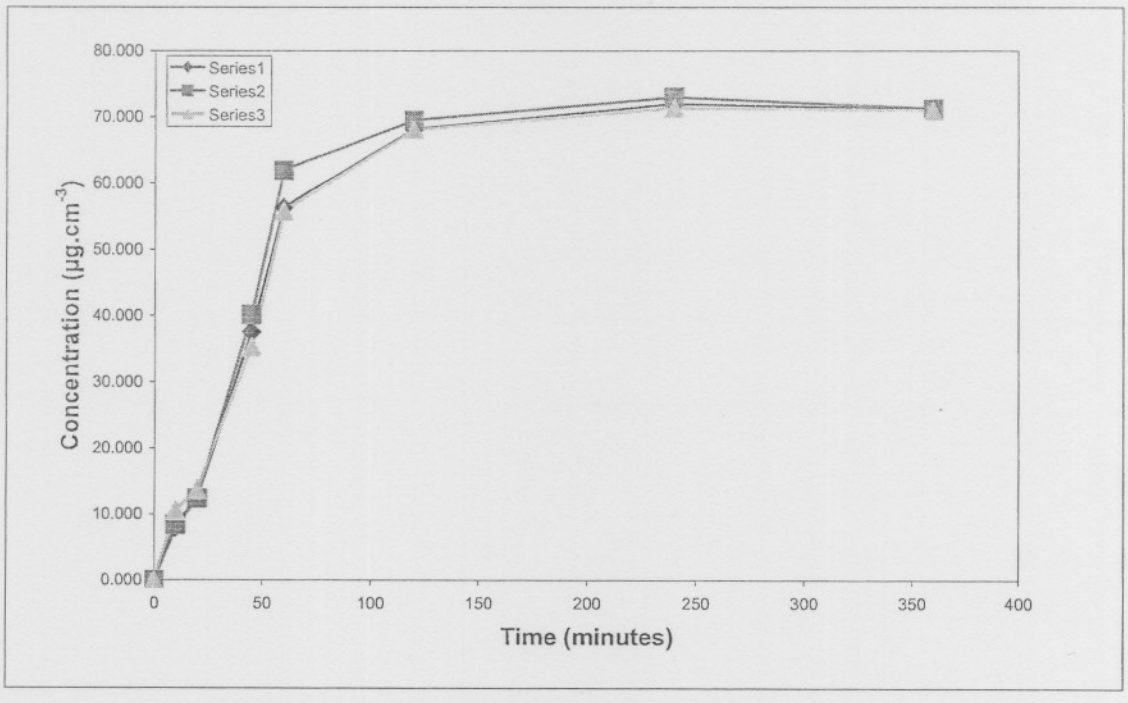

Figure A2.9: Dissolution profiles of individual stations.

FORMULATIONS TESTED IN SÖRENSEN BUFFER (pH ~ 4.5).
Inderal® LA 80 mg

Table A2.10: Dissolution data for three repetitions.

Time	R 1	R 2	R 3	Average	[1]Cave	s	%RSD
0	0.000	0.000	0.000	0.000	0.000	0.000	0.000
10	0.004	0.006	0.014	0.008	0.000	0.005	66.143
20	0.033	0.034	0.044	0.0371	0.000	0.006	16.439
45	0.141	0.137	0.157	0.145	3.905	0.010	7.298
60	0.203	0.205	0.227	0.211	7.909	0.013	6.291
120	0.439	0.423	0.442	0.434	21.204	0.010	2.349
240	0.733	0.726	0.722	0.727	25.782	0.005	0.765
360	0.901	0.911	0.893	0.901	49.101	0.009	1.000
^2DR_i	0.185						
^3AUC	8236.18						

[1]*Corrected samples average concentration ($\mu g.cm^{-3}$)*
[2]*DR_i = initial dissolution rate ($\mu g.cm^{-3}.min^{-1}$)*
[3]*AUC = area under curve ($\mu g.min.cm^{-3}$)*

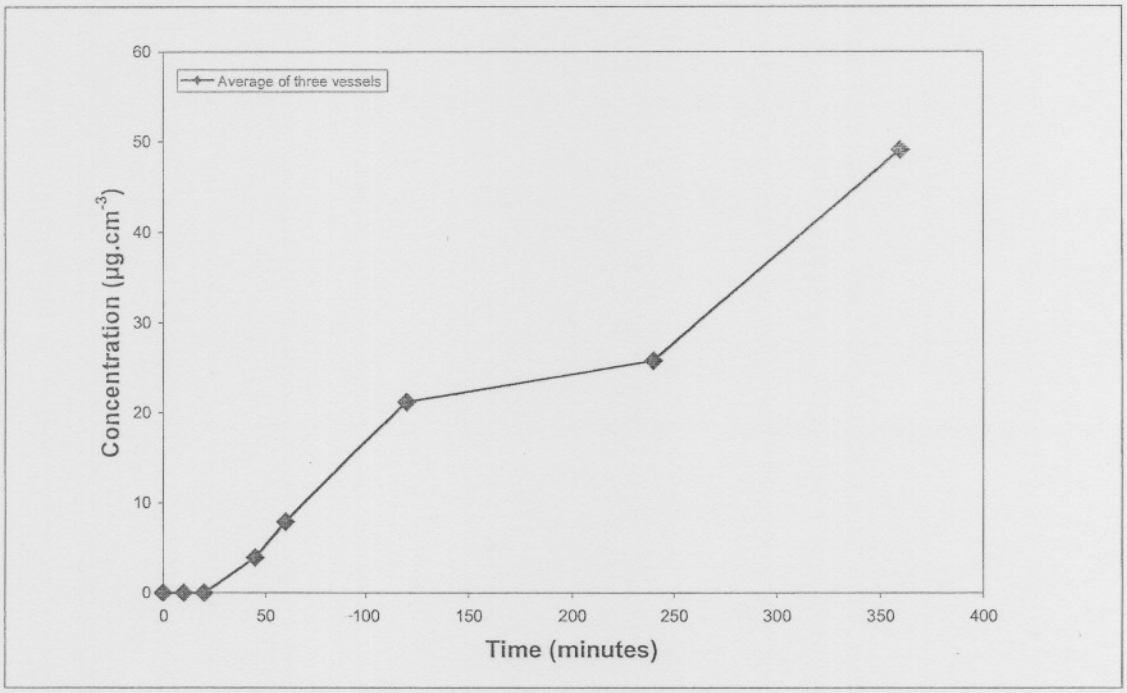

Figure A2.10: Dissolution profiles of individual stations.

8.2 ANNEXURE B: DETERMINING THE DRUG RELEASE MECHANISM OF PROPRANOLOL HYDROCLHORIDE FROM SPHERICALLY AGGLOMERATED CHITOSAN TABLETS

a)	
First order I	
Time (minutes)	Log % Dissolved
0	0
10	8.189
20	11.031
45	12.400
60	14.326
120	39.660
240	63.657
360	69.429

b)	
First order II	
$kW_0 - kQ'$	dQ'/dt
0	0.82
8.189	0.28
11.031	0.05
12.401	0.13
14.326	0.42
39.660	0.20
63.657	0.05
69.429	

c)	
Matrix dissolution	
Time (minutes)	$W^{1/3}$-$W^{1/3}$
0	4.642
10	2.626
20	2.416
45	2.327
60	2.213
120	1.231
240	0.649
360	0.532

d)	
Zero order	
Time (minutes)	Dissolved (%)
0	0
10	8.189
20	11.031
45	12.401
60	14.326
120	39.600
240	63.657
360	69.429

e)	
Matrix diffusion I	
$\sqrt{\text{Time}}$	Dissolved (%)
0	0
3.162	8.189
4.472	11.031
6.708	12.401
7.746	14.326
10.954	39.659
15.492	63.657
18.974	69.429

f)	
Matrix diffusion II	
Log Time	Log % Dissolved
1	0.913
1.301	1.043
1.653	1.093
1.778	1.156
2.079	1.598
2.380	1.804
2.556	1.842
N/d	N/d

8.3 ANNEXURE C: PRESENTATION AT THE 25TH SILVER JUBILEE ACADEMY OF PHARMACEUTICAL SCIENCE CONFERENCE, GRAHAMSTOWN, SOUTH AFRICA, 2004

Slide 1

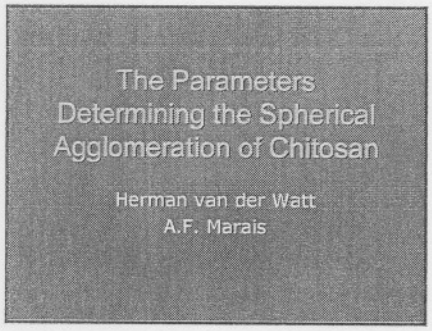

Slide 2

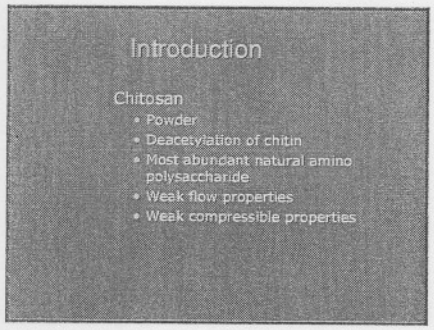

Slide 3

Introduction

Chitosan

- Microscopic structure → weak flow and compressibility properties
- Milling
- Liquid nitrogen

Slide 4

Scanning electron microscopy

- Figure 1. Chitosan Powder

Slide 5

Size enlargement

Controlled manner

- Wet granulation
  - Failed with conditions applied
- Spherical agglomeration

Slide 6

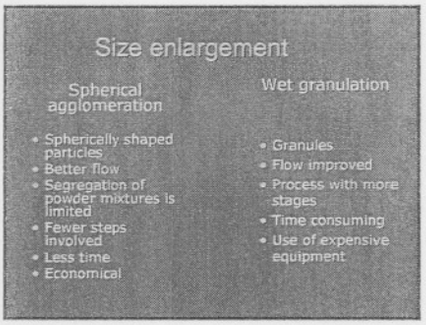

Slide 7

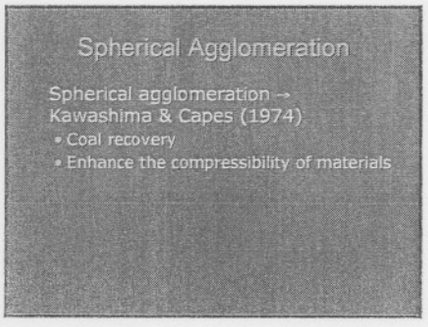

Slide 8

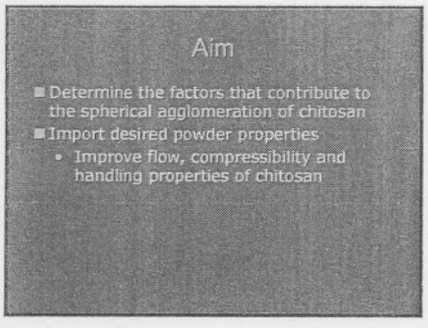

Slide 9

Method

- Suspension / External phase
  - agitated by mechanical stirrer → turbulence
  - Ethyl acetate
- Bridging liquid / Internal phase
  - dissolves the binder
  - wets the suspended particles → transfer binder to particles
  - immiscible with external phase
  - 5% glacial acetic acid
- External phase removed → agglomerates dried, evaluated

Slide 10

Setup

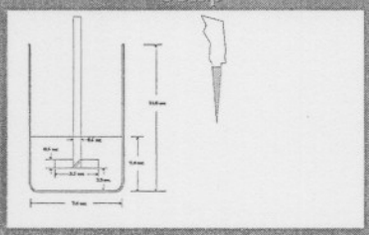

→ Found 2. Experimental setup

Slide 11

Factorial design

Exploratory experimental study
- Five predominant factors, two levels
- Carefully selected subset/fraction
  - Fractional factorial design

Slide 12

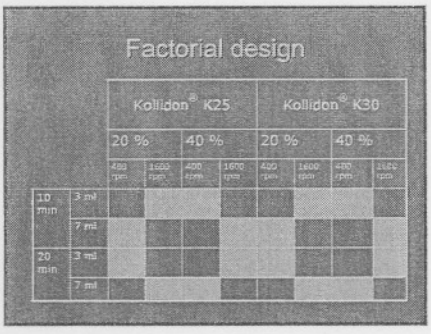

Slide 13

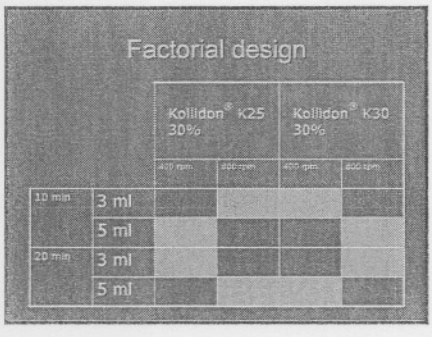

Slide 14

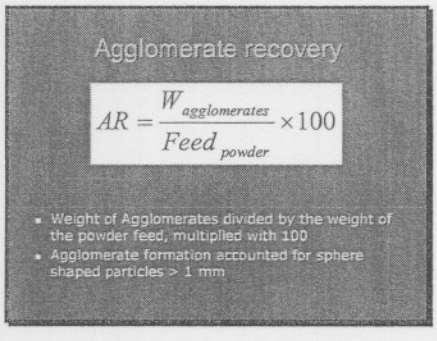

Slide 15

Results and discussion

		Kollidon K25				Kollidon K30			
		20 %		40 %		20 %		40 %	
		400 rpm	1600 rpm	400 rpm	2400 rpm	400 rpm	1600 rpm	400 rpm	2400 rpm
10 min	3 ml							29.5 %	
	7 ml								
20 min	3 ml	4.83 %				2.55 %			
	7 ml								

Slide 16

Results and discussion

- Kollidon® K25 and Kollidon® K30
- 2^5 factorial design
- 8 : 2 ratio weak, brittle → insufficient binder concentration

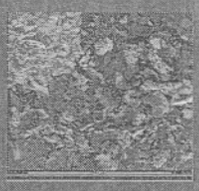

Slide 17

Agitation speed

- 1600 rpm, 800 rpm failed
- Small, irregularly shaped
- Size → Partial comminution
  - Collisions with cell walls, blades, other

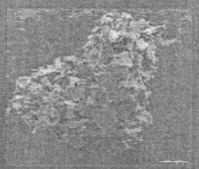

Slide 18

Bridging liquid volume

- 7 ml / 3 g
  - ↑ agglomerate recovery
  - ↑ size
  - irregular particle size distribution
- 3 ml / 3 g
  - ↓ agglomerate recovery, ↓ size
  - free flowing
  - uncovered and inadequately agglomerated

Slide 19

Effect of agglomeration time

- Minimum effect
- 15 / 20 minutes → sphere shaped agglomerates

Slide 20

Results and discussion

		Kollidon K25 30 %		Kollidon K30 30 %	
		400 rpm	800 rpm	400 rpm	800 rpm
10 min	3 ml		1.75%	29.2%	
	5 ml	66.3%			2.1%
20 min	3 ml	31.5%			1.8%
	5 ml		1.88%	51.2%	

Slide 21

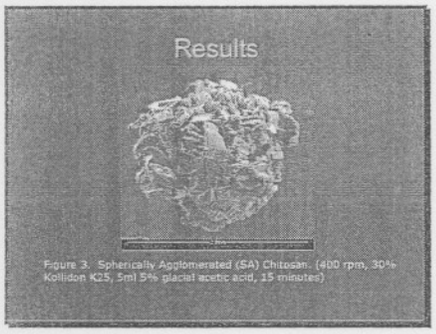

Slide 22

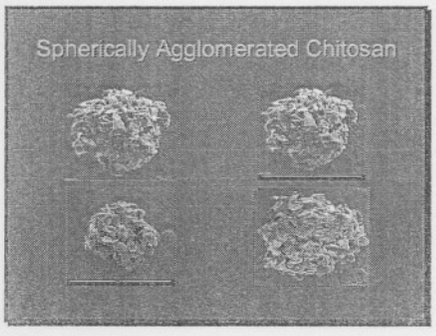

Slide 23

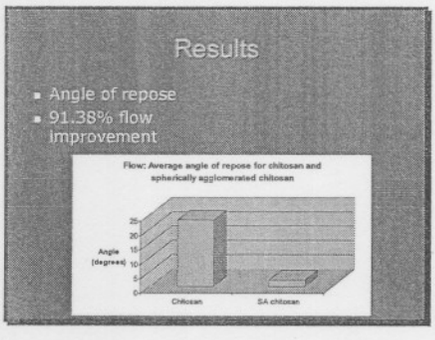

Slide 24

Conclusion

Agitation speed	400 rpm
Agglomeration time	15 minutes
Bridging liquid volume	5 ml
Binder concentration	30%

Slide 25

Conclusion

Spherically Agglomerated Chitosan vs. Chitosan

- Flow improved
- Compressibility improved
- Dust free particles

Future prospects

- Alternative binder in less quantities
- Size reduction of the chitosan agglomerates
- Incorporation of weakly compressible drugs

MALVERN MASTERSIZER X

Version 1.2a

Tue, Sep 16, 2003 9:29AM

Chitosan :Run Number 3

Batch nr.: 021010 Drum: 115
Dispersant: 15 ml Ethanol in MSX1

Sample 2
Sample File Name: JOE_01 , Record: 3 Source: Analysed
Measured on: Fri, Jan 04, 1980 6:56PM Last saved on: Fri, Jan 04, 1980 6:57PM

Presentation: 2THD
Very Polydisperse model

Volume Result

Focus = 300 mm.

Residual = 0.818 %
d (0.5) = 193.99 µm
D [4, 3] = 208.86 µm
Sauter Mean (D[3,2]) = 123.69 µm
Specific Surface Area = 0.0485 sq. m. / gm

Concentration = 0.062 %
d (0.1) = 77.22 µm
Span = 1.46

Obscuration = 19.72 %
d (0.9) = 359.54 µm

Mode = 229.54 µm
Density = 1.00 gm. / c.c.

Size (Lo) µm	Result In %	Size (Hi) µm	Result Below %
0.50	0.00	1.32	0.00
1.32	0.00	1.60	0.00
1.60	0.00	1.95	0.00
1.95	0.00	2.38	0.01
2.38	0.01	2.90	0.02
2.90	0.02	3.53	0.04
3.53	0.05	4.30	0.09
4.30	0.08	5.24	0.17
5.24	0.09	6.39	0.26
6.39	0.10	7.78	0.36
7.78	0.12	9.48	0.48
9.48	0.14	11.55	0.61
11.55	0.17	14.08	0.78
14.08	0.21	17.15	0.99
17.15	0.27	20.90	1.26
20.90	0.37	25.46	1.63

Size (Lo) µm	Result In %	Size (Hi) µm	Result Below %
25.46	0.52	31.01	2.15
31.01	0.74	37.79	2.89
37.79	1.11	46.03	4.00
46.03	1.61	56.09	5.61
56.09	2.36	68.33	7.97
68.33	3.47	83.26	11.45
83.26	4.80	101.44	16.25
101.44	7.22	123.59	23.47
123.59	9.72	150.57	33.19
150.57	12.74	183.44	45.93
183.44	14.76	223.51	60.70
223.51	14.85	272.31	75.54
272.31	11.08	331.77	86.63
331.77	7.23	404.21	93.86
404.21	3.83	492.47	97.69
492.47	2.31	600.00	100.00